Journal of Structural Geology 32 (2010) 1519–1551

Contents lists available at ScienceDirect

Journal of Structural Geology

journal homepage: www.elsevier.com/locate/jsg

Review Article

Structural geology, petrofabrics and magnetic fabrics (AMS, AARM, AIRM)

Graham J. Borradaile [a,*], Mike Jackson [b]

[a] Faculty of Science, Lakehead University, Thunder Bay P7B 5E4, Canada
[b] Institute of Rock Magnetism, University of Minneapolis, MN 55455, USA

ARTICLE INFO

Article history:
Received 14 April 2009
Received in revised form
19 August 2009
Accepted 13 September 2009
Available online 2 December 2009

Keywords:
Magnetic fabrics
Petrofabric
Anisotropy of magnetic susceptibility
AMS

ABSTRACT

Anisotropy of magnetic susceptibility (AMS) was recognized as a feature of minerals in 1899, and petrofabric-compatible AMS fabrics were reported from 1942–1958. Shortly thereafter, cleavage and mineral lineation were associated with the principal axes of the AMS ellipsoid. AMS is describable by a magnitude ellipsoid, somewhat similar in concept to the finite strain ellipsoid, with principal susceptibilities (κ_{MAX}, κ_{INT}, κ_{MIN}) as its axes and their average value being the mean susceptibility (κ). Orientations of the AMS axes usually have a reasonably straightforward structural significance but their magnitudes are more difficult to interpret, being the result of mineral abundances and different mineral-AMS. The strain ellipsoid is dimensionless (i.e., of unit-volume) and readily compared from one outcrop to another but the AMS ellipsoid represents the anisotropy of a physical property. Thus, (κ) determines the relative importance of AMS for different specimens, or compared outcrops, or component AMS subfabrics. AMS provides a petrofabric tool, unlike any other, averaging and sampling the orientation-distribution of all minerals and all subfabrics in a specimen. Sophisticated laboratory techniques may isolate the AMS contributions of certain minerals from one another, and of certain subfabrics (e.g. depositional from tectonic). However, suitable data processing of the basic AMS measurements (κ_{MAX}, κ_{INT}, κ_{MIN} magnitudes and orientations, and the mean susceptibility, κ) may provide the same information.. Thus, AMS provides the structural geologist with a unique tool that may isolate the orientations of subfabrics of different origins (sedimentary, tectonic, tectonic overprints etc.).

1. Purpose and background

Structural geology infers the axes of finite strain or solid-state flow from the orientations of crystals *or* the orientation of grain shapes. Preferred crystallographic orientation (PCO) is less easily measured and interpreted than preferred dimensional orientation (PDO) but received attention earlier mainly due to brilliant insights based on field studies, Universal stage and early X-ray methods (March, 1932; also by Schmidt, 1917–1929 and Sander, 1909–1948, summarized in Sander, 1970). They associated girdle-cluster orientation distributions (ODs) of crystals (and in some cases grain shapes) on the stereogram (Fig. 1) with macroscopic structures (folds, cleavage and mineral lineation). Now we accept that a homogeneous single fabric (e.g. "D_1") comprises a composite lineation-schistosity fabric of minerals described in the L-S continuous spectrum (Flinn, 1962, 1965) (Fig. 1a–e). We may readily identify orientation-distributions (ODs) of aligned elements or the shapes of strained objects and perhaps quantify these in terms of a strain or fabric ellipsoid (Flinn, 1965; Ramsay, 1967). PCOs are quantifiable by the Eigenvectors method (Scheidegger, 1965; Woodcock, 1977) but usually they do not directly relate to strain. The finite strain ellipsoid, and by analogy the fabric ellipsoid, range over a smooth continuum of shapes ranging from oblate ($X = Y > Z$), through neutral ($X/Y = Y/Z$) to prolate ($X > Y = Z$). Thus, no homogeneous single-event fabric may possess any symmetry lower than orthorhombic and only the extreme end-cases are tetragonal. Flinn's fabric scheme (L, $L > S$, $L = S$, $L < S$, S) is universally accepted in structure (Fig. 1a) but the Cartesian graph of ($a = max/int$, $b = int/min$) has an awkward asymmetric radial shape parameter [$=(a-1)/(b-1)$]. For applications in magnetic fabrics, in which anisotropy is usually rather low, Jelinek (1981) introduced improved parameters; Pj for the eccentricity of the ellipsoid ("anisotropy degree") and Tj for its shape. These are equally valid for strain, fabric ellipsoids and ODs.

$$T_J = \frac{\ln(F) - \ln(L)}{\ln(F) + \ln(L)} \quad \text{where } L = \left(\frac{\kappa_{MAX}}{\kappa_{INT}}\right) \; F = \left(\frac{\kappa_{INT}}{\kappa_{MIN}}\right) \qquad (1)$$

* Corresponding author at: Department of Geology & Physics, Lakehead University, 955 Oliver Road, Thunder Bay, Ontario P7B 5E4, Canada. Tel.: +1 807 683 0680.
E-mail addresses: borradaile@lakeheadu.ca (G.J. Borradaile), irm@tc.umn.edu (M. Jackson).

0191-8141/$ – see front matter © 2010 Published by Elsevier Ltd.
doi:10.1016/j.jsg.2009.09.006

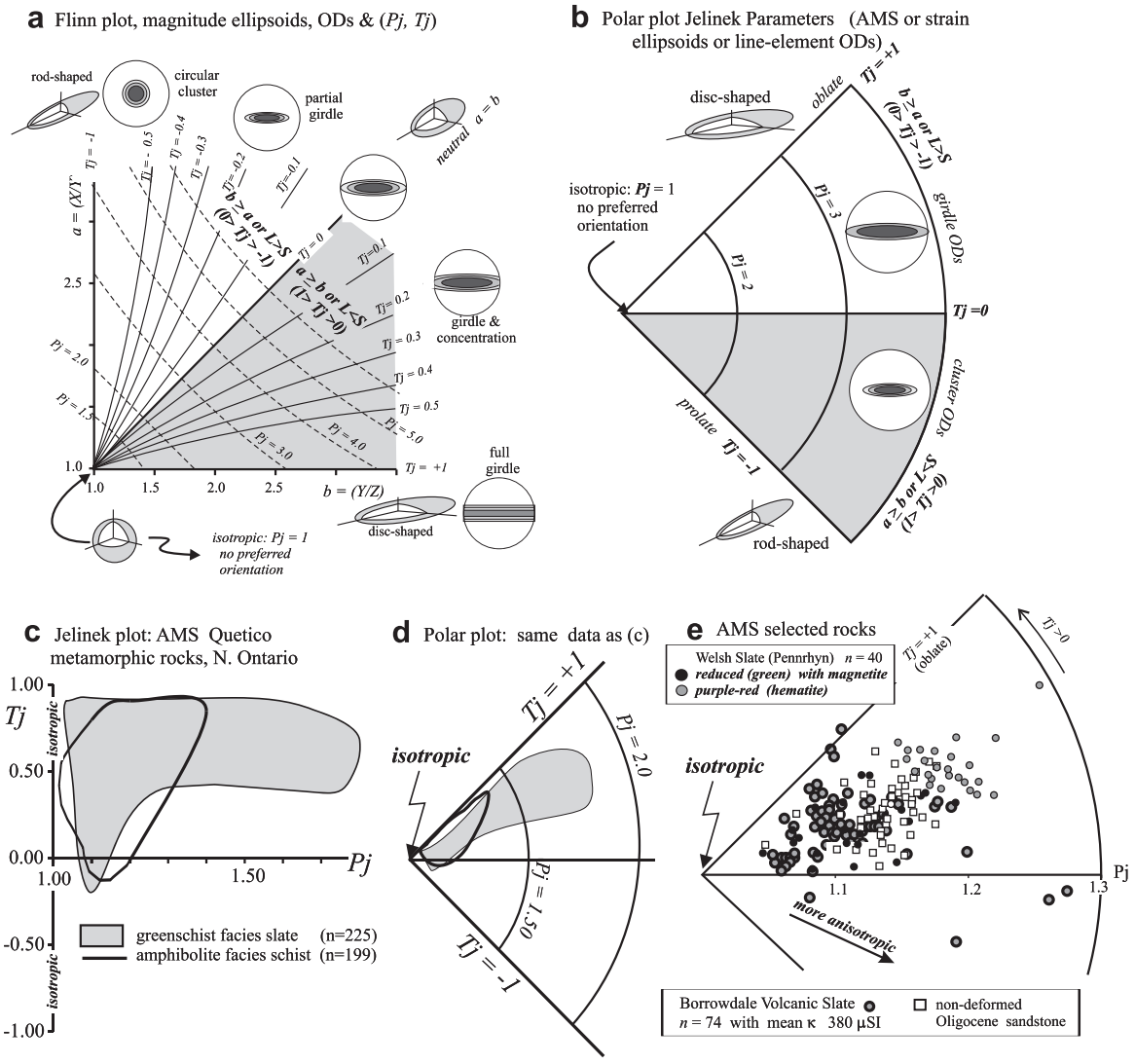

Fig. 1. Structural geologists define homogeneous, anisotropic preferred crystallographic orientations (PCO) and preferred dimensional orientations (PDO) in terms of fabric ellipsoids (Flinn, 1962, 1965;Scheidegger, 1965; Woodcock, 1977) that relate to the finite strain ellipsoid (Ramsay, 1967). (a) In structural geology, the ellipsoid is plotted on Cartesian axes. (b) However, for magnetic fabric ellipsoids which usually have very low anisotropy degree, Jelinek's (1981) more symmetric parameters (Pj for anisotropy degree (eccentricity) and Tj for shape) are greatly preferred. These plot more faithfully on a polar plot. (c, d) Samples for AMS ellipsoids on a Cartesian and on a polar plot compared. The isotropic case occurs at a unique location in (d). (e) AMS ellipsoids compared for some well-known metamorphic rocks and a non-deformed sandstone.

Tj ranges symmetrically over the spectrum of ellipsoid shapes: $Tj = +1$ for oblate, $Tj = -1$ for prolate, $Tj = 0$ for neutral and $+1 > Tj > -1$ for the general ellipsoid.

Jelinek's parameter for the degree of anisotropy is

$$\ln(P_J) = \sqrt{2}\left(\left(\ln\left(\frac{\kappa_{MAX}}{\kappa}\right)\right)^2+\left(\ln\left(\frac{\kappa_{INT}}{\kappa}\right)\right)^2+\left(\ln\left(\frac{\kappa_{MIN}}{\kappa}\right)\right)^2\right)^{\frac{1}{2}} \quad (2)$$

It includes a reference to shape and is therefore is preferable to an older but still commonly used simple ratio ($P = \kappa_{MAX}/\kappa_{MIN}$) of Nagata (1961). It is derived from older Nagata's P-values with

$$\ln(P_J) = \ln(P)\sqrt{\left(1+\frac{T_J^2}{3}\right)} \quad (3)$$

A polar plot of (Pj, Tj) (Fig. 1b) gives an unbiased distribution of ellipsoid shapes (Fig. 1c–d), especially for those with low Pj, (Borradaile and Jackson, 2004). Importantly, the isotropic case plots uniquely whereas Cartesian plots of (Pj, Tj) are ambiguous.

1.1. Why magnetic fabrics?

The OD of a certain mineral is remarkably difficult to measure and is restricted to oriented thin-sections or slabs cut for X-ray work. Before many such ODs were available from Universal-stage microscopy, a remarkably early study recognized that the L–S scheme of crystal ODs would arise if crystals were to spin passively without -impingement (March, 1932). Subsequently, field or laboratory tests verified that March's hypothesis was an acceptable qualitative approximation, albeit with many caveats (Frost and Siddans, 1979; Oertel, 1983; Tullis, 1976; Hobbs et al., 1976). More recently, neutron texture goniometry has overcome some of the difficulties of PCO quantification – the large penetration depth allows analysis of volumes of material comparable to AMS specimens without any special surface preparation and complete pole figures can be measured with only one specimen

(Brokmeier, 1994; Ullemeyer et al., 2000). However, neutron diffraction instrumentation is not readily accessible to most researchers. The impetus to develop or apply magnetic techniques to determine ODs stalled until the early 1980s until continuum mechanics (Ramsay, 1967; Ramsay and Huber, 1983) and material science concepts verified that PCOs were a readily interpretable consequence of tectonic strain. Concepts concerning crystal plasticity, dynamic recrystallization, diffusive mechanisms, pressure solution and particulate flow were not absorbed into structural analysis until relatively recently (e.g., Boland and Fitzgerald, 1993; Blenkinsop, 2000; Knipe and Rutter, 1994; .Nicolas and Poirier, 1976; Nicolas, 1987; Poirier, 1985; Paaschier and Trouw, 2005).

Armed with means to interpret ODs, it became reasonable to apply magnetic methods to measure PCOs. Magnetic properties, especially low field susceptibility (κ) have large ranges and are readily measured by mostly non-destructive methods. The development of the "personal" computer in 1980 expanded the routine measurement of anisotropy of low field susceptibility (AMS) for suitably prepared standard-size specimens. Finite strain, ODs and AMS have all in common the underlying convenience that as homogeneous fabrics, they may be visualized as a magnitude ellipsoid with orthogonal principal axes. Their relative magnitudes will determine whether a point-cluster, a partial girdle or a full-girdle exist for the crystal OD. For AMS, as long as all principal susceptibilities have the same sign, a homogeneous sub-fabric or a single crystal, will have a magnitude ellipsoid, or AMS ellipsoid with orthogonal axes (κ_{MAX}, κ_{INT} and κ_{MIN}). The magnitude ellipsoids in these cases are properties of a state of matter, the permanent features of a *material tensor* (Nye, 1957) like finite strain ($X \geq Y \geq Z$). In contrast, to the dismay of structural geology, stress is an ephemeral *field tensor* (Nye, 1957) that rarely correlates directly with any specific finite strain, orientation-distribution or instant in time. There is a major difference between the strain ellipsoid concept in structural geology and the AMS ellipsoid. *Strain ellipsoids are dimensionless, with axes normalized so that the ellipsoid has the same volume as the initial sphere*. However, AMS ellipsoids vary in shape (anisotropy) *but also in magnitude because specimens differ in mean susceptibility* (κ). Thus, AMS ellipsoids carry an inherent weighting factor. Whereas strain ellipsoids for different specimens are directly comparable, AMS ellipsoids are generally not!

The attraction of AMS as a petrofabric detector is that it sums influences from all minerals in a small sample, in a matter of minutes, with a higher reproducibility and precision than any other petrofabric method. If sufficiently homogeneous, the rock-AMS corresponds to the ODs of significant minerals. The most abundant, high-κ, and strongly anisotropic minerals control the rock-AMS. The AMS of minerals was first measured more than a century ago (Voight and Kinoshita, 1907) and used as a petrofabric petrofabric marker by Ising (1942) and Graham (1954). Fuller (1963), Nagata (1961), Stacey and Banerjee (1974), Uyeda et al. (1963) and Hrouda (1982) developed fundamental concepts in landmark studies. Applications to structural and metamorphic problems, including multiple sub-fabrics are found in Borradaile and Henry (1997), Rochette et al. (1992), Tarling and Hrouda (1993), Jackson and Tauxe (1991) and Borradaile and Jackson (2004). Anisotropy of remanence is a more specialized field and a powerful supplement for a complete evaluation of AMS (Jackson, 1991; Potter, 2004).

2. Quantifying κ and AMS

2.1. Low-field susceptibility measurements

To measure susceptibility, a specimen is exposed to a weak laboratory field, typically an AC field with an RMS intensity of tens to hundreds of A/m and a frequency in the range 100 Hz to 20,000 Hz. The applied field ($\vec{H}_A$) produces an induced magnetization $\vec{M}_i$ in *any* substance (section 3). The two vectors are parallel only for isotropic materials or for fields applied along one of the principal susceptibility axes of the sample. Most AC susceptibility instruments measure only the coaxial response $M_{i//}$, i.e., the component of induced magnetization parallel to the applied field. The scalar (directional) susceptibility κ is the dimensionless ratio $M_{i//}/H_A$. DC magnetometers can in many cases be configured to apply weak steady fields and to measure the full induced magnetization vector (Schmidt et al., 1988), but in most laboratories, single-axis AC instruments are used for measurements of κ and AMS. Low-field and high-field torque magnetometers are much less common than AC instruments and are used specifically for measuring magnetic anisotropy (Banerjee and Stacey, 1967; Jelinek, 1985; Martín-Hernández and Hirt, 2001, 2003, 2004).

Of all the petrophysical properties, bulk susceptibility (κ) shows the widest range of values (e.g., Hunt et al., 1995). For pure, ideal minerals, chemical composition and crystal structure controls susceptibilities. Pure examples of quartz, calcite and feldspars may have values $\sim -15 - 10^{-6}$ or 15 μSI. Relatively pure clay minerals, chlorites and micas may range from 100 to 1500 μSI. The theoretical upper limit for paramagnetic mafic silicates is calculated at $\sim$ 2000 μSI (Syono, 1960). Due to their high susceptibility, the common oxides and sulfides of iron, despite low concentrations, must always be considered when interpreting κ or AMS. For example, magnetite has $\kappa > 2$ SI, and titanomagnetites, titanohematite, hematite and pyrrohotite all have high κ-values, e.g. 10^{-2}–10^{0} SI. Magnetite is always of particular concern in any magnetic-petrofabric interpretation since its susceptibility is so high and its average concentration in continental and oceanic crust is at least 2% (Taylor and McLelland, 1985).

2.2. Anisotropy of low-field magnetic susceptibility (AMS) quantification

The structural geologist is interested primarily in anisotropy; differences in susceptibility along different axes determined during the same experiment. Since minerals are anisotropic, their alignment will cluster their maximum susceptibilities along one axis, and their minimum susceptibilities along another axis. AMS is most commonly determined from sets of directional susceptibility measurements. Using the common Kappabridge (AGICO, Czech Republic) or Sapphire Instruments (Kingsville, Ontario, Canada) susceptibility-anisotropy systems, reproducible values of κ (for a particular specimen in a particular orientation) are obtained routinely to four significant figures. Derived parameters describing anisotropy (e.g., *Pj*, *Tj*) are valid to three significant figures. Torsion magnetometers measure torques due to directional susceptibility differences rather than directional susceptibilities (e.g., Banerjee and Stacey, 1967; Bergmüller et al., 1994). Because of space limitations, and because directional susceptibility instruments are far more common, we will not describe torque-based measurements in any detail.

For instruments that sense only the component of magnetization parallel to the applied field, we denote the directional (parallel) susceptibilities as $\kappa_{//} = M_{//}/H = (\vec{M}\cdot\hat{H})/H = ([\kappa]\hat{H}\cdot\hat{H})/H^2$, and we write the matrix equation for any arbitrary set of n applied field orientations in terms of the "design matrix" A $(n \times 6)$ relating the corresponding array of parallel directional susceptibilities $\kappa_{//}$ $(n \times 1)$ to the 6 independent tensor elements:

$$\begin{pmatrix} \kappa_{//1} \\ \kappa_{//2} \\ \kappa_{//3} \\ \vdots \\ \kappa_{//n} \end{pmatrix} = \left(\frac{1}{H^2}\right) \begin{pmatrix} H_{x1}^2 & H_{y1}^2 & H_{z1}^2 & 2H_{x1}H_{y1} & 2H_{y1}H_{z1} & 2H_{z1}H_{x1} \\ H_{x2}^2 & H_{y2}^2 & H_{z2}^2 & 2H_{x2}H_{y2} & 2H_{y2}H_{z2} & 2H_{z2}H_{x2} \\ H_{x3}^2 & H_{y3}^2 & H_{z3}^2 & 2H_{x3}H_{y3} & 2H_{y3}H_{z3} & 2H_{z3}H_{x3} \\ \vdots & \vdots & \vdots & \vdots & \vdots & \vdots \\ H_{xn}^2 & H_{yn}^2 & H_{zn}^2 & 2H_{xn}H_{yn} & 2H_{yn}H_{zn} & 2H_{zn}H_{xn} \end{pmatrix} \begin{pmatrix} \kappa_{xx} \\ \kappa_{yy} \\ \kappa_{zz} \\ \kappa_{xy} \\ \kappa_{yz} \\ \kappa_{zx} \end{pmatrix} \quad (4)$$

(Girdler, 1961; Tauxe, 1998; Owens, 2000a; Borradaile, 2003). In the inverse problem, where we have n measured values of directional susceptibility, the best-fit values for the tensor elements are given by $(\mathbf{A}^T\mathbf{A})^{-1}\mathbf{A}^T\kappa_{//}$. Eigenvalues and eigenvectors are then calculated by iterative diagonalization methods. The same mathematical treatment applies equally to directional measurements of low-field susceptibility, high-field susceptibility (Kelso et al., 2002; Martin-Hernandez and Ferre, 2007), and resolved field-parallel components of ARM (McCabe et al., 1985; Trindade et al., 2001).

The choice of measurement axes for the determination of AMS is critical. A minimum of six is necessary to solve for the six unknown tensor components but their orientation must be selected carefully and appropriately programmed (Hext, 1963; Girdler, 1961; Jelinek, 1978; Borradaile and Stupavsky, 1995; Owens, 2000a). Schemes in common use (for AMS and/or ARM anisotropy) include $n = 7$ (Borradaile and Stupavsky, 1995), 9 (Girdler, 1961), 12 (Hext, 1963), 15 (Jelínek, 1976), 18 (Trindade et al., 2001), 24 (Kelso et al., 2002), 192 (Jelínek and Pokorný, 1997) or more directional measurements. Fig. 2 shows some common schemes of measurement axes. A key advantage of least-squares estimation of κ is that also allows quantitative assessment of the uncertainties in the best-fit values and in the parameters derived from them. There are two main approaches in use for this: linear perturbation analysis (Hext, 1963; Jelinek, 1976) and re-sampling or bootstrapping (Constable and Tauxe, 1990; Owens, 2000a,b; Tauxe, 1998). Werner (1997) compares the methods for the same data sets.

The second rank tensor may be represented by a quadric surface that is fortunately usually an ellipsoid; this may be inverted to yield a magnitude ellipsoid (Nye, 1957) for which shape and orientation are defined by its orthogonal principal axes of susceptibility ($\kappa_{MAX} \geq \kappa_{INT} \geq \kappa_{MIN}$ or $\kappa_1 \geq \kappa_2 \geq \kappa_3$). Structural geologists may, after some consideration relate this to an orientation-distribution ellipsoid of some important minerals, or even to the orientation of a finite strain ellipsoid or some kinematic axis. Of course, for the strain ellipsoid axes are always positive since they are the stretches (l_{NEW}/l_{OLD}). Thus, finite strain is always described by an ellipsoidal quadric that yields a magnitude ellipsoid. Unfortunately, for certain rocks such as some quartzite, limestone, tonalite, and rhyolite, susceptibilities may be very low ($\kappa \sim 0$), bridging the response between paramagnetism and diamagnetism. Measurements along some axes may yield $\kappa > 0$ and others may yield $\kappa < 0$; a magnitude ellipsoid is therefore indeterminate. Fortunately, this situation is rare and mostly we deal with AMS suites in which all specimens have $\kappa_{MIN} > 0$ or, more rarely with $\kappa_{MAX} < 0$ (diamagnetic), so that an ellipsoidal description of AMS is always possible. For rocks with $\kappa < 0$, AMS requires careful consideration in plotting and interpreting fabric shapes and in its kinematic interpretation (Hrouda, 2004; Hamilton et al., 2004).

3. Mineral sources of susceptibility and of AMS

All materials, including rocks, magnetize in response to an applied field (H_A). Pure materials may be broadly classified (Figs. 3 and 4) as magnetically disordered (diamagnetic or paramagnetic) or ordered (ferromagnetic, ferromagnetic, or antiferromagnetic) at ambient temperatures (e.g., Dunlop and Özdemir, 1997). For disordered materials and for certain ordered ones ("perfect antiferromagnets"), the induced magnetization M_i is a linear and reversible (single-valued) function of applied field over the range attainable in conventional laboratory instruments ($H_A < 10^5$–10^6 A/m), according to $M_i = \kappa H_A$ (Fig. 4b). In such linear materials no magnetization remains when the applied field is removed; these include virtually all of the major rock-forming minerals and most important accessory minerals. Most magnetically ordered materials (ferromagnets, ferrimagnets, and imperfect antiferromagnets) exhibit nonlinear (and commonly irreversible) dependence of M upon H_A, with magnetization approaching saturation in sufficiently strong applied fields, and with a remanent magnetization Mr commonly remaining after removal of the applied field (Fig. 3c). Such behavior occurs only in a relatively small number of minerals, chiefly iron oxides (Fig. 4c) and iron sulfides. In sufficiently weak applied fields (the threshold of ~10–100 A/m depending on material), ferri- and ferromagnets also behave linearly, allowing simple definition of *low-field susceptibility* according to $M_i = \kappa_{lf} H_A$ (Fig. 3c,d).

Diamagnetic susceptibility is very weak ($\kappa_d = \sim -15$ μSI for most materials) but is accurately measurable with modern instruments. It is independent of temperature. Fe^{2+}, Fe^{3+} and Mn^{2+} are the major sources of paramagnetism in minerals. At room temperature (~300 K), when these magnetic ions are present in non-negligible quantities (~0.5% or more by mass) their positive susceptibilities outweigh the diamagnetic susceptibilities of the bulk material. If pure, chlorites, micas, pyroxenes, amphiboles and other mafic minerals are paramagnetic. Syono's (1960) formula is equivalent to

$$\kappa = \mu_0 \left(x_{Fe^{2+}} \mu_{Fe^{2+}}^2 + x_{Fe^{3+}} \mu_{Fe^{3+}}^2 + x_{Mn^{2+}} \mu_{Mn^{2+}}^2 \right) \Big/ (3k_B T) \quad (5)$$

where μ_0 is the permeability of free space, k_B is Boltzman's constant, $\mu_{Fe^{2+}} \approx 5.3\mu_B$ is the moment per Fe^{2+} ion, $x_{Fe^{2+}}$ is the number of Fe^{2+} ions per cubic meter of sample, and so on for the other ions ($\mu_{Fe^{3+}} \approx \mu_{Mn^{2+}} \approx 5.3\mu_B$). Paramagnetic susceptibility varies inversely with absolute temperature.

In magnetically ordered materials, the atomic magnetic moments are usually arranged into parallel (ferromagnetic) or antiparallel (antiferromagnetic) sublattices. For perfect antiferromagnets the sublattice magnetizations cancel and there is no net spontaneous magnetization. Imperfect cancellation due to spin canting or other mechanisms results in a weak "parasitic ferromagnetism" in materials like hematite. Ferrimagnets (e.g., magnetite, maghemite) have strongly unbalanced sublattices and intense resultant spontaneous magnetization. Spontaneous magnetization is largely independent of external applied fields, but varies strongly with temperature, disappearing at the Curie temperature (for ferromagnets) or Néel temperature (for antiferromagnets) where thermal fluctuations become large enough to break down the magnetic ordering. Above their ordering temperatures, ferromagnetic materials behave paramagnetically, with linear $M(H)$ dependence, but their susceptibilities vary with temperature in distinctive ways (e.g., Petrovsky and Kapicka, 2006).

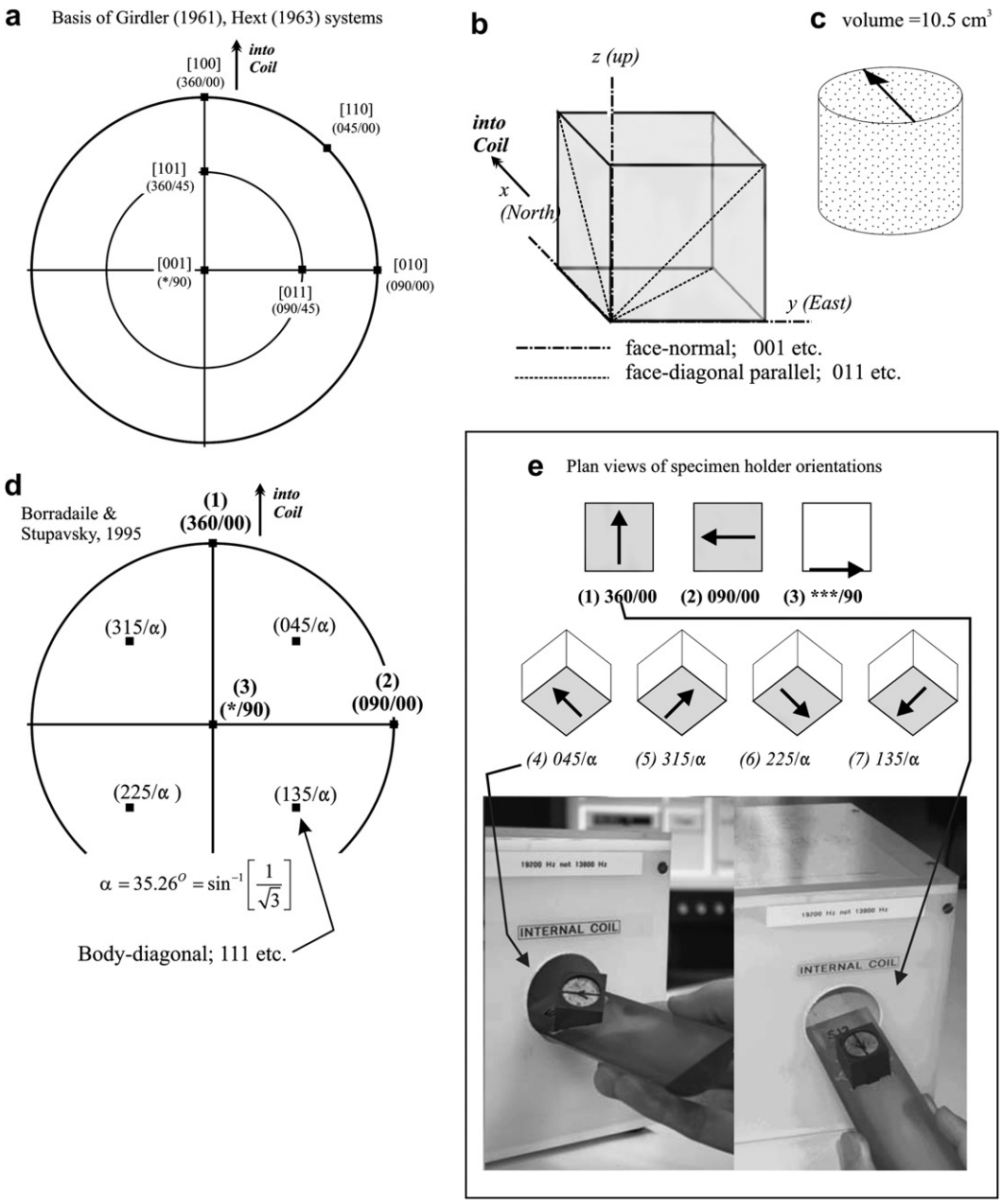

Fig. 2. (a) Traditional orientations of the core-specimen axis, relative to the induction coil, for successive measurements in an AMS determination. Repeat measurements along the same axis, or along anti-parallel axes are sometimes made to improve averaging. (b) Rectangular outline of specimen with measurement axes corresponding to (a). (c) Typical core specimen with orientation mark. (d) An improved tensor-matrix design for AMS measurement; the "body-diagonal" axis (045/α), provides better orientation-coverage of the specimen. (e) Specimen orientations, plan-view, required by (d). Two measurement steps using method (d-e) with the Sapphire Instruments.

3.1. Grain-scale AMS

3.1.1. Shape anisotropy

Magnetostatic self-demagnetization strongly affects the susceptibility of ferromagnetic and ferrimagnetic particles. The internal demagnetizing field is proportional to magnetization:

$$H_d = -NM \tag{6}$$

The proportionality constant N is called the demagnetizing factor. The net internal field in a grain exposed to an external field H_o is then $H_i = H_o + H_d = H_o - NM$. Measured susceptibility κ_o ($=M/H_o$) relates to intrinsic susceptibility κ_i ($=M/H_i$) through the demagnetizing factor:

$$\kappa_o = \frac{\kappa_i}{1 + N\kappa_i} \tag{7}$$

For weak intrinsic susceptibilities ($\kappa_i << 1$, typical of diamagnets, paramagnets and antiferromagnets) self-demagnetization is negligible, and the observed and intrinsic susceptibilities are equal (Fig. 5a). These materials have anisotropy controlled entirely and directly by crystallography. For very high intrinsic susceptibilities ($\kappa_i >> 1$, e.g., magnetite), the observed susceptibility reaches the "self-demagnetization limit" of $1/N$ (Fig. 5a). N is a tensor with a mean value in SI units of 1/3 (for any 3 orthogonal axes $N_1 + N_2 + N_3 = 1$). Thus, high intrinsic-susceptibility minerals like magnetite have mean external susceptibilities of around 3 SI, with anisotropy controlled dominantly by particle shape.

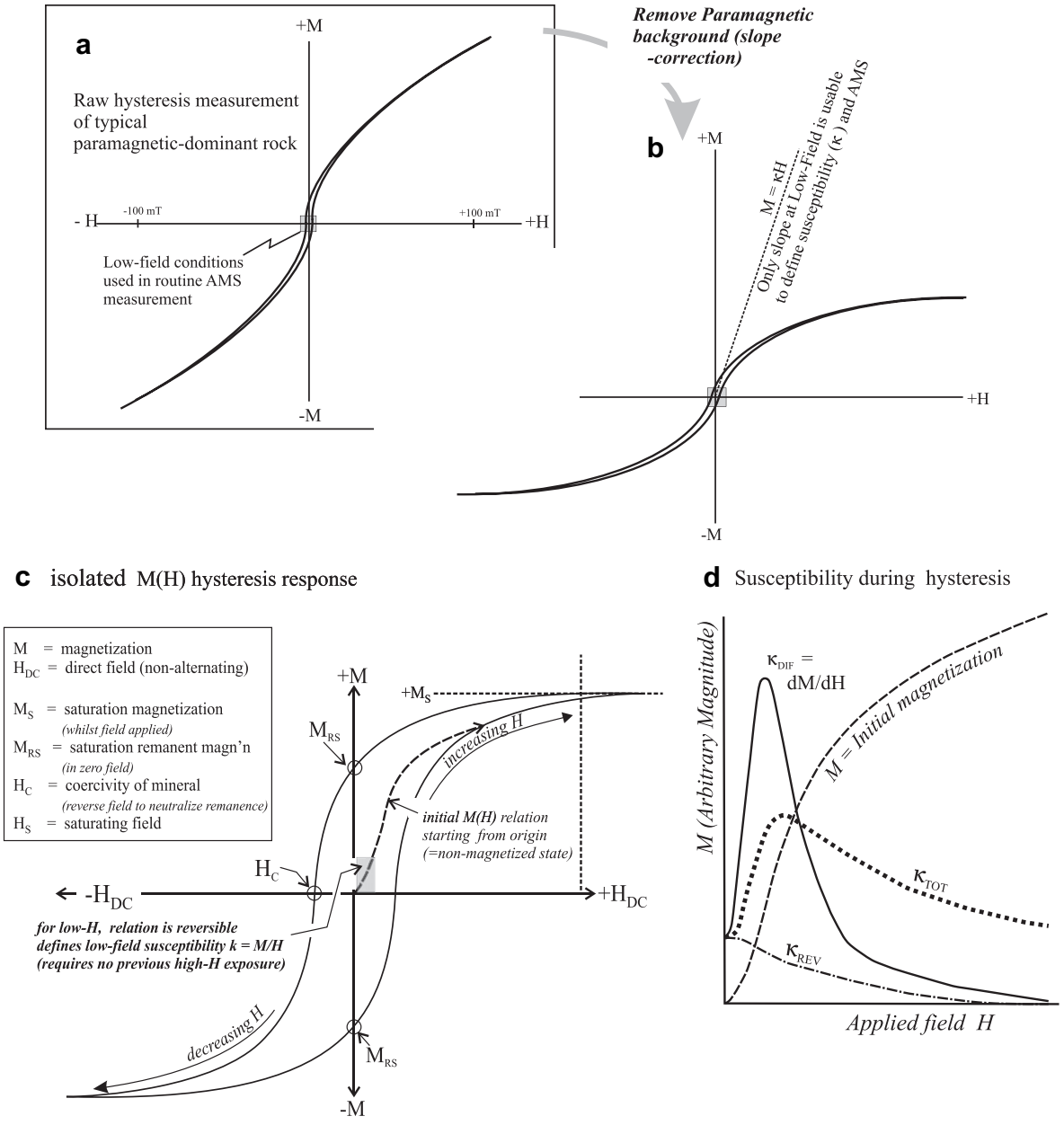

Fig. 3. (a)Typical hysteresis curve for a rock with *RBM* in paramagnetic matrix. To ensure accurate AMS measurements, applied fields must be constrained to low values (shaded near origin). (b) The hysteresis characteristics of the *RBM* may be isolated by subtracting the background paramagnetic slope. (c) Details of the hysteresis behaviour of the *RBM*. (d) Complexity of ferromagnetic susceptibility. The initial magnetization curve, starting from a demagnetized state, has a moderate slope in low fields (initial susceptibility or low-field susceptibility). The slope increases in fields strong enough to produce irreversible magnetization changes (i.e., fields comparable to the coercivity of the material). Slope decreases on approach to saturation. Because of nonlinearity and irreversibility, susceptibility can be defined in several ways. Total susceptibility (κ_{tot}) is simply the ratio M/H; differential susceptibility (κ_{dif}) is the slope of the initial magnetization curve. Reversible susceptibility (κ_{rev}) is the slope of a minor loop obtained by interrupting the initial magnetization process and reducing the field slightly before resuming. In sufficiently low fields these susceptibilities all have the same value.

M and H_d are in general non-uniform in arbitrarily-shaped grains, but they are uniform in ellipsoidal grains. Stoner (1945) calculated N for uniaxial ellipsoidal grains (i.e., grains having rotational symmetry about a unique axis). For such grains the shape can be described by the dimension ratio $\beta = d_p/d_e$ = polar axis/equatorial axis. Limiting cases are $(N_p, N_e) = (0, 0.5)$ for needle-like grains, (1/3, 1/3) for spheres and (1,0) for flat disks (Fig. 5b). For high intrinsic susceptibilities, the observed directional and mean susceptibilities change systematically with grain shape; the self-demagnetization limit in SI units is $(\kappa_p, \kappa_e) = (\kappa_i, 2)$ for needles, (3, 3) for spheres, and $(1, \kappa_i)$ for disks (Fig. 5c). The grain-scale AMS ratios due to self-demagnetization thus depend on both intrinsic susceptibility and grain shape, and may reach P values as high as 10 or more. For dimension ratios that are not too extreme ($0.1 < \beta < 10$) and sufficiently high κ_i, the AMS ratios are closely equal to the dimension ratios (Fig. 5d). Thus, conveniently, the susceptibility ellipsoid has the same orientation and aspect ratio as the grain itself. For a population of grains with dominant shape anisotropy, the measured AMS represents a composite of grain shapes and preferred orientations (as observed e.g., by Grégoire et al., 1995, 1998).

Stable single-domain (SSD) grains are an interesting and important special case. Because a stable SD grain is magnetized to saturation along its easy axes, even in the absence of an applied field, it has essentially zero low-field susceptibility parallel to its

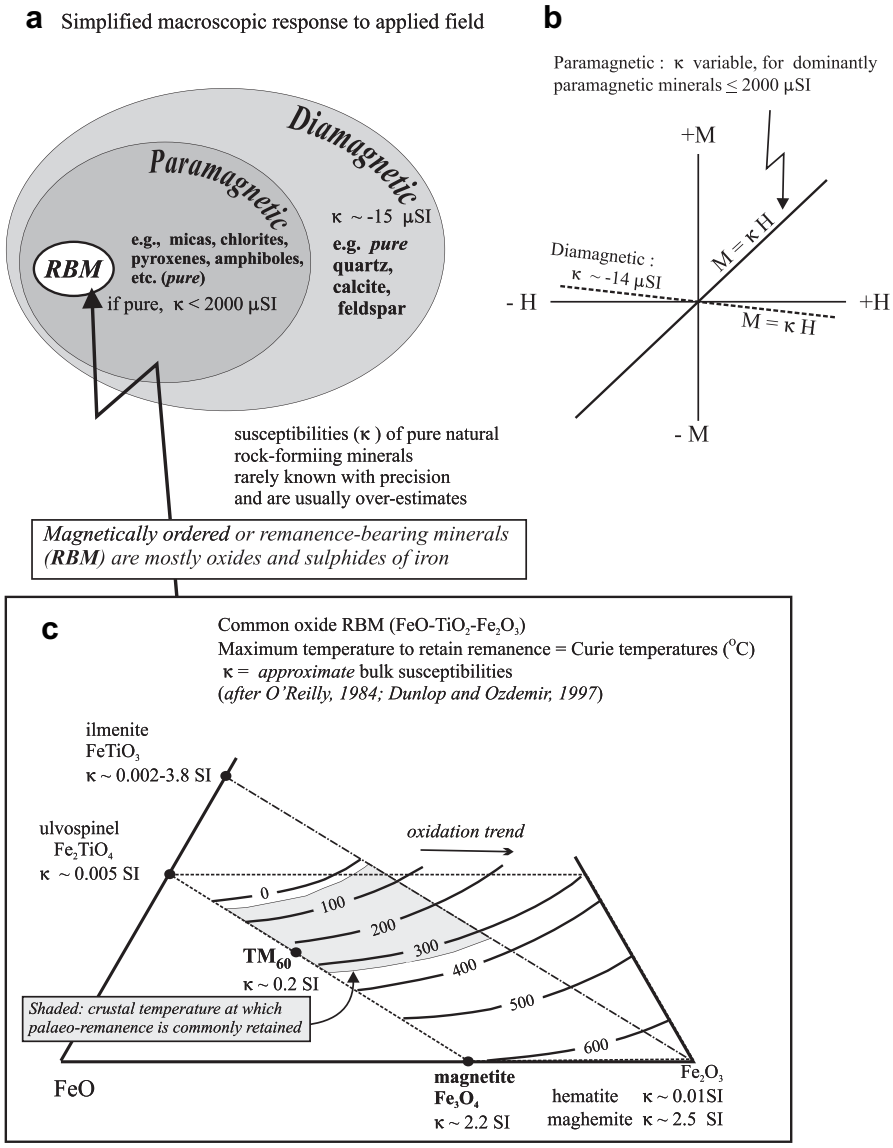

Fig. 4. (a) The three broad categories of magnetic response. *RBM* = remanence-bearing minerals. (b) The ephemeral paramagnetic or diamagnetic responses to an applied field that characterize most pure rock-forming "matrix" minerals. (Paramagnetic materials include a diamagnetic component that is usually negligible in comparison). (c) Some details of the important accessory minerals of the Fe–Ti–O system; note some compositions preclude remanence at temperatures available in the earth.

long dimension. Weak perpendicular fields, however, are able to rotate the grain moment slightly away from the easy axis, and thus there is a finite susceptibility normal to the easy axis. This "single-domain effect" (Potter and Stephenson, 1988) is an important mechanism introducing a component of "inverse AMS" in magnetite-bearing rocks. Other high susceptibility minerals that may show an inverse-AMS include maghemite (Borradaile and Puumala, 1989), suitable titanomagnetite compositions and greigite (Aubourg and Robion, 2002). Anisotropy of remanence, in contrast is "normal" (i.e. the shape of the magnetic ellipsoid resembles that of the grain, at least qualitatively) for SD as well as for MD grains (Stephenson et al., 1986).

3.1.2. Magnetocrystalline anisotropy

For paramagnetic and antiferromagnetic materials, magnetization intensities are too low for self-demagnetization to be important. Instead, crystallography mainly controls magnetic anisotropy through anisotropic exchange interactions. Magnetocrystalline anisotropy also plays an important role in the behavior of ferrimagnets with low crystal symmetry (e.g., monoclinic pyrrhotite). For paramagnetic minerals, the susceptibility ratio $\kappa_{max}/\kappa_{min}$ rarely exceeds 1.4 (see summary in Borradaile and Jackson, 2004) but is often strongly influenced by ferromagnetic inclusions (Borradaile, 1994; Borradaile and Werner, 1994; Lagroix and Borradaile, 2000a). Ferromagnetic minerals with strong magnetocrystalline anisotropy, including pyrrhotite (Martin-Hernandez et al., 2008) and hematite (Hrouda, 2002a,b), have larger reported P ratios, extending into the range 10–100.

For most minerals, there is a strong (albeit imperfect) correspondence between crystal habit and AMS (Figs. 6 and 7); in general, crystallography determines both AMS and grain-shape. Chain and sheet silicates form elongate and platy grains, respectively, and are commonly paramagnetic. Generally, they have κ_{MAX} sub-parallel to their long dimension and κ_{MIN} at a high angle to a basal c-plane. This approximation suffices for petrofabric interpretations with most chlorites, clays and micas. However, we should consider the *shape-symmetry-AMS* angular relationships individually for each pure mineral.

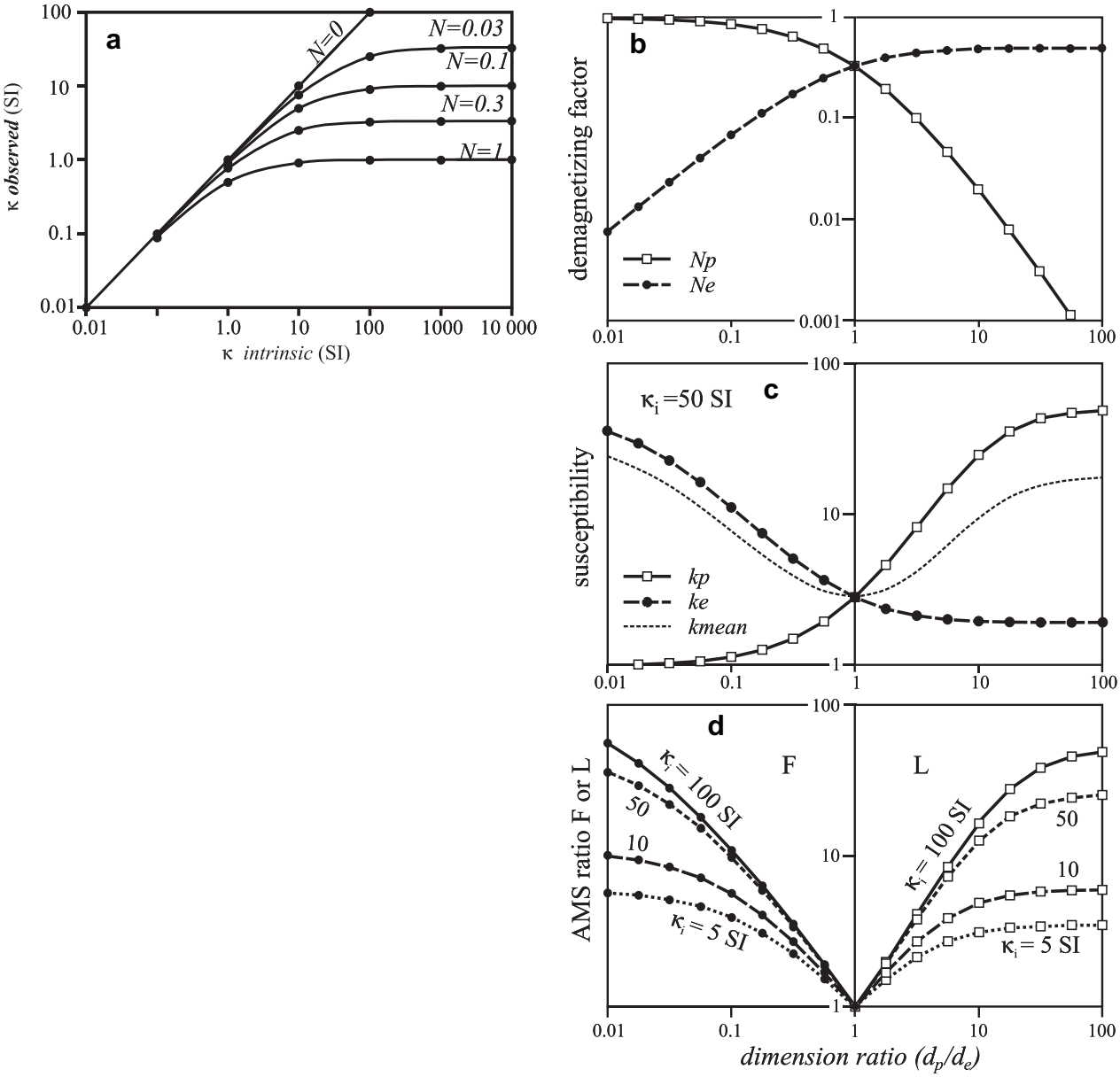

Fig. 5. (a) Measured susceptibilities are always less than or equal to the intrinsic susceptibility due to the "screening" effects of self-demagnetization, quantified by the demagnetizing factor N (a tensor whose principal magnitudes sum to 1 in SI units). Self-demagnetization becomes significant for intrinsic susceptibilities greater than about 0.1 SI. Observed susceptibility reaches a limiting value of $1/N$ ($\sim$3 SI) for high intrinsic susceptibilities. (b–d) Shape anisotropy results from differences in N in different orientations; for ellipsoidal particles with rotational symmetry around a polar axis, the demagnetizing factors along the polar (N_p) and equatorial (N_e) axes can be calculated from the dimension ratio d_p/d_e (b), and the directional susceptibilities (c) follow from N and κ_i.. (d) For low to moderate dimension ratios (0.1 to 10), the AMS ratios are approximately equal to the corresponding dimension ratios (i.e., $L = \kappa_p/\kappa_e \sim d_p/d_e$ and $F = \kappa_e/\kappa_p \sim d_e/d_p$).

"Inverse" anisotropy is a feature of uncommon paramagnetic minerals. Tourmaline, for example, is *c*-elongate but the *c*-axis corresponds with κ_{MIN}, and cordierite may also have inverse AMS (Rochette et al., 1992). Unfortunately, only a few studies relate AMS to crystallography and composition for common rock-forming, stoichiometrically-variable matrix minerals such as amphibole and phyllosilicates (Borradaile and Werner, 1994; Friederich, 1995; Martín-Hernández and Hirt, 2003).

3.1.3. Magnetostriction and stress effects

Magnetization produces small spontaneous strains (e.g., of order 10^{-5}) in most ferromagnetic materials, which may expand or contract in the direction of magnetization (positive or negative magnetostriction, respectively) (Flanders, 1974; Klerk et al., 1977; Moskowitz, 1993). Conversely, applied stresses produce a magnetoelastic anisotropy that increases or reduces the energy associated with magnetization in the direction of compressive or tensile stress, according to the sign of the magnetostriction coefficients for the material. For positive isotropic magnetostriction, remanent magnetization rotates away from the orientation of an applied compressive stress, and susceptibility decreases along the load axis; these effects may be transient, disappearing on removal of the applied stress, or permanent, depending on stress magnitudes and material properties (Nagata, 1970; Revol et al., 1977; Appel, 1987).

3.2. Whole-rock anisotropy

Of course rocks are always composed of mixtures of minerals, each of which contributes to low-field susceptibility. Neglecting (for the moment) caveats related to magnetostatic interactions

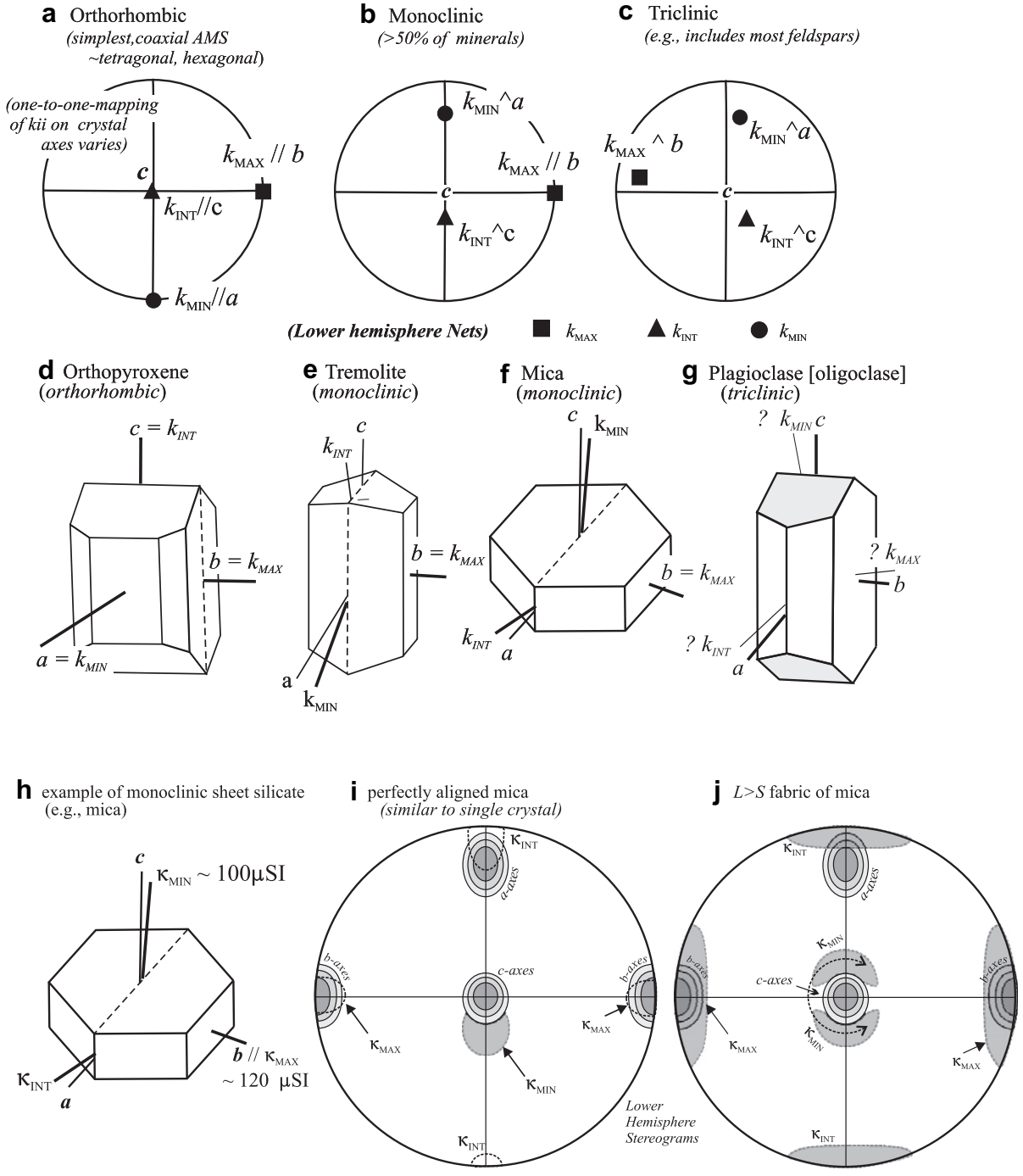

Fig. 6. (a–g) For most pure minerals, the orientation of principal susceptibility axes is crystallographically controlled. Whereas AMS is a tensor and its axes must be orthogonal, the crystal axes will only be orthogonal in systems of high symmetry (e.g., cubic, tetragonal, orthorhombic). Therefore, since most rock-forming minerals are monoclinic or triclinic there may be no close correspondence in orientation between AMS axes and crystal axes. (h) Fortunately, a large number of minerals useful in petrofabrics are monoclinic, with one AMS axis corresponding to a crystal axis, and relatively small angular discrepancies between the other two AMS axes and their closest crystal axis. (i) If perfectly aligned, such crystals, e.g., phyllosilicates, produce an imperfectly aligned AMS fabric. (j) When the crystals have some variation in orientation, the AMS axes become further disoriented.

among mineral grains, the susceptibility of a rock specimen is simply the sum of individual mineral contributions:

$$\kappa_{\text{specimen}} = \sum \kappa_i f_i \quad \text{where} \quad \sum f_i = 1 \tag{8}$$

where f_i is the volume fraction in the specimen of mineral phase i and k_i is the volumetric susceptibility of the pure phase. The mixing equation can include mineral classes (e.g., diamagnetic, paramagnetic, and ferrimagnetic) as well as individual minerals. When dealing with anisotropy we are concerned with tensors rather than scalars but we can still write

$$[\kappa]_{\text{specimen}} = \sum [\kappa]_i f_i, \quad \sum f_i = 1 \tag{9}$$

where the mineral tensors being summed in turn represent summations over large numbers of individual-grain tensors, each expressed in the specimen coordinate system. It is clear that the susceptibility tensor for a geological specimen depends on the

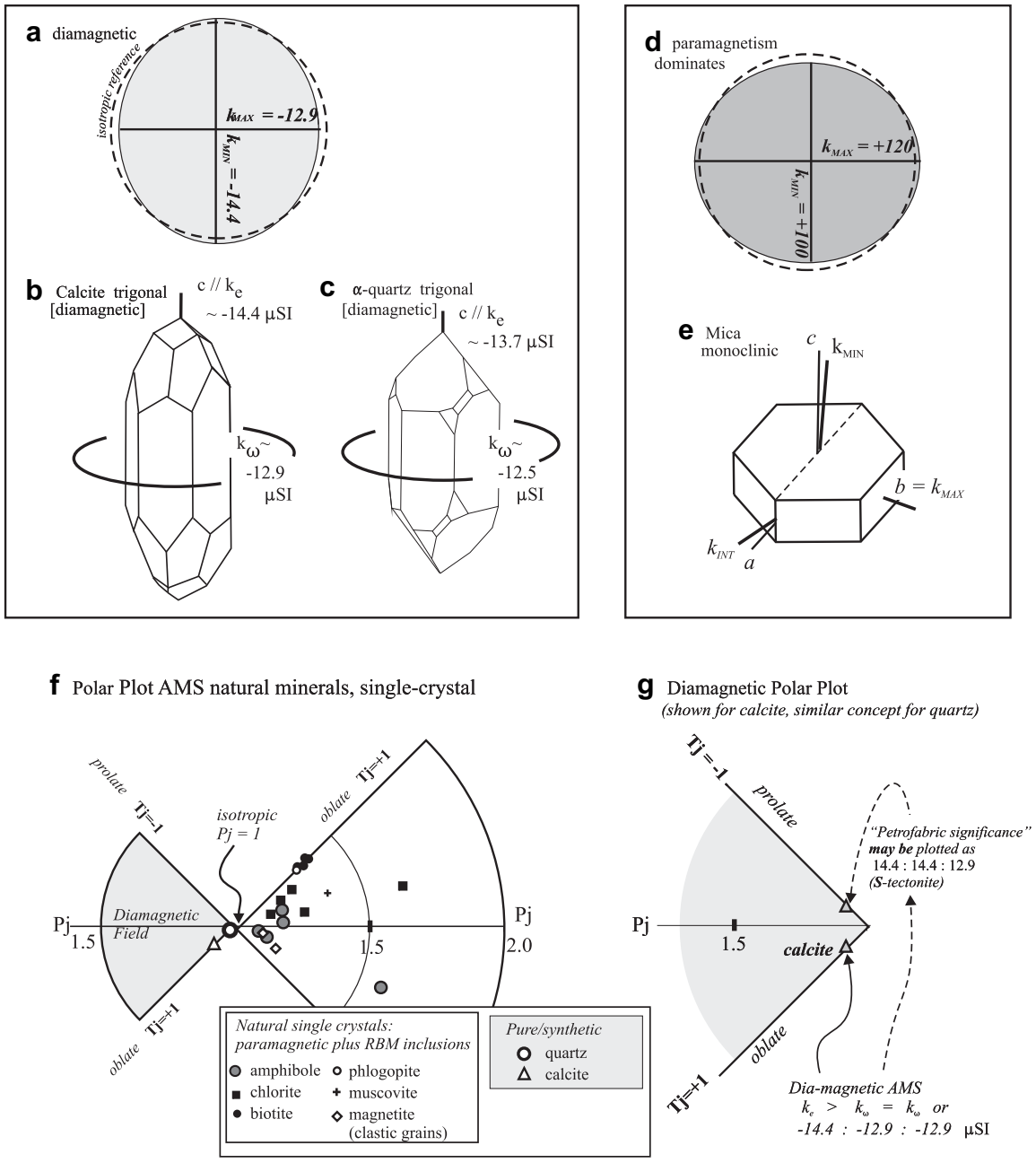

Fig. 7. (a–c) Diamagnetic minerals, such as calcite and quartz have an AMS ellipsoid for which the longest (most negative susceptibility axis) corresponds to the c-axis. The c-axes also align normal to schistosity due to basal glide under most tectono-metamorphic conditions. (Thus, quartz and calcite produce "inverse" fabrics, for a very different reason than SD magnetite, of course.) Ferroan calcites have positive susceptibility with a maximuim along the c axis and thus also have "inverse" AMS. (d–e) Paramagnetically dominant rock-forming minerals, such as phyllosilicates may mix with quartz and calcite to form mixed or blended fabrics with principal susceptibility axes not simply related to petrofabric. (f–g) The polar plot for AMS requires a switched field on which to plot diamagnetic minerals.

minerals present, their relative abundances, their specific susceptibilities, their grain-scale anisotropies, and their orientation distributions (e.g., Owens, 1974; Jezek and Hrouda, 2004). The automatic averaging over large numbers of grains is one of the chief advantages of AMS for petrofabric characterization, although quantitative interpretations are hampered by the dependence on mineralogic abundances and on the unknown weighting factors *f*.

For this reason, significant efforts have been made to separate the AMS contributions of different minerals or classes of minerals, using a variety of sophisticated laboratory techniques. These include high-field hysteresis or torque measurements, variable-temperature susceptibility measurements, and studies of anisotropic remanence (Ihmlé et al., 1989; Borradaile and Werner, 1994; Hamilton et al., 2004; Kelso et al., 2002; Ferré et al., 2004; Hrouda et al., 1997; Martín-Hernández and Hirt, 2001, 2003, 2004; Martín-Hernández and Ferré, 2007; Richter and van der Pluijm, 1994; Parés and van der Pluijm, 2002a,b). Remanence-based methods of anisotropy measurement focus exclusively on the ferromagnetic (*s.l.*) minerals, and they may be even more selectively focused through the use of partial remanences that target specific ranges of coercivity or blocking temperature (Fuller, 1963; Daly, 1967; McCabe et al., 1985; Jackson, 1991; Potter, 2004).

Moreover, as discussed later in this paper, the AMS of deformed rocks almost always represents the integrated effects of a complex

thermochemical/mechanical history: discrete sub-fabrics may form at different stages, by different mechanisms, involving different mineral and/or grain-size fractions, accompanied by metamorphism, mineral transformations, recrystallization, etc. Differential techniques of magnetic fabric analysis may resolve certain details of complex tectono-metamorphic histories in ways that are not possible by traditional structural or strain analysis (see examples in Borradaile and Jackson, 2004).

3.3. Mineral-specific magnetic fabric components

Anisotropy in pure paramagnetic minerals is an intrinsic property, independent of particle size and shape, and practically independent of applied field strength. This invariance of mineral-specific grain-scale anisotropy for pure grains makes it attractive to consider straightforward quantitative relationships between AMS and PCO (e.g., Jezek and Hrouda, 2004). Several x-ray and/or neutron texture goniometry studies now document a correspondence between paramagnetic phyllosilicate orientation and AMS (Richter et al., 1993a,b; Chadima et al., 2004; Cifelli et al., 2009). Paramagnetic AMS is isolated in anisotropy measurements at low temperature (amplifying the paramagnetic susceptibility) and/or in high-fields (reducing or eliminating ferromagnetic contributions). However, even in such ideal cases, the AMS-PCO relationship may show surprising complexities and the technology is challenging (e.g., Debacker et al., 2009).

Fe-Ti oxides and sulfides are worthy of special mention due to their high susceptibilities (κ up to a few SI) and their highly variable grain-scale anisotropies, although they generally occur as accessory or trace minerals. Because of these factors, the RBM contribution to AMS can swamp that from the rock matrix. This is however not a general rule and in some sense its importance was exaggerated in early AMS studies at the expense of the rock-forming or matrix minerals. Now, we appreciate the importance of mafic rock-forming silicates (Rochette, 1987a; Borradaile, 1987, 1988), and the need to quantify the relative contributions to κ and to AMS from each mineral present. Nevertheless, ferromagnetic (s.l.) minerals deserve special attention because they exhibit a much wider variety of behavior than disordered minerals do in response to applied fields, temperatures and other experimental variables, and this variety provides us with a versatile set of tools for "deconstructing" magnetic fabrics. Moreover, due to their generally low relative abundance and their chemical differences, ferromagnetic oxide and sulfide minerals invariably experience deformation and metamorphism differently than the more abundant silicate minerals do.

Another phenomenon exclusively associated with ferromagnetic (s.l.) particles is "distribution anisotropy" (Hargraves et al., 1991; Stephenson, 1994; Cañon-Tapia, 1996; Muxworthy and Williams, 2004; Gaillot et al., 2006), in which anisotropic magnetostatic interactions among grains affect bulk sample properties.. An externally-applied field produces an induced magnetization in each grain but their resultant fields increase the effective susceptibility of the population. The spatial distribution of the grains, as well as their orientation distribution and individual-grain anisotropies, determine the collective AMS of the group. This may in some cases cause inverse magnetic fabrics, even when the individual-grain anisotropies are normal.

If we suspect magnetite is contributing to κ and to AMS, some other aspects should be considered. *First*, one must know whether the magnetite grains are independent, their alignment directly controlled by the structural mechanism acting on their shape. Alternatively, if the magnetite is included or attached to rock-forming minerals, its contribution to AMS will be a complex interaction with the structural process that aligned the host minerals. *Second*, magnetite's AMS will mostly be due to grain-shape. Grain-shape alignments are unlikely to have the same causes as the crystallographic alignments of minerals in deformed and metamorphic rock. They also behave differently in magmatic flow environments. In rocks with a sedimentary origin, the paleo-field may align magnetite during deposition, although this effect is generally very weak. *Third*, we should be able to infer from structural history if the magnetite is highly strained or annealed. This is important since dislocation-density influences κ and AMS, and in some cases the reliability of their measurement. *Fourth*, it is attractive to assume that petrographic measurements of magnetite-shape should be correlatable with AMS. Apart from ignoring the aforesaid caveats, some optimistic studies along these lines neglected sampling effects especially the deceptive cut-effect on fortuitous grain aspect ratio in thin-section, and few were statistically sound. Other RBM such as hematite and pyrrhotite, with strong magnetocrystalline anisotropies (Hrouda, 2002a,b; Martin-Hernandez et al., 2008), may possess complex polycrystalline structure in metamorphic rock and the ways in which this may complicate the relationships between the orientations of principal susceptibilities and crystal axes are areas for future study. With hindsight, it is evident from first principles that the contribution of high-κ accessory minerals (not all of which are RBM) must be treated separately from the rock-forming paramagnetic and diamagnetic minerals in all aspects of magnetic fabric studies (Figs. 3 and 4).

Remanence-based methods (Potter, 2004) are sensitive exclusively to the ferromagnetic minerals and their statistical characteristics (relative abundances, magnetizability, grain-scale anisotropies and PCO/PDO). These include anisotropy of anhysteretic remanent magnetization (AARM) (McCabe et al., 1985), anisotropy of isothermal remanence (AIRM) (Fuller, 1963; Daly and Zinsser, 1973; Stephenson et al., 1986) and anisotropy of gyroremanence (AGRM) (Stephenson, 1993; Stephenson and Potter, 1987). Thermal magnetization methods are used less often because they tend to alter the mineralogy and/or magnetic properties. With isothermal methods, applied field strength and mineral coercivity are key parameters. The ARM magnetizing process involves a weak (50–100 microT) DC field superposed on a strong AC field that decays with time from a maximum of 100–200 mT depending on the instrument used. ARM therefore effectively magnetizes "soft" ferrimagnets (e.g., magnetite) but is less efficient at magnetizing hard antiferromagnets, with coercivities exceeding the maximum AC field. Partial ARMs (pARMs) are imparted by applying the DC field over only a selected portion of the AC decay, thereby magnetizing a discrete coercivity fraction (which may represent a range of grain sizes or grain shapes). AIRM involves DC fields alone, and therefore much stronger fields are accessible (up to a few Tesla), sufficient to produce significant magnetization of hematite, goethite, and other "hard" magnetic phases. Strong-field IRM is rarely a linear function of applied field, and therefore the tensor calculations used for AMS and AARM are not valid for AIRM. Nevertheless, semi-quantitative magnetic fabric characterization is useful in many cases. AGRM is in some ways analogous to torque-based AMS measurement: it is sensitive to directional differences in OD and yields a deviatoric tensor. GRM is acquired in an AC field with or without a superposed DC bias field, and is preferentially carried by fine (single-domain) ferrimagnetic particles; its anisotropy therefore reflects the PDO of those particles.

In conclusion, all minerals have a diamagnetic component but for practical purposes only calcite, quartz and some feldspar may be abundant and pure enough for this to be important. Most rock-forming minerals are paramagnetic and may provide possible structural interpretations of AMS if their orientation distribution and crystal-susceptibility relations are simple (Fig. 6). High

susceptibility minerals such as magnetite have AMS orientations controlled by shape. Single domain magnetite may show an inverse AMS and the question of "inverse" and "normal" magnetite-fabrics features prominently in the literature. Magnetite-inverse fabrics, although rare, may propose paradoxical tectonic interpretations, for example with κ_{MIN} parallel to grain long axis. However, we should note that in low susceptibility rocks, sub-equal contributions from diamagnetic and paramagnetic sources may also produce another type of "inverse" fabric for quite different reasons (Fig. 7). The matter simply concerns the fact that diamagnetic minerals such quartz and calcite have negative susceptibilities so that their "maximum" value is actually most negative. The polar plot facilitates the interpretation of such fabrics. Ferroan calcites have positive susceptibility with a maximuim along the c axis and thus have "inverse" AMS (Rochette, 1988). The second aspect of this problem is that crystal plastic processes commonly use a basal glide mechanism which aligns c-axes. For micas, this is helpful for structural interpretation since it approximately aligns κ_{MIN} with their c-axes (Fig. 6h–j). Unfortunately, the situation is more complex for calcite and quartz where basal glide mechanisms (approximately) align the most negative (κ_{MIN}) susceptibility axis with their c-axes, perpendicular to rock-foliation (Fig. 7).

Diamagnetic-dominant minerals complicate plotting AMS shapes. Dominantly paramagnetic specimens have oblate and prolate fields switched with respect to those of diamagnetic specimens. This is shown with respect to some single mineral AMS values (Fig. 7f–g). In general, interpretation of AMS must always include knowledge of the metamorphic conditions. Alignment by crystal plastic processes or neo-crystallization will produce strong PCOs and a strong correlation of AMS axial orientations with crystallographic/mineral orientations. Preferred dimensional alignments (PDOs) due to mechanical moments turning objects towards the maximum extension direction will generally produce a lower correlation between the orientations of crystal axes and crystallographic AMS axes with structurally significant axes.

4. AMS and crystallography: symmetry considerations

Physicists early noted that certain minerals showed anisotropic susceptibility (Voight and Kinoshita, 1907) using torque-magnetometry for anisotropy (AMS) and fundamental measurement techniques for κ. Early in the 20th century, the tensor nature of physical properties for ideal crystals was appreciated as was the influence of crystal-symmetry on the anisotropy of physical, lattice-scale properties (Nye, 1957). Fortunately, AMS is represented by a second-rank tensor, visualized as a magnitude ellipsoid for our convenience, and for analogy with ellipsoids describing orientation distributions or finite strain in structural geology. The orientations of the orthogonal principal susceptibilities (axes of the AMS magnitude ellipsoid) are constrained in their angular relationship to crystallographic axes although the relative magnitudes of the susceptibility axes are not predictable from crystallography. For orthorhombic and tetragonal crystals, principal susceptibilities and crystal axes are parallel; they show a one-to-one mapping of orientations. Some rock-forming minerals, such as quartz and calcite have high symmetry and an important axis [*c*] and a basal plane correspond to the symmetry of an AMS ellipsoid. Unfortunately, most rock-forming minerals are of lower symmetry; for example about 50% of silicates are monoclinic in which only one axis (usually *b*) corresponds to one of the principal susceptibilities. In triclinic crystals no susceptibility axis may be parallel to a crystal axis. A further subtle point is that the symmetry of anisotropic physical properties, including susceptibility, must include that of the crystal symmetry point-group. Thus, the symmetry of physical properties commonly exceed that of the crystal (Nye, 1957). The best expected correspondence between principal susceptibility axes and crystal axes is only obtained within the limits of measurement for pure minerals (Figs. 6 and 7).

Even if a polycrystalline aggregate is mono-mineralic and has a perfect ("saturation") alignment of the crystal in question, its AMS ellipsoid will not be related directly to the axes of the alignment mechanism, nor in a simple way to the preferred crystallographic orientation (PCO). This is because most rock-forming minerals are monoclinic or triclinic so that at least one AMS axis is inclined to a crystal axis (Fig. 6h). Since the fabric will be imperfect, the dispersion of susceptibility axes must be even less favourable (Fig. 6i–j). There have been successful hypothetical mathematical solutions relating ODs to AMS but these are restricted to grains ("minerals") that have orthorhombic dimensional symmetry corresponding to their AMS ellipsoid and simple finite strain history (Hrouda and Schulmann, 1990; Jézek and Hrouda, 2002, 2004; Henry, 1983, 1989, 1990, 1992; Henry and Daly, 1983; Owens, 1974) and some extensions to natural examples with suitable allowance for metamorphic effects (Henry, 1990). Clearly, in a polymineralic rock with a PCO fabric somewhere in the L-S range, possibly even with each mineral in a different part of the L-S range we may at best only expect the rock's AMS to be a complex blend of the contributions of different minerals (Eqs. (8) and (9)). Fortunately, in many rocks only two or three minerals control the distribution of κ and of AMS and some simple data treatments discussed below permit us to analyze the sources of remanence.

Thus, as a general rule, AMS intensity degree (*Pj*) must underestimate the strength of the crystal orientation-distribution. However, the *orientations* of the principal axes of AMS are invariably more consistent and more readily correlated with structural features such as finite strain axes, flow-axes or some axis of kinematic importance such as a bedding-cleavage intersection lineation. The shape of the AMS ellipsoid (*Tj*) is influenced by the grain-scale anisotropy shape of the dominant mineral (i.e., most abundant and high-κ) in the rock and its orientation distribution. Thus, it need not necessarily correspond to the shape of the dominant orientation distribution in the *L-S* scheme. For example, some slates have $S > L$ strain ellipsoids but may have ($Tj < 0$) AMS ellipsoids if their AMS is partly controlled by grains with a well-defined uniaxial crystal-AMS (e.g., amphibole) or uniaxial shape-AMS (prolate magnetite grains).

5. AMS data for individual minerals

Magnitudes of κ, κ_{MAX}, κ_{INT} and κ_{MIN} have been determined in numerous specialized studies for suitable rock-forming minerals and important iron-bearing accessories (e.g. see Borradaile and Jackson, 2004). Unfortunately, the precise orientations of κ_{MAX}, κ_{INT} and κ_{MIN} with respect to crystal axes or crystal habit are less well documented, despite theoretical expectations (e.g., Figs. 6 and 7). Values of κ, and especially AMS published for specific mineral examples must not be accepted as standard values since stoichiometry and impurity-content vary. Such values serve only as guidelines in the qualitative interpretation of AMS as a combination from contributory minerals.

Structural interpretation of tectonite-AMS requires some knowledge of the partitioning of κ and AMS between different minerals. Sophisticated supplementary experimental methods including hysteresis (Fig. 3), measurements in high field (Figs. 8 and 9), at different frequencies, and different temperatures, paleomagnetic techniques, acquisition and demagnetization of remanence, anisotropy of remanence may resolve these issues. However, in most situations of interest to the structural geologist the raw data itself, obtained solely with the AMS instrument (i.e. κ and the magnitudes and orientations of κ_{MAX}, κ_{INT} and κ_{MIN}) provide sufficient

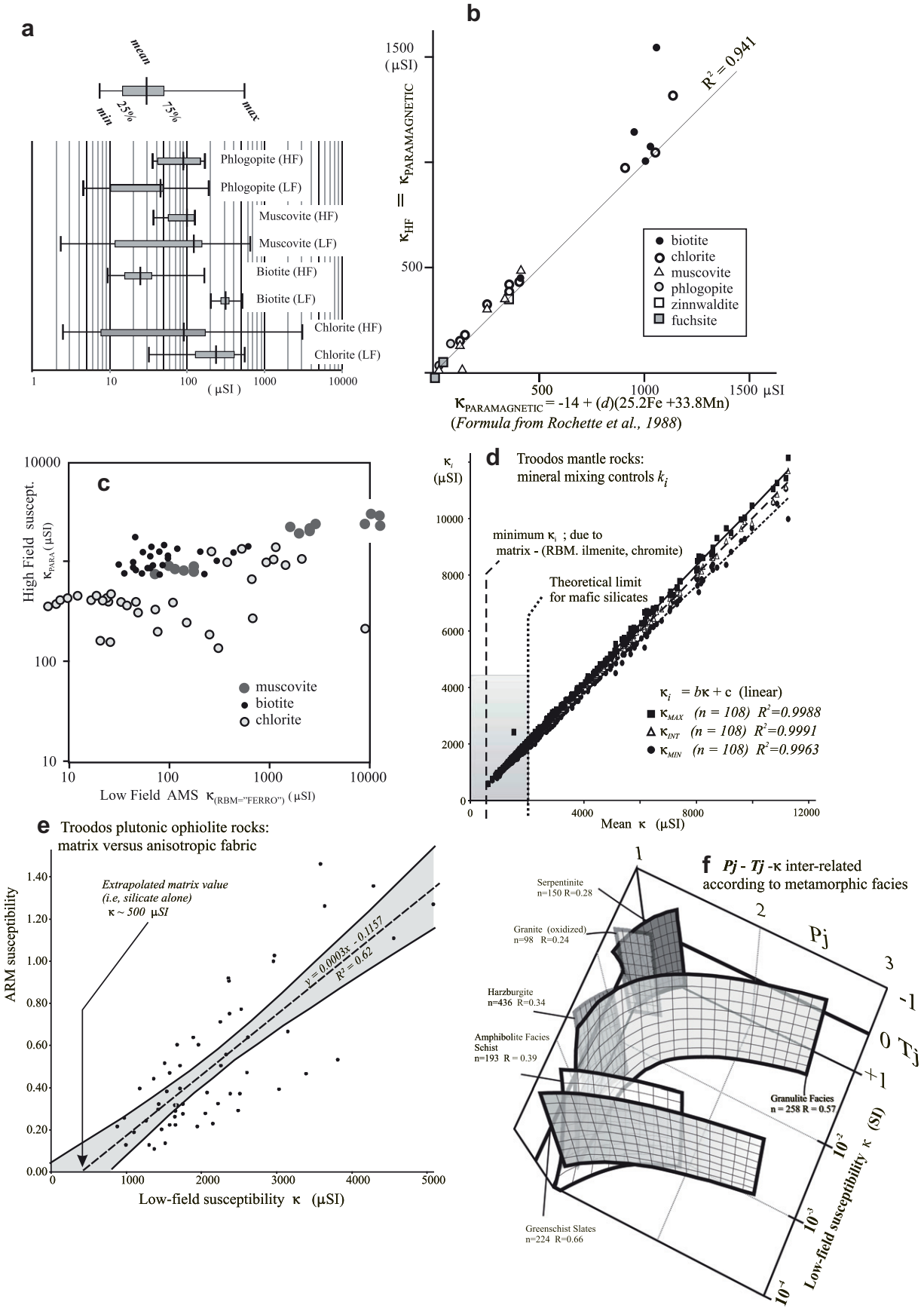

Fig. 8. (a) Single mineral susceptibility varies widely due to RBM inclusions (maximum pure silicate is 2000 μ-SI). (b) High field-susceptibility for the paramagnetic (lattice) component of susceptibility depends on lattice composition . (c) Thus, high-field susceptibility is independent of low-field AMS that is strongly dependent on RBM concentrations. (d) Individual principal susceptibility magnitudes may depend linearly on bulk susceptibility. (e) Correlation of ARM on bulk susceptibility for the same rocks shows influence of RBM. (f) Mutual dependence of Pj, Tj and κ shows that AMS is compositionally controlled (Borradaile and Lagroix, 2001; Borradaile and Werner, 1994; Nakamura and Borradaile, 2004).

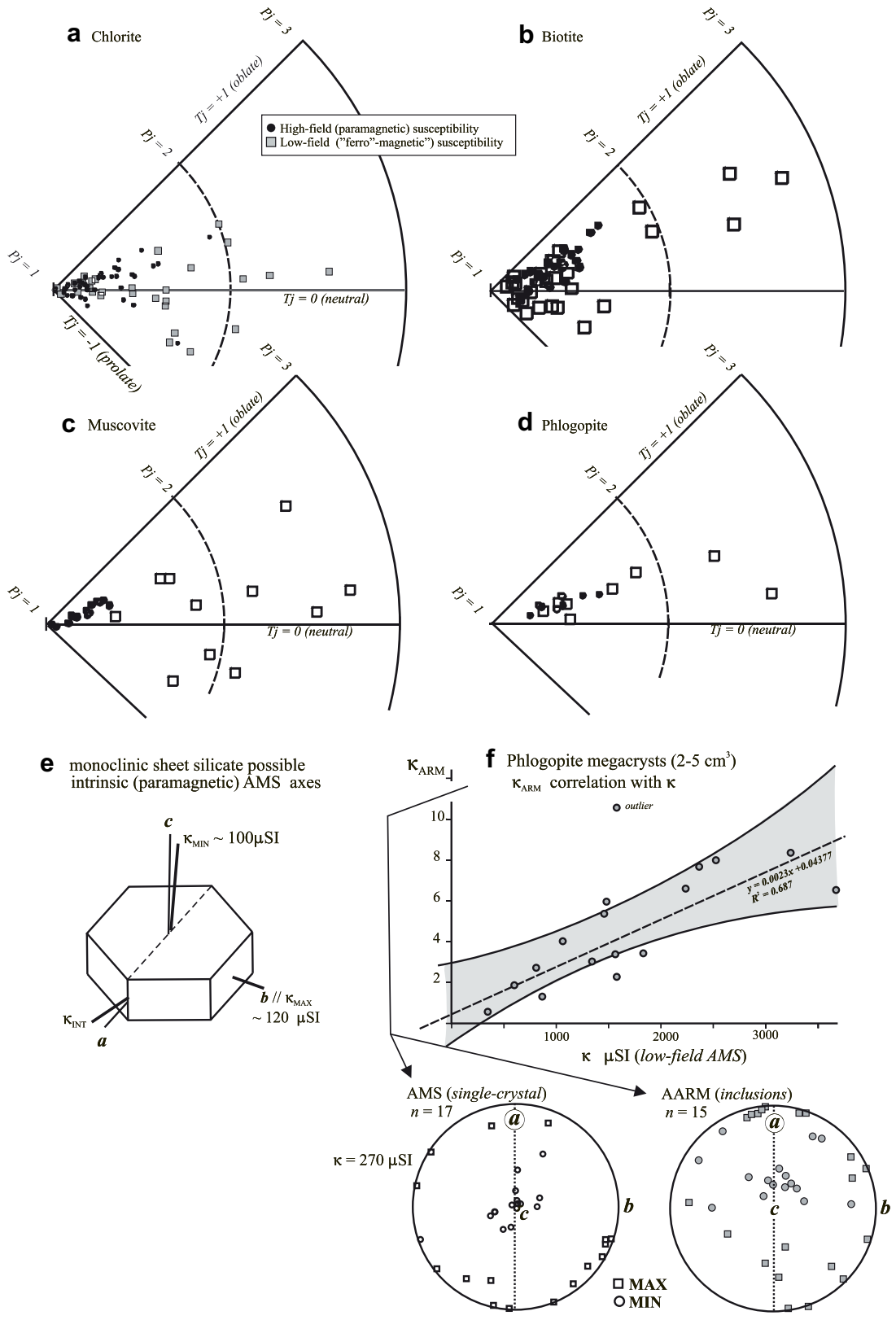

Fig. 9. (a–d) AMS for typical phyllosilicate from metamorphic rocks. (e) Typical mismatch of orthogonal AMS axes with monoclinic crystal axes for a phyllosilicate. (f) Dependence of ARM on low field susceptibility shows importance of RBM inclusions. Stereograms beneath show AMS and AARM in crystal-coordinates.

information to understand the mineralogical and sub-fabric contributions to AMS. Commonly, this is because most simple structural and metamorphic suites have rocks in which two different minerals, or two different sub-fabrics control κ and AMS.

Fortunately, for an approximately homogeneous sample suite, with some variation of κ_{MAX}, κ_{INT} and κ_{MIN} against κ, there is normally some underlying control of AMS by the rock-κ (Henry and Daly, 1983; Rochette, 1987a; Borradaile and Sarvas, 1990; Johns and

Jackson, 1991). Some recent data illustrate the point here; usually some small degree of fabric/strain variation may show a nearly linear distribution against κ (Figs. 8d and 12c). Here as is commonly the case, larger differences between κ_{MAX}, κ_{INT} and κ_{MIN} (larger *Pj*) usually occur at high- κ values, indicating that some high-κ mineral and more anisotropic mineral controls AMS. The suite comprises plutonic ophiolite rocks with a modest L-S fabric with a matrix of aligned pyroxene. The high- κ petrofabric element is known to be magnetite but chromite is also occasionally present. Measurements of anhysteretic remanence confirm that magnetite is present and dictating the relationship (Fig. 8d–e). Such AMS-data explorations substantiate relations between anisotropy and κ, without further sophisticated experiments. Clearly AMS (considered as *Pj* but even identified in data lists as (κ_{MAX} / κ_{MIN}) depends on mineral abundances and is unrelated quantitatively to fabric-strength or finite strain. AMS shape parameters (*Tj*) may be more useful than *Pj* since they may share the sense of symmetry of the overall petrofabrically controlled PCO. Compositional control on AMS is especially obvious when κ, (*Tj*) and (*Pj*) correlate in three-dimensions (Fig. 8f) (Nakamura and Borradaile, 2004). Despite low correlation coefficients, those trend surfaces are all significant at the 95% level due to the large sample-sizes. This emphasizes the notion that AMS is commonly compositionally controlled, not strain-controlled (Borradaile, 1987; Borradaile and Jackson, 2004).

Phyllosilicates are an important and strongly anisotropic component of tectonites and their contributions to AMS has been well documented (Borradaile, 1994; Borradaile and Werner, 1994; Borradaile and Sarvas, 1990; Johns and Jackson, 1991; Johns et al., 1992; Henry, 1990, 1992; Jackson and Borradaile, 1991; Zapletal, 1990). Most have a modest paramagnetic intrinsic lattice κ, which is similar to that of many tectonites such as slate or schist (Fig. 9) (Borradaile, 1994; Borradaile and Werner, 1994). Due to impurities, susceptibilities may exceed the theoretically predicted values from ideal chemical compositions (Rochette et al., 1992). High-field measurement (κ_{HF}) compared with the theoretically calculated value for κ (Fig. 8a–c) confirm the view that high- κ RBM inclusions mask the intrinsic lattice AMS. An alternative demonstration is that for most of the common micas we studied, low-field or normal susceptibility κ is variable and κ_{HF} is almost constant and independent of those values. The AMS of single crystals is measured with less precision than for specimens but we have previously done this by measuring in microscopically identified crystallographic directions and for small macroscopic crystals by using a special specimen holder that orients the crystal, somewhat like a microscope universal stage. Micas (as with many other rock-forming minerals) show rather high anisotropy degree (*Pj*). For the micas studied, *Pj* ranges commonly up to 2.0 (Figs. 9 and 10) whereas the schist and slate in which they dominate AMS commonly has $Pj \leq 1.2$ (Fig. 1e). Mica shape parameters (*Tj*) that will usually be in a similar shape-field to that of the parent tectonite (i.e. "flat" ellipsoid versus "constricted" ellipsoid shape). The AMS of individual crystals is naturally influenced by RBM inclusion and exsolution sub-grains, most of which are detectable only under SEM. Micro-hysteresis measurements of the single crystal micas show that the inclusions may respond generally with a SD or PSD structure (Borradaile and Werner, 1994; Borradaile, 1994).

Thus, intrinsic silicate AMS complicates the interpretation of AMS even for a perfect alignment of grains (Fig. 6h–j). The presence of RBM inclusions may complicate matters further (Figs. 9 and 10). In the example shown, AARM isolated the orientation distribution of RBM inclusions and, since κ_{ARM} correlates well with low field κ, RBM appear to control AMS. Plotted in crystallographic coordinates, their AMS axes are rather scattered which is disappointing for the purposes of studying the AMS of host-rocks (Figs. 9 and 10e). The orientation of the RBM inclusions (magnetite), isolated by AARM explains the imperfect correlation of AMS with crystal axes but it is noteworthy that the AARM axes suggest the RBM inclusions have some alignment due to the host lattice. This was corroborated by a previous palaeomagnetic study in which AF demagnetization showed the phlogopite contained RBM inclusions with a crystallographically significant demagnetization path (Borradaile, 1994).

Other rock-forming minerals useful in petrofabric studies of plutonic and metamorphic rock also commonly have κ far above the theoretical limit for mafic silicates (~2000 μSI) (Rochette et al., 1992). Again this can only be attributed to high-κ inclusions, usually of RBM and usually magnetite, but pyrrhotite, titanomagnetite, ilmenite, hematite, and chromite are also common high-κ (10^{-2}–10^{0} SI) inclusions (Hunt et al., 1995). Their presence is confirmed with suitable instrumentation that identifies some characteristic physical response, e.g., field-dependence (i.e. remanence), frequency-dependence or temperature-dependence (Borradaile and Jackson, 2004; Borradaile et al., 1992; Borradaile et al., 2008; Dunlop and Özdemir, 1997; Ellwood et al., 1993; Hrouda, 2002a,b; Hrouda, 2007, 2009; Hrouda et al., 1997a,b, 2000, 2002, 2009; Jackson et al., 1998; Parés and van der Pluijm, 2002a,b; Pokorny et al., 2004; Rochette and Fillion, 1988; Schmidt et al., 2007a,b; Worm, 1998; Vincenz, 1965). Simple examples of high-symmetry orthopyroxene and monoclinic serpentine, both well known for inclusions of magnetite, titanomagnetite or ilmenite are shown in Fig. 10a,b (Lagroix and Borradaile, 2000a; Renné et al., 2002). Thus, AMS axes may correlate rather poorly with crystal axes. However, a sufficiently large sample of specimens seems to overcome this problem from this (and other) ophiolite mantle sequences, the AMS axes define macroscopic L-S mineral fabrics. This success may be because such rock-forming mineral hosts are rich in high-κ inclusions, their high anisotropy degree (mostly $Pj > 1.5$; Figs. 9 and 10).

Another mineral-level problem arises relates to the relation between the host lattice and high-κ inclusions. Whereas the AMS or ARM principal axes indicate that high-κ inclusions are approximately controlled by the symmetry of the host crystal's lattice, the mapping may not show a simple one-to-one correspondence, e.g., with κ_{MIN} parallel to a certain crystal axis, e.g., *c*. Paradoxical associations, sometimes termed "inverse" arise through quite different causes. The first concerned some mineral with a counter-intuitive AMS with respect to crystal habit. Single-domain magnetite was the first recorded "inverse fabric" mineral (Potter and Stephenson, 1988) but low anisotropy calcite and quartz (Hrouda, 1986, 2004; Hamilton et al, 2004; Owens and Rutter, 1978; Rochette, 1988; Schmidt et al., 2006) may also yield inverse fabrics due to their diamagnetism (Fig. 7). For the important examples in question, both quartz and calcite align their c-axes perpendicular to cleavage or foliation by the most common crystal plastic mechanisms. The c-axes also yield the most negative κ-values, thus defining the long axes of the diamagnetic-AMS ellipsoid (Hamilton et al., 2004). The symmetry switch of the polar AMS plot assists in interpreting petrofabric from their AMS (Fig. 7f–g). Thus, calcite schistosity occurs with diamagnetic, *most negative* κ, perpendicular to foliation (Almqvist et al., 2009; de Wall, 2000; de Wall et al., 2000; Hamilton et al., 2004; Hrouda, 2004; Lagroix and Borradaile, 2000b). The authors have similarly determined inverse quartz AMS fabrics in tonalite-schist in northern Ontario.

A further usage of "inverse fabric" describes the superposition of competing sub-fabrics with differently oriented AMS axes (Ferré, 2002; Rochette et al., 1992). These may produce AMS axial orientations that are counter-intuitive to the tectonic framework. The first example was described where a stylolitic AMS sub-fabric overprinted a bedding-AMS to yield a composite depositional-tectonic AMS (Borradaile and Tarling, 1981). Other examples have been described that produce net fabrics inverse to the expected

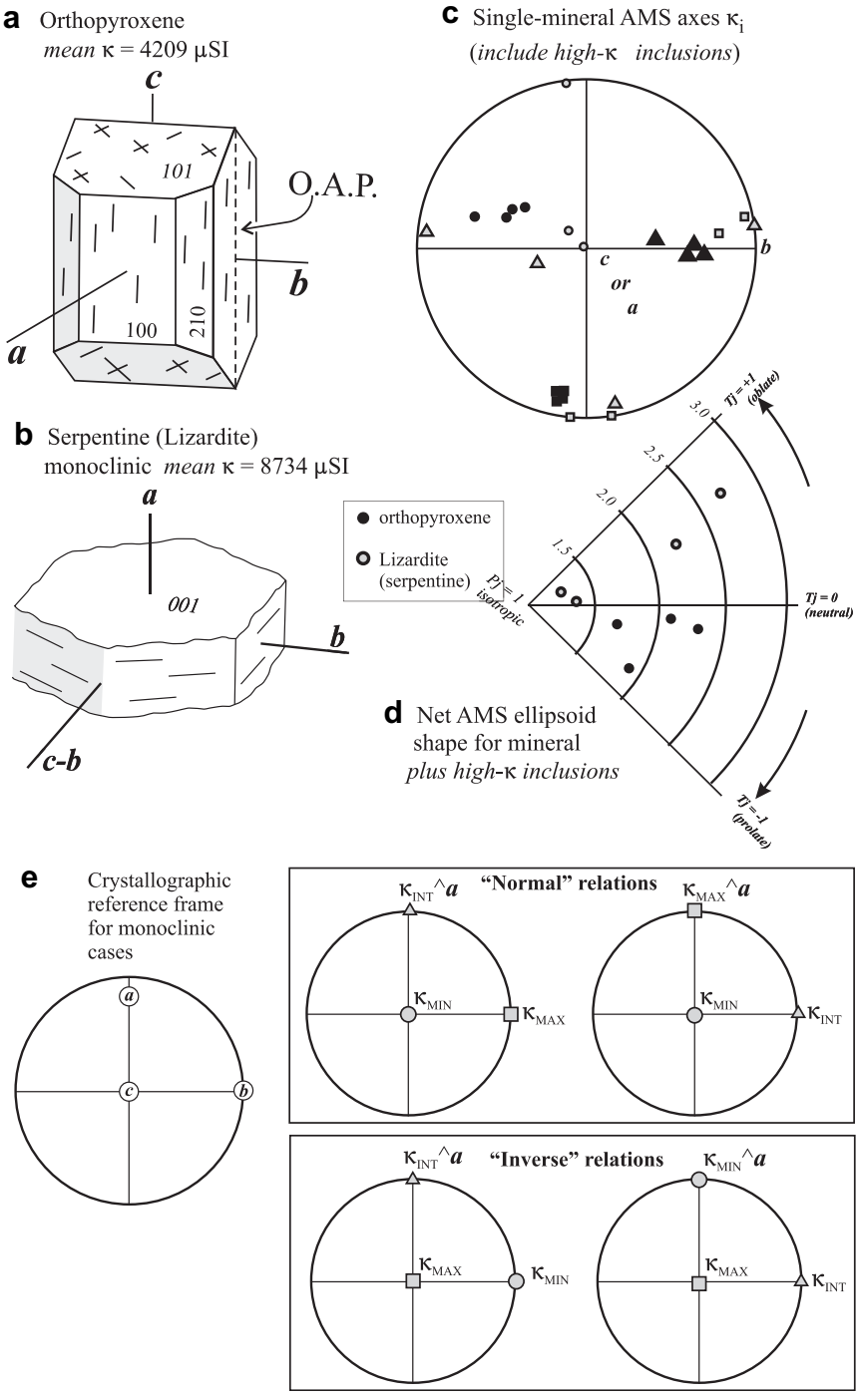

Fig. 10. (a–d) Despite low shape aspect ratios minerals such as orthopyroxene and lizardite contribute significantly to L–S fabrics and AMS due to their high intrinsic susceptibility in the Troodos ophiolite. However, the crystallographic control on AMS axes is imperfect due to high-κ inclusions. (e) Relative to the host-mineral crystallography, various permutations of susceptibility axes and crystal axes are possible.

tectonic arrangement of AMS axes. The differently oriented sub-fabrics must occur at a scale below that of the size the specimen so that they blend homogeneously to produce a combined and different AMS fabric from each component sub-fabric.

6. Interpreting AMS of rocks

The AMS of a tectonite depends upon the number of rock-forming minerals, their κ, their intrinsic AMS (possibly modified by high-κ inclusions) and their relative abundances (Borradaile, 1987; Borradaile and Jackson, 2004; Johns and Jackson, 1991; Rochette, 1987a,b). However, Henry (1983) recognized that nature commonly reduces complexity to a situation with two important minerals of contrasting κ and AMS (e.g., a mafic silicate and magnetite or a sheet-silicate and a diamagnetic mineral). The universal caveat is that rock-AMS underestimates *Pj* of the most anisotropic and well-aligned minerals (Fig. 6h–j). Similarly, the tectonite's *Tj* will underestimate that of the minerals but qualitatively represents symmetry of the strain or flow alignment mechanism. Earlier discussions concerning mineral anisotropy and

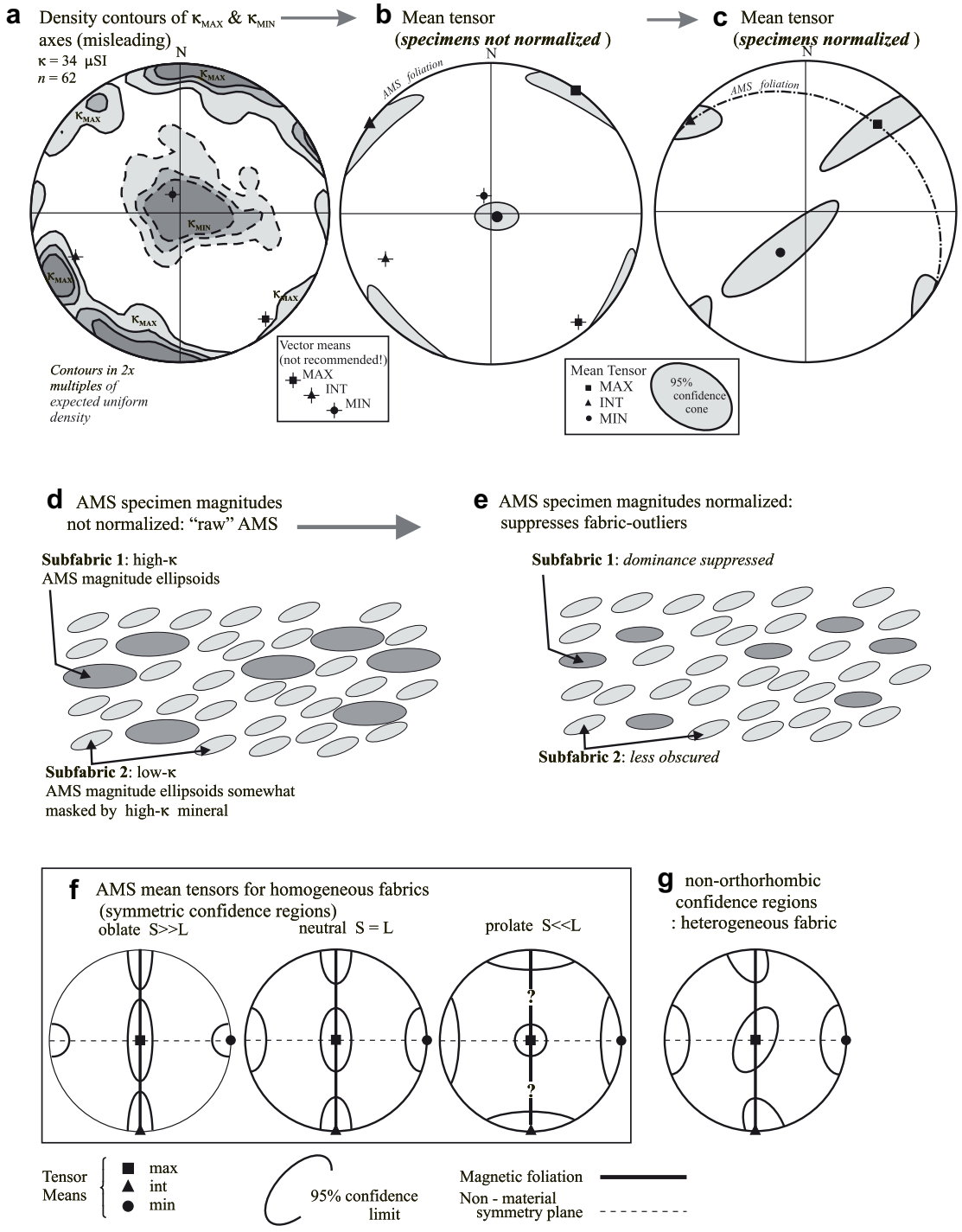

Fig. 11. (a) Density contours are imperfect for the representation of AMS axes since they fail to preserve perpendicularity of the mean principal axes. (κ_{MAX}, κ_{INT}, κ_{MIN}). (b) Since the mean AMS ellipsoid for a sample of specimens must have orthogonal axes, it is essential to use the statistical procedures of Jelinek (1978). (c) The mean tensor may be calculated for the raw data in which specimens are weighted by their κ-values, or for normalized specimens which are reduced to unit-susceptibility. (d) An anomalous sub-fabric of higher-κ may smear the AMS axes distribution. Normalizing the data and re-calculating the mean tensor suppresses the contribution of that sub-fabric. (f) Typical mean tensor and confidence-regions associated with L–S (Flinn, 1965) fabric types. (g) Heterogeneous fabrics may show asymmetric confidence regions.

crystallography indicate that in general strain magnitudes cannot correlate with magnitudes of principal susceptibilities as tested examples show (Fig. 12a,b; Borradaile, 1991; Borradaile and Jackson, 2004).

Below we describe techniques mainly limited to comparison of values of κ with ODs, and of the values and orientations of the κ_{MAX}, κ_{INT} and κ_{MIN} axes. These permit the structural geologist using little more than an AMS instrument to interpret which different minerals or sub-fabrics control AMS and κ within a tectonite by data manipulation. Of course, experimental methods at different temperatures, fields and frequencies may provide diagnostic criteria but they demand considerable resources, especially where RBM are present.

Subsequently, we need to present and compare AMS orientations for samples of many specimens. Being a tensor, a sample of AMS measurements present a fundamental problem when plotted on

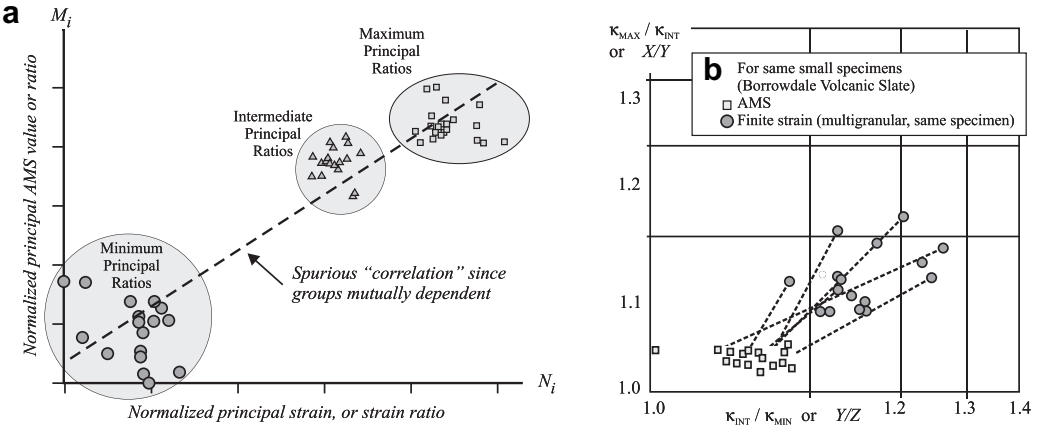
a
Mi
Maximum Principal Ratios
Intermediate Principal Ratios
Minimum Principal Ratios
Spurious "correlation" since groups mutually dependent
Normalized principal AMS value or ratio
Ni
Normalized principal strain, or strain ratio
b
For same small specimens (Borrowdale Volcanic Slate)
AMS
Finite strain (multigranular, same specimen)
κMAX / κINT or X/Y
κINT / κMIN or Y/Z

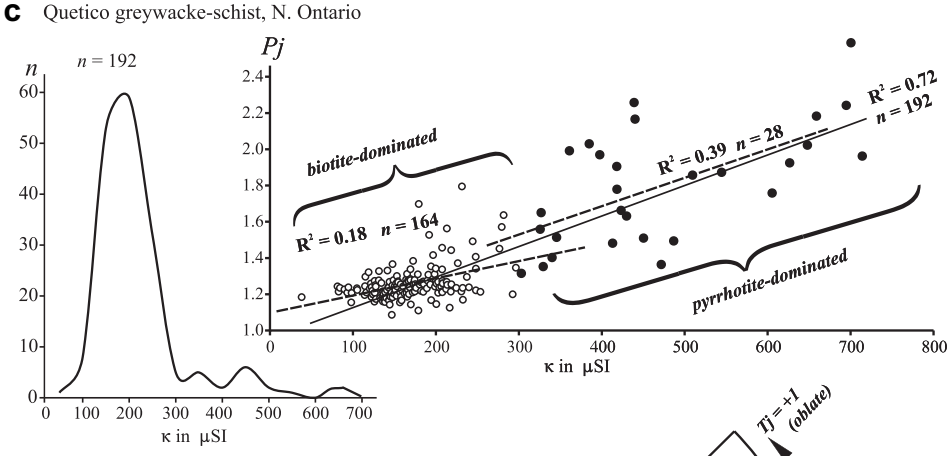
c Quetico greywacke-schist, N. Ontario
n = 192
Pj
biotite-dominated
R² = 0.18 n = 164
R² = 0.39 n = 28
R² = 0.72 n = 192
pyrrhotite-dominated
κ in μSI

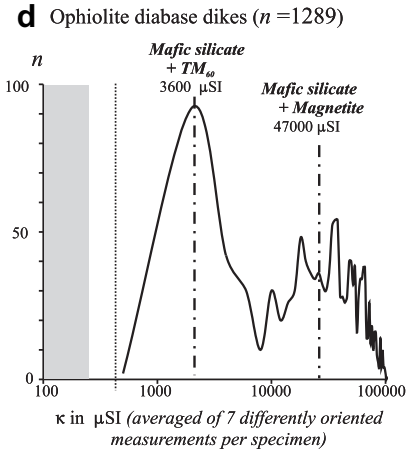
d Ophiolite diabase dikes (n =1289)
n
Mafic silicate + TM60
3600 μSI
Mafic silicate + Magnetite
47000 μSI
κ in μSI (averaged of 7 differently oriented measurements per specimen)

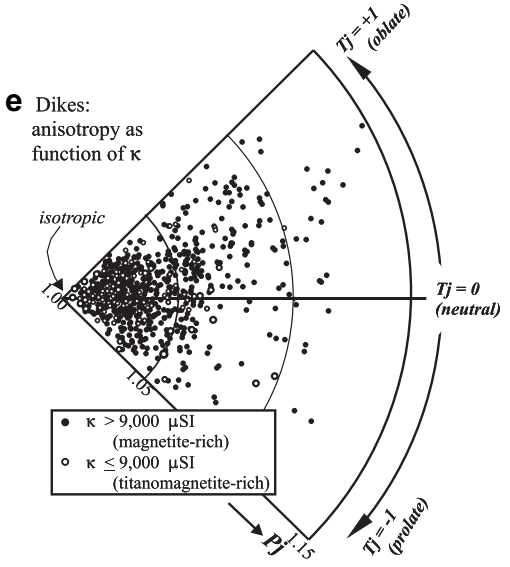
e Dikes: anisotropy as function of κ
isotropic
Tj = +1 (oblate)
Tj = 0 (neutral)
Tj = -1 (prolate)
Pj
κ > 9,000 μSI (magnetite-rich)
κ ≤ 9,000 μSI (titanomagnetite-rich)

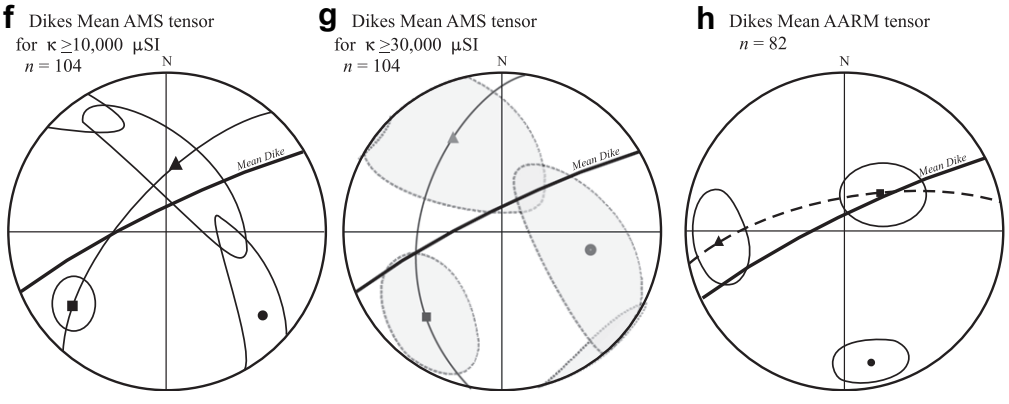
f Dikes Mean AMS tensor for κ ≥10,000 μSI n = 104
g Dikes Mean AMS tensor for κ ≥30,000 μSI n = 104
h Dikes Mean AARM tensor n = 82
N
Mean Dike

a stereogram. The traditional and objective use of density-contours is valid for axes and unit-vectors but not for tensors (Borradaile, 2003). For example, the peak densities, or vector-means calculated independently for κ_{MAX}, κ_{INT} and κ_{MIN} are not orthogonal (Fig. 11a). Alternative, computational approaches such as the "bootstrap" method, when applied to the principal axes independently, are theoretically and practically unsatisfactory (Werner, 1997). The only valid approach is a computationally complex tensor-statistical algorithm (Jelinek, 1978) that determines the *orthogonal* axes of the mean tensor (Fig. 11b). Each specimen has a different κ so that specimens with anomalous values may weight and skew the mean tensor orientation. Standardization of specimen tensors overcomes this; dividing each specimen's κ_{MAX}, κ_{INT} and κ_{MIN} by its κ reduces all specimens to unit susceptibility (Fig. 11c–e). The confidence regions around the mean-tensor axes correspond in symmetry to the L-S OD for the sample of specimens (Fig. 11f) however, where the rock includes two differently oriented, competing AMS sub-fabrics the confidence regions may be asymmetric (Fig. 11g) and this feature may persist after standardization (Fig. 11c).

6.1. Compare principal susceptibilities (κ_i) with κ for a sample of similar specimens

Particularly where an anisotropic silicate and a high- κ RBM control susceptibility, rather simple relationships may exist when κ_i plots against κ (Henry, 1983). An example from ophiolite-mantle S > L tectonites is shown (Fig. 8d). Anisotropy increases with κ and the κ_i curves intersect at the mean matrix susceptibility. A plot of ARM against κ verifies this (Fig. 8e). The κ_i versus κ plot works well where the mineralogy and fabric are reasonably homogeneous for the whole sample. A successful relation shows that rock-AMS is controlled by the relative abundance of the high-anisotropy, lower-κ mineral and the lower anisotropy, high- κ mineral.

6.2. Compare Pj, Tj for specimens of different κ

For a specimen, κ sums the partial contributions of minerals (Eq. (8)) and in a more complex manner (*Pj*, *Tj*) represent a more complex summation of mineral anisotropies and mineral ODs with imperfectly aligned minerals. (Attempts to write relationships inevitably simplify the situation to one where mineral alignments are perfect.) A pragmatic approach nevertheless throws light on the mineral sub-fabrics controlling rock-AMS. The samples must comprise specimens that are reasonably uniform with regard to AMS orientation and derive from a rock-type with mineralogy varying within reasonable limits. The most obvious examples possess a high-κ mineral such as mica in a meta-sandstone (Fig. 12c) or an iron oxide/sulphide in a silicate rock (Fig. 12d–e). A frequency-distribution of κ-values permits selection of sub-samples with suitably different κ-range (Fig. 12c, d) (Borradaile et al., 1988; Borradaile and Spark, 1991). A plot of *Pj versus* κ reveals that AMS for the rock is controlled by the relative abundances of well-aligned biotite ($\kappa \sim 200$–400 μSI) and a high-κ accessory (pyrrhotite $\kappa \sim 0.5$ SI, Worm et al., 1993) or in some sub-areas, magnetite ($\kappa \sim 2.5$ SI) (Borradaile and Sarvas, 1990; Werner and Borradaile, 1996). Similarly, an ophiolite mantle sample shows hydrothermal sea-floor metamorphism with an isotropic sub-fabric of secondary magnetite overprinting an earlier flow-aligned pyroxene-titanomagnetite (TM_{60}) in ophiolite dikes.. The bimodal histogram shows relative contributions from flow aligned pyroxene ($\kappa \sim 500$ μSI if pure) plus early TM_{60} ($\kappa \sim 2.2$ SI) or late isotropic magnetite ($\kappa \sim 2.5$ SI) (Fig. 12d). A polar (*Pj, Tj)* plot clearly distinguishes their different AMS (Fig. 12e) (Borradaile and Gauthier, 2003, 2001).

6.3. Compare mean-tensor for standardized versus non-standardized AMS specimens

The AMS ellipsoid represents a material tensor whose axes have magnitudes κ_{MAX}, κ_{INT} and κ_{MIN} characteristic of the specimen, for example, they may have magnitudes of 845: 822: 782 μSI. Specimens with high bulk κ dominate the suite and skew the orientation of the mean tensor (Fig. 11a–c). This effect is suppressed by normalizing all specimen susceptibilities to bulk unit-susceptibility (dividing specimen κ_{MAX}, κ_{INT} and κ_{MIN} magnitudes by κ) . For the example, principal values 845: 822: 782 μSI are each divided by the mean ($\kappa = 816$) to yield normalized values 1.035: 1.007: 0.958 for the "unit-susceptibility"; in other words specimens may then be compared on the basis of their normalized AMS ellipsoids Thus, sub-fabrics of aberrant orientation and κ may be identified (Borradaile, 2001, 2003; Borradaile and Gauthier, 2001, 2006) (Fig. 11d–e).

The Archaean MacKenzie plutonic granitoid of NW Ontario is deformed with the usual NW-dipping, NE-striking single foliation. It shows well-defined shape fabrics and PCOs of feldspar, quartz and biotite with subordinate magnetite. AMS fabrics corroborate the field-foliation orientation but the normalized mean tensor suppresses the magnetite sub-fabric revealing a more symmetric *S > L* fabric (Fig. 13a). A polar *Pj–Tj* plot shows the high anisotropies developed and essentially neutral ellipsoid shapes (*Tj* ~ 0) (Fig. 13e). The analysis may be extended, repeating this procedure for sub-samples of high and low κ (>5000 μSI; < 2000 μSI), revealing different aspects of the sub-fabrics homogeneity of orientation (Fig. 13b–c) and anisotropy (Fig. 13f,g).

A similar analysis of AMS and, AARM orientations provides even more information in a different suite. The rocks are supra-ophiolite limestone, dipping gently southward with a gently northward-dipping stylolitic cleavage. Cleavage accompanies S-closing, or S-vergent folds, of mappable dimensions near Limassol (Fig. 14). The limestone has low susceptibility, in some cases dominated by the diamagnetic calcite matrix but mostly with κ and AMS controlled by small PSD magnetite (Fig. 14b) (Hamilton et al., 2004; Lagroix and Borradaile, 2000a,b). Raw AMS axes define a sub-horizontal magnetic foliation, close to the stylolitic cleavage, with κ_{MAX} aligned N-S, parallel to the axis of subduction of the African Plate beneath Cyprus (Fig. 14c–e). By normalizing the AMS tensor, the sub-fabric contribution of the magnetite is suppressed and the intrinsic clay-calcite matrix fabric is emphasized, revealing a steeper foliation, dipping ~15° NE, similar to the average stylolitic cleavage. The somewhat complex and demanding AARM technique isolates RBM fabrics due to magnetite (using an AF window used of 0-60 mT). In subareas with the best-developed stylolitic cleavage and smallest bedding-cleavage angle, the AARM tensor is similar in orientation to cleavage and the normalized AMS fabric (Fig. 14f). Where stylolitic cleavage is less well developed, the AARM tensor defines a steeper N-dipping foliation (Fig. 14f–g) which probably indicates a later development of the magnetite-sub-fabric.

Fig. 12. (a) Early claims that strain-AMS correlations exist (e.g. here for the Borrowdale Volcanic Slate) were incorrect since dependent variables (the axial values) were correlated against one another. In any case, we now understand that mineral abundances and grain-AMS control rock AMS. (b) Even simple ratio comparisons, from the same specimens show that strain and AMS do not correlate (Borradaile, 1991; Borradaile and Mothersill, 1984). (c) Metamorphic rocks in which κ is controlled chiefly by two anisotropic minerals usually show a correlation of anisotropy (here Pj versus κ), but see Fig. 8d. (d–e) Ophiolite dikes in Cyprus have bimodal κ and bimodal Pj. (f–h) Their mean tensor may be calculated and compared for sub-samples of different mean-κ.

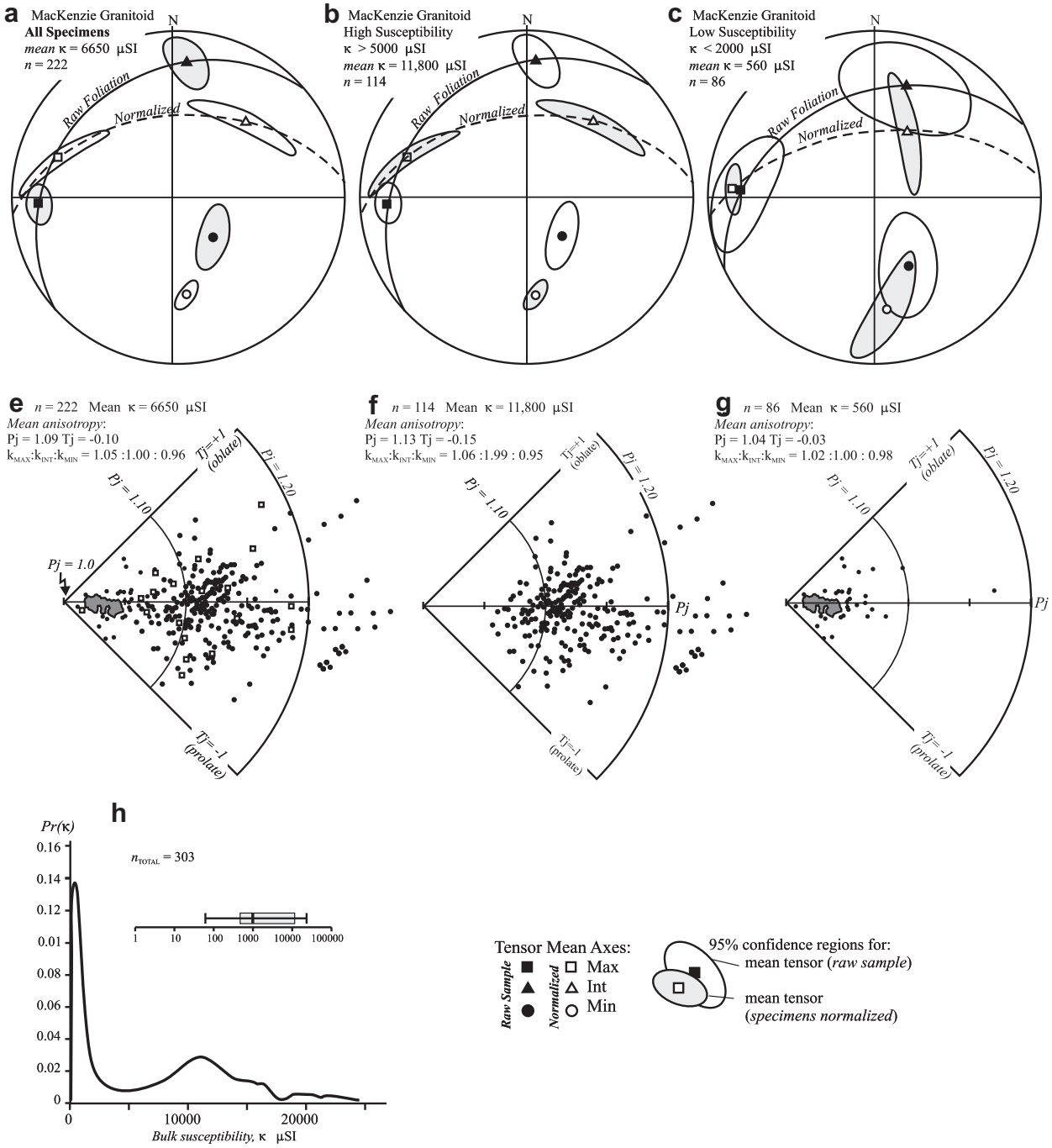

Fig. 13. (a) MacKenzie plutonic granitic gneiss has a broad distribution of specimen-κ values (see h). Raw AMS foliation is unrelated to field S-fabric but normalization yields magnetic foliation that is parallel to regional schistosity. High-κ specimens act as outliers distorting the interpretation of the raw AMS data. (b-c) Sorted into low-κ and high-κ subgroups, anomalous specimens still define foliation incompatible with the field L–S fabric but in both cases the *normalized fabric* has a magnetic foliation parallel to S in the field. However, the shapes and orientations of the confidence regions show that for the κ > 5000 μSI subgroup, the AMS fabric has S > L but for the κ < 2000 μSI the AMS fabric has L > S. (e-g) Considerable differences are seen in anisotropy degree (*Pj*) for the different subgroups, depending on the predominance of magnetite, biotite or amphibole in the particular sub-sample.

6.4. Analyze mineral separations

This instructive approach is time-consuming and specimen-destructive but requires only normal lapidiary facilities (Borradaile et al., 1987, 1990). SEM-EDA technology is available in most Geology Departments and this may greatly assist (Jackson and Borradaile, 1991). Most commonly, specimens are gently crushed to liberate individual grains. Liquid density separation using non-toxic sodium polytungstate ($Na_6[H_2W_{12}O_{40}]$) efficiently separates lighter versus denser minerals. Those fractions are further separated magnetically using the vibrating separator (e.g., Franz Magnetic Separator). Subsequently, hand-picking under the microscope isolates desirable mineral grains. Weighing separated fractions estimates mineral abundances but losses during separation may make this unreliable. Modal analysis of suitably oriented thin-sections may provide a more reliable estimate of mineral abundances. A known mass of suitable grains is aligned in epoxy in a standard 2 cm^3 specimen container. Magnetic alignment produces an *L*-fabric which blurs the κ_{INT} and κ_{MIN} values. Manual alignment in successive, thin layers of fast-setting layers of epoxy is preferable to

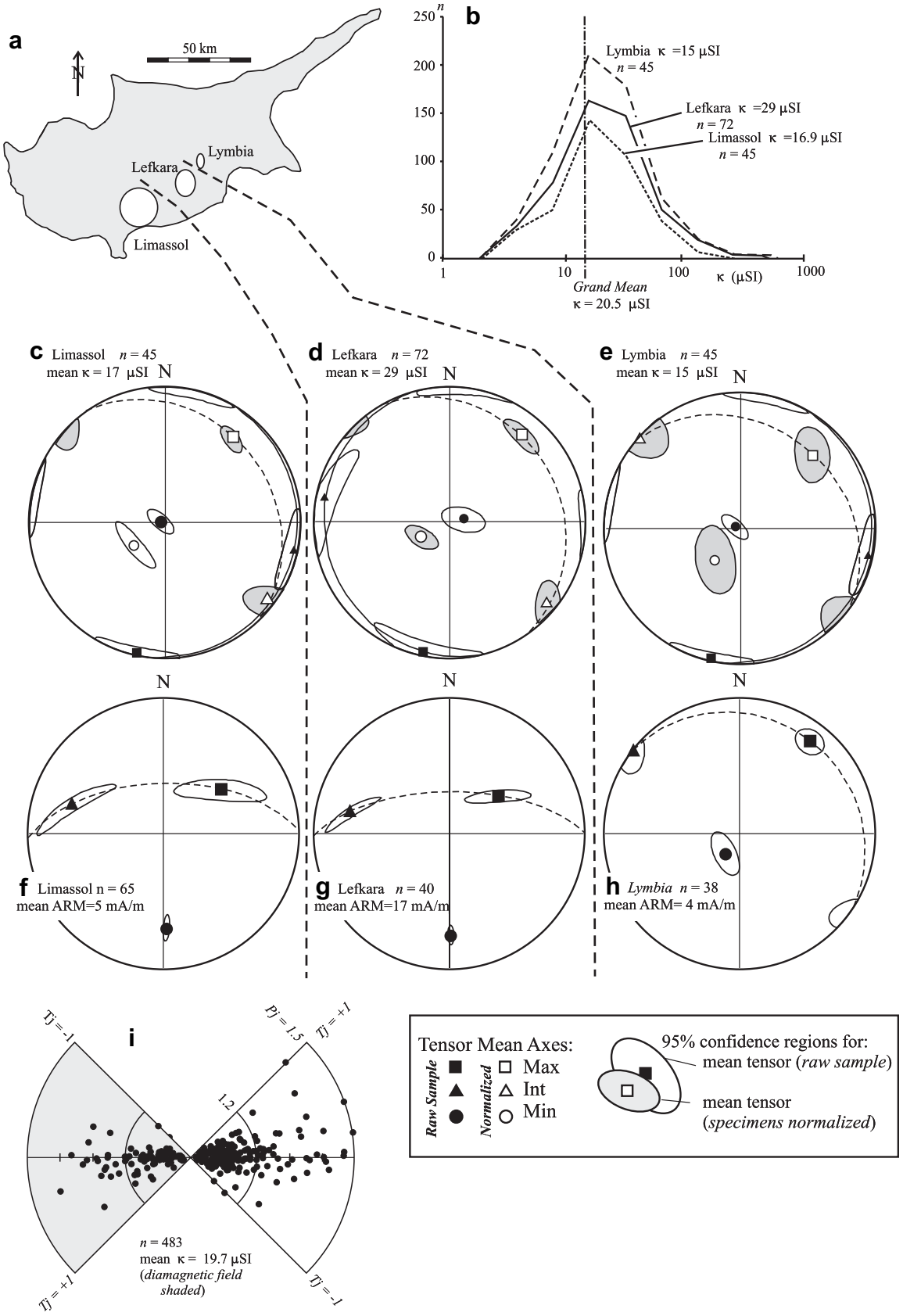

Fig. 14. (a) The Cyprus supra-ophiolite limestone sequence is deformed with S or SW-vergent cleavage above the north-dipping subduction zone, along which the African plate descends. (b)The limestones have low-κ due to volcaniclastic magnetite and, more rarely, clay minerals. Diamagnetic specimens have been excluded from this histogram. (c–e) Raw AMS axes are essentially controlled by bedding; normalization suppresses high-κ subfabric contributions and all normalized fabrics have S > L fabrics, parallel to the stylolitic cleavage. (f–g) AARM *determined in MD, magnetite-rich specimens* isolates the magnetite's subfabric contribution. The AARM S > L fabric mostly has a steep, northward dip, corresponding to later stages of the southward regional shortening.

estimate minimum values for each of the three κ_i. This tedious approach provides approximate but underestimated principal susceptibilities for the minerals. Of course, even the best-aligned tectonite provides lower estimates of mineral anisotropies. An adaption used in the cited papers is the progressive leaching and repeated AMS-measurement of specimens, first rendered more permeable by fine saw-cuts and drill-holes. This progressively emphasizes the AMS, or κ, or both for the least soluble remaining mineral or sub-fabric. Single mineral anisotropy may be measured more precisely using a micro-hysteresis instrument (Micromag 2900; Borradaile and Werner, 1994) or from large single crystals (e.g. Borradaile, 1994).

6.5. Anisotropy of remanence

The preceding methods used only the actual AMS measurements, or simple sample investigation, to partition κ, and AMS between different minerals and between different sub-fabrics. They are attractive for structural studies since equipment is limited to an AMS instrument and the workers do not have to sidetrack into the highly technical field of rock magnetism with experiments that yield relatively little useful information. However, the AMS measurements are inscrutable and potentially misleading without the foregoing types of analysis. The main sources of concern are due to minerals that compete strongly to control either AMS or κ, or both.

Rock magnetists would immediately proceed to techniques including hysteresis, high-field versus low-field susceptibility, and susceptibility versus temperature (inter alia) to characterize and isolate RBM versus paramagnetic/diamagnetic matrix responses (Daly, 1967; Hrouda, 2002a,b, 2009; Hrouda and Jelinek, 1990; Borradaile and Jackson, 2004). Here, we wish only to advise that with relatively sophisticated equipment available in an equipped paleomagnetic laboratory, it is also possible to determine the *anisotropy of remanent magnetization*. In the simplest terms, the specimen is magnetized and its remanence measured using a low DC field. This procedure is repeated along sufficient appropriate axes to determine a tensor describing the anisotropy of isothermal remanence (AIRM) (Daly and Zinsser, 1973; Jelinek, 1993). To achieve a measurable remanence the required field magnitude may introduce a non-linear response. Anisotropy of anhysteretic remanence (AARM) (McCabe et al., 1985; Jackson et al., 1988; Jackson, 1991; Stephenson et al., 1986) overcomes this by using a weak DC field during the application of a decaying alternating field in a suitably modified AF demagnetizer. The AF commences at a high value, randomizing the magnetic moments of the specimen. As the AF decays the DC field progressively aligns successively less coercive grains thereby producing a significant remanence with an essentially linear relation between the weak DC field and the magnetization. Furthermore, the DC field may be applied over a selected part of the AF range so that only a certain range of grain-sizes or domain-structures are included in the AARM measurement (Jackson et al., 1988, 1989). The method is restricted to RBM that are easily demagnetizable and re-magnetizable by otherwise non-destructive laboratory methods, usually magnetite. However, where available, AARM *combined* with the preceding data-analysis approaches usually effectively isolates the different mineralogical and sub-fabric sources of AMS. This ability is unavailable by any other petrofabric or structural technique.

7. Interpreting magnetic fabrics of tectonites (chiefly AMS)

Although second-rank tensors, visualized as ellipsoids represent finite strain and AMS, the latter is complicated in that its axial magnitudes have material values with fundamental significance. Strain axes sum the accumulated increments of processes acting within a continuum and the strain ellipsoid is a flexible property during geological processes, free to change shape in response to the demands of imposed tectonic strains as long as the rock remains a continuum at the scale of the strain ellipsoid (Ramsay, 1967; Ramsay and Huber, 1983) (e.g., Fig. 15a). This is possible and repeatedly observed because rocks undergo particulate flow in which grains may change shape, rotate and switch neighbours in a complicated pattern of *particulate flow* at every metamorphic grade (Borradaile, 1981; Borradaile and Tarling, 1984; Paaschier and Trouw, 2005).

In contrast, the AMS ellipsoid sums contributions from different minerals with crystal-AMS magnitudes that affect the orientation of the rock's AMS axes. Even if the rock was mono-mineralic and perfectly aligned, the mismatch between crystal and AMS axes (Fig. 6) prohibits any simple correlation of rock AMS axes with finite strain axes (Borradaile, 1991; Borradaile and Jackson, 2004), or with any metamorphic process. Conceptually, the rock's bulk κ (and more complexly AMS) is a balance between mineral abundances and mineral-κ values (Eqs. (8) and (9); Borradaile, 1987; Johns et al., 1992). A model calculation shows that dramatically different rock AMS (*Pj, Tj*) arise from different proportions of just two coaxially aligned minerals (Fig. 15e). Fig. 15f shows more complex, but still very simplified examples.

Thus, AMS ellipsoid cannot be flexible in harmony with the shape of the strain ellipsoid and strain events. It is controlled by discrete metamorphic and solid-state flow events that determine the abundances and alignments of individual minerals (Borradaile, 1987; Borradaile and Jackson, 2004; Rochette, 1987a,b; Robion et al., 1995, 1997). Changes in a rock's AMS may only occur if κ, AMS, or abundances change as a result of discrete events. Metamorphism or the superimposition of a sub-fabric would be just two examples where the composite AMS could not correlate with strain. Thus, it is misleading to compare the deformation path of a continuum strain ellipsoid (Fig. 15a) with the distribution-pattern of successive AMS states of essentially different mineral-assemblages on an AMS plot (Fig. 15e–f). Where such situations are suspected, careful analysis is needed (e.g., Frizon De LaMotte et al., 2002; Parés, 2004; Parés et al., 1999).

Close angular relations between strain or fabric axes and AMS axes usually requires some specialized conditions. These include situations in which a *progressive* tectonic-metamorphic process and a *progressive* change in AMS occur, so that successive discrete mineralization controls or influences the AMS orientation at certain points in the strain history. Favourable conditions include neocrystallization, pressure-solution, progressive metamorphism or stress-controlled mineralization, especially in low vorticity strain histories (Aubourg and Robion, 2002; Aubourg et al., 1995; Borradaile et al., 1985, 1987; Borradaile and Jackson, 2004; Housen and van der Pluijm, 1990, 1991; Housen et al., 1993a,b; Hirt et al., 2004; Jackson and Borradaile, 1991; Kissel et al., 1986; Rochette and Vialon, 1984; Rochette et al., 1999). Original and imposed sub-fabrics only blend in a readily comprehended fashion if the new mineral sub-fabric develops while principal tectonic axes are reasonably stably oriented with respect to material axes (Fig. 16a). For the example chosen, relative susceptibilities permit simple orientation-switching of the rock's κ_{MAX}, κ_{INT} or κ_{MIN}. The first studies of sub-fabric-blending recorded the transition from outcrops with bedding-controlled fabrics to those dominated by stylolitic cleavage with strain tests for strain-axis orientations. (Fig. 16b–d; Borradaile and Tarling, 1981, 1984). Another example, from AMS cores sampled across a 1 m thick graded bed shows some "axis-switching" as slaty cleavage refracts from the silty base to the pelitic top (Borradaile and Sarvas, 1990) (Fig. 16e).

Rochette et al. (1992), and subsequently Ferré (2002) advanced numeric modeling of sub-fabrics blending, considering the

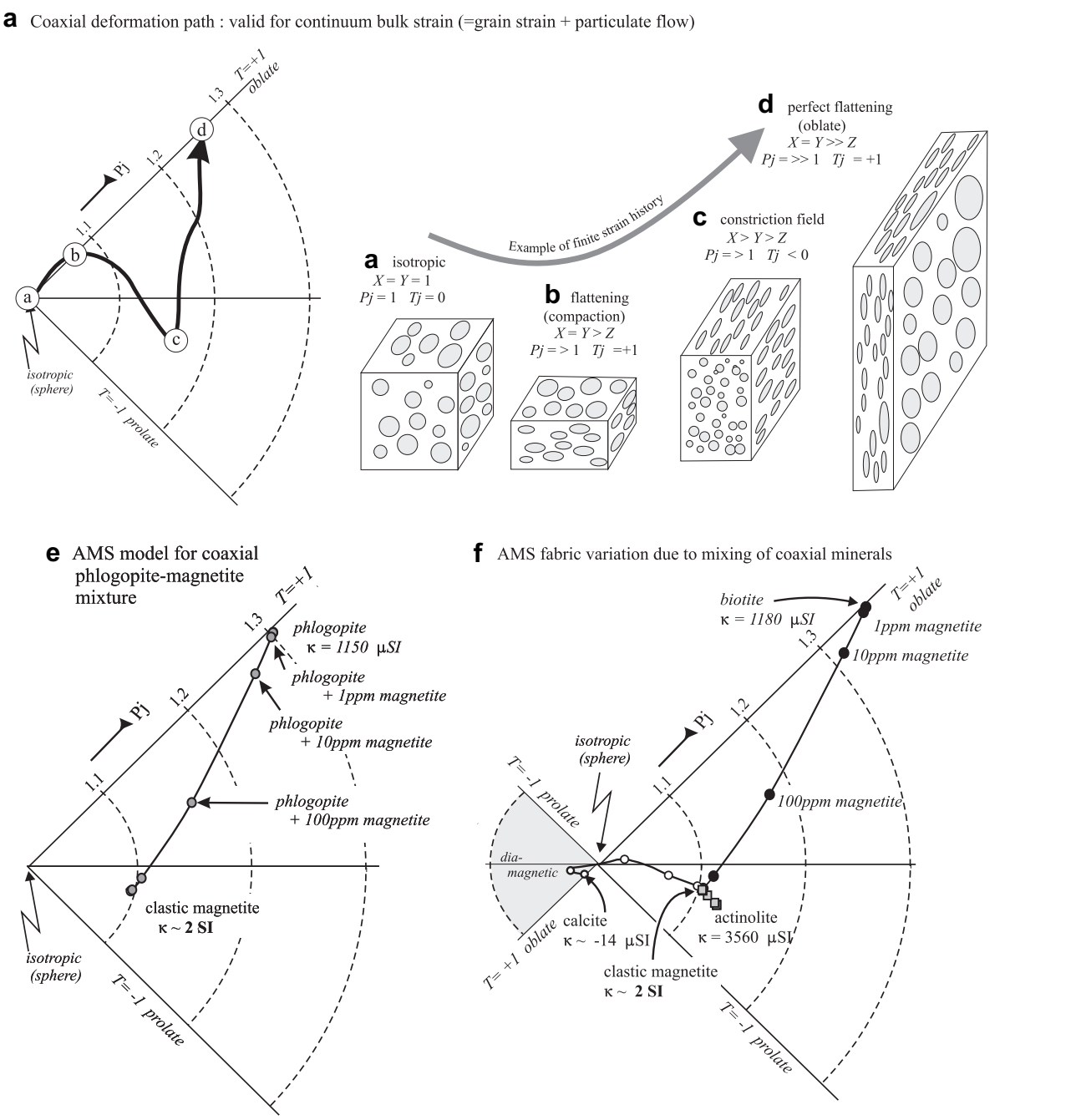

Fig. 15. (a–d) Continuum mechanics permit the assumption that the finite strain ellipsoid is plastically transformable in a progressive strain history at a scale on which the rocks are homogeneous and not disrupted. The elements involved must be ideally passive (i.e., no physical properties) but in finite strain studies this is not too restrictive and a smooth passage of fabric shapes may be a reasonable assumption. (e–f) AMS fabric variations between specimens and outcrops is due to a combination of different minerals, in different abundances, with different intrinsic anisotropies. These minerals evolve in discrete events and therefore, changes in AMS do not correspond to changes in strain.

different magnitudes and (coaxial) orientations of κ_{MAX}, κ_{INT} or κ_{MIN} (Fig. 16f–h). Further potential complications may be due to single-domain magnetite, for which the AMS ellipsoid is counter intuitively aligned to grain-shape (just one use of the term "inverse AMS"). In general, precisely inverse fabrics are very rare, more usually some blend exists between AMS sub-fabrics that result in a rock AMS counterintuitive to known structural elements, such as mineral lineation and foliation. Inverse fabrics are more common in limestone and quartzite, where *c*-axes align perpendicular to the foliation and the matrix diamagnetic-AMS causes an inverse fabric (Hamilton et al., 2004; Hrouda, 2004). However, alignment mechanisms or orientations for rock-forming minerals cannot be assumed; they depend on crystal plastic processes controlled by metamorphic conditions, their results are not simply predictable (Paaschier and Trouw, 2005). Nevertheless, the prima facie problem of sub-fabric mixing, even restricted to the case of two coaxial end-members gives rise to some possibly unexpected complications (Fig. 16f–h). Sub-fabric blending also causes changes in both *P* and *Tj* that are not readily predictable without calculation. The change in shape of rock's AMS ellipsoid is due to the combination of discrete mineral sub-fabrics' mixing steps, each with different magnetic properties. Numerous blended fabric and fabric overprint

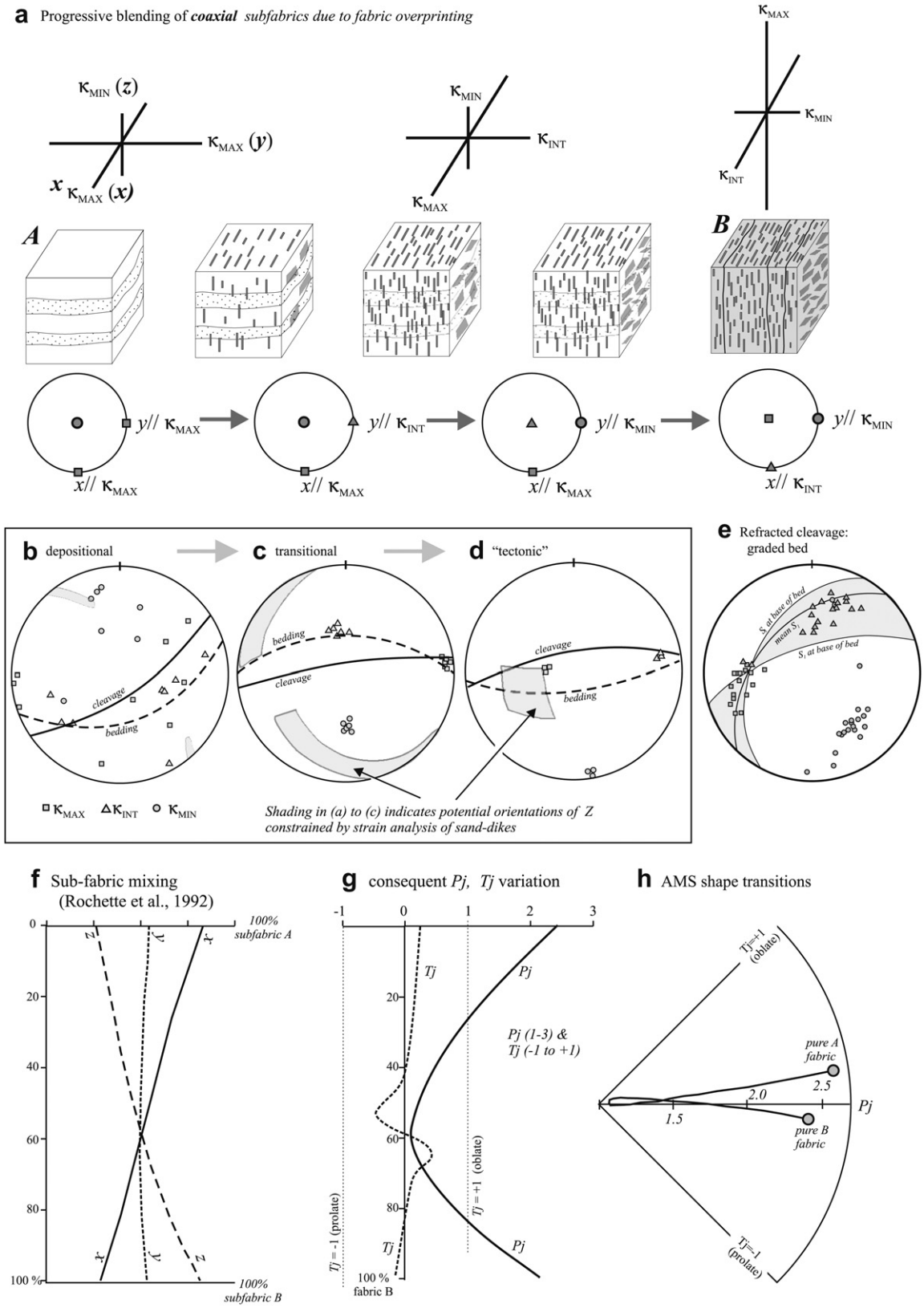

Fig. 16. (a) Differently oriented subfabrics may combine so that the end-member AMS axial configurations blend or switch. The end-members here are a bedding-fabric (left) and a cleavage fabric (right) with various blends in between. (b–d) The first recorded example of such subfabric blending, causing a switch in AMS axial orientations between outcrops. (e) AMS variation through a 1 m thick graded bed in which the cleavage (and AMS axes) refract. This causes some axis-switching (subfabric-blending) at different layers through the graded bed. (f–h) Represent an example of AMS fabric blending and axis-switching in various graphical forms.

studies are available (Borradaile and Genvicienne, 2008; Borradaile and Tarling; 1981, 1984; Hrouda, 1992; Hrouda et al., 2002; Housen et al., 1993a,b; Parés, 2004; Parés et al., 1999; Robion et al., 1995; Rochette et al., 1992, 1999).

8. AMS and finite strain

Many field studies and a few specialized laboratory studies verify that AMS axial *orientations* are commonly similar in orientation, if not parallel to the macroscopic fabric axes (L–S) (Ising, 1942; Graham, 1954, 1966; Granar, 1958). Correlations of strain *magnitudes* with AMS magnitudes (e.g., Rathore, 1979, 1980) mostly failed on statistical grounds (see Borradaile, 1991; Fig. 12a). However, in some cases the level of strain heterogeneity was not recognized so that specimen AMS was non-correlatable with strain for geological reasons as shown by Borradaile and Mothersill (1984) (see Fig. 12b). In other cases, other *prima facia* geological reasons negate a correlation (Nakamura and Borradaile, 2001). Only a few successful correlations have been found using special classes of strain markers and lithologies (Hirt et al., 1988, 1993; Siddans et al., 1984) or in experimental studies in which there was an isotropic initial fabric (Borradaile and Alford, 1987, 1988; Jackson et al., 1993). However, in almost all cases, *mineral abundances control rock-AMS* (Figs. 14a and 19e–f) (Borradaile, 1987; Borradaile and Sarvas, 1990; Borradaile et al., 1990; Borradaile and Jackson, 2004; Johns et al., 1992; Nakamura and Borradaile, 2004; Sun et al., 1995), a concept summarized here in Fig. 15.

The earliest notion relating finite strain to preferred orientation was due to March (1932) who investigated the concept of rotation of a *passive* linear marker, i.e., one with no particular physical properties and free to spin in space without changing dimensions or interfering with other particles. An original uniform OD of such lines, follows motion paths away from the axis of maximum shortening (Z) towards the X-axis as shown in Fig. 17a, with the density of poles (ρ) in any direction P defining the stretch in that direction as $\rho^{-1/3}$. The path depends on the Y-value of finite strain and does not follow the shortest route and is specific to the $X:Y:Z$ ratio. To describe the motion of poles to passive planar elements (i.e., mica poles), one simply reverses the direction of the movement arrows in Fig. 17a. This may approximately verify phyllosilicate alignment in slate (Oertel, 1983). Laboratory experiments (Tullis, 1976) and some X-ray or neutron goniometry work of low-strain slates approximately corroborates March's relationship. Some of these studies also made comparisons with AMS (Chadima et al., 2004; Cifelli et al., 2009; Hirt et al., 2004; Siddans et al., 1984; Sun et al., 1995). However, the initial OD is never uniform, particles impinge during rotation and they are *never* passive. These problems severely hinder the quantitative application of March's model.

Some simple triaxial rig experiments compared AMS with finite strain using analogue calcite-cement-magnetite aggregates and oolitic limestone in triaxial rigs (100–150 MPa confining pressure, 10^{-5} s^{-1} strain rate, some with pore fluid-pressure) (Borradaile and Alford, 1987, 1988; Borradaile and McArthur, 1990; Jackson et al., 1993). By using Teflon specimen jackets, such experiments were interrupted at various stages to re-measure AMS, thus documenting the progressive change in AMS with applied strains. Maximum shortening strains were ~30%. Internal specimen-piston arrangements also permitted shear configurations as well as the more traditional axial shortening tests. Broadly, such test show that the AMS axes spin approximately in the sense predicted by March (1922) (Fig. 17a) although more quickly that the applied strains would predict (Fig. 17b–d). Other experiments have been performed using laboratory bench analog experiments with plasticene or silicone-putty matrices and either PSD magnetite accessory grains or inverse-SD maghemite (Borradaile and Puumala, 1989). Progressive re-orientations of AMS axes agree only qualitatively with the March model (Fig. 17d–f) due to extreme material heterogeneity and non-uniform initial ODs.

The strain histories considered above (e.g. Figs. 15 and 16 consider that the strain axes remain parallel to the same material reference lines. Such *coaxial strain histories* are rare in nature and theoretically no history of finite strain in a heterogeneous material can be so simple (Ramsay, 1967; Ramsay and Huber, 1983). In general, successive increments of strain add obliquely to earlier ones so that the finite strain ellipsoid spins during its development. If the vorticity is rather low, the ellipsoid may become progressively more elongated but for high vorticities later strain increments may "undo" or de-strain earlier increments and the strain is non-progressive. For low vorticities, the finite strain ellipsoid continues to increase in eccentricity and, being a passive ellipse, it spins more quickly than any material markers such as mineral alignments (Fig. 18a). During most strain histories, there are discrete metamorphic effects and microcrystalline deformation mechanisms (Blenkinsop, 2000; Paaschier and Trouw, 2005) that block in new mineral sub-fabrics at different stages. From our studies in northern Ontario and northern Minnesota we generally find that mineral sub-fabrics usually develop in the sequence quartz and feldspar, biotite, chlorite, magnetite/pyrrhotite (Borradaile and Dehls, 1993; Borradaile et al., 1988, 1993; Johns et al., 1992; Sun et al., 1995). Each sub-fabric aligns parallel to the contemporary XY plane. Comparisons of AMS and anisotropy of remanence differentiate the influence of successive sub-fabrics (Fig. 18a). In Northern Ontario and Minnesota, E-W terrane boundaries have vertical terrane contacts sometimes obscured by later faulting but all characterized by early dextral transpression associated with the climax of metamorphism ~2700 Ma. The relative orientations of early-developing AMS fabrics and later superposed AARM sub-fabrics corroborate this dextral transpression at several hundred outcrops (Borradaile and Dehls, 1993; Borradaile and Sarvas, 1990; Borradaile and Spark, 1991; Werner and Borradaile, 1996) (Fig. 18b). A similar example of progressive sub-fabric superposition during non-coaxial strain is evident during the inflation of the Ash Bay Gneiss Dome of northern Ontario (Borradaile and Gauthier, 2003) (Fig. 18c). The gentle dome shows a circular outcrop of amphibolite gneiss in country rock of leucogranitic gneiss. The schistosity defined as a preferred dimensional orientation of quartz and feldspar, dips radially from the centre of the dome, a typical feature in the region. Interestingly however, the AMS foliation, attributed to late retrogressive phyllosilicates defines a *less* gently dipping radial foliation, as shown by the site-stereograms. Thus, the later and less domed mica-controlled AMS fabric overprinted the more obviously domed quartz-feldspar schistosity.

More precise, outcrop-scale evidence of non-coaxial AMS, AARM and petrofabric is found in well known simply deformed rocks such as the Welsh Slate of Penrhynn, North Wales and the Borrowdale Volcanic Slate, of Kentmere, Cumbria (Nakamura and Borradaile, 2001a,b). These rocks have provided many studies of stain, petrofabric and the Welsh slate outcrops defined the term "slaty cleavage". In the Borrowdale volcanic slate, elegant strained ellipsoidal accretionary lapilli permit strain analyses and define X, Y and Z orientations (Borradaile and Mothersill, 1984) (Fig. 1e, Fig. 12a, b). The Welsh slate is largely purple-red due to hematite; this conceals the underlying green colour of the chlorite slate which appears as cleavage-parallel reduction spots and lenses, or as persistent green beds. The ellipsoidal spots are not in fact strain markers, as commonly assumed,; they are simply post-cleavage colour-change patches located around suitable nuclei and adopting a shape controlled by anisotropic diffusion along the slaty cleavage (Nakamura and Borradaile, 2001a,b). Thus, the spots mimic X, Y and Z orientations and are sub-parallel to the AMS axes (Fig. 19). Slaty

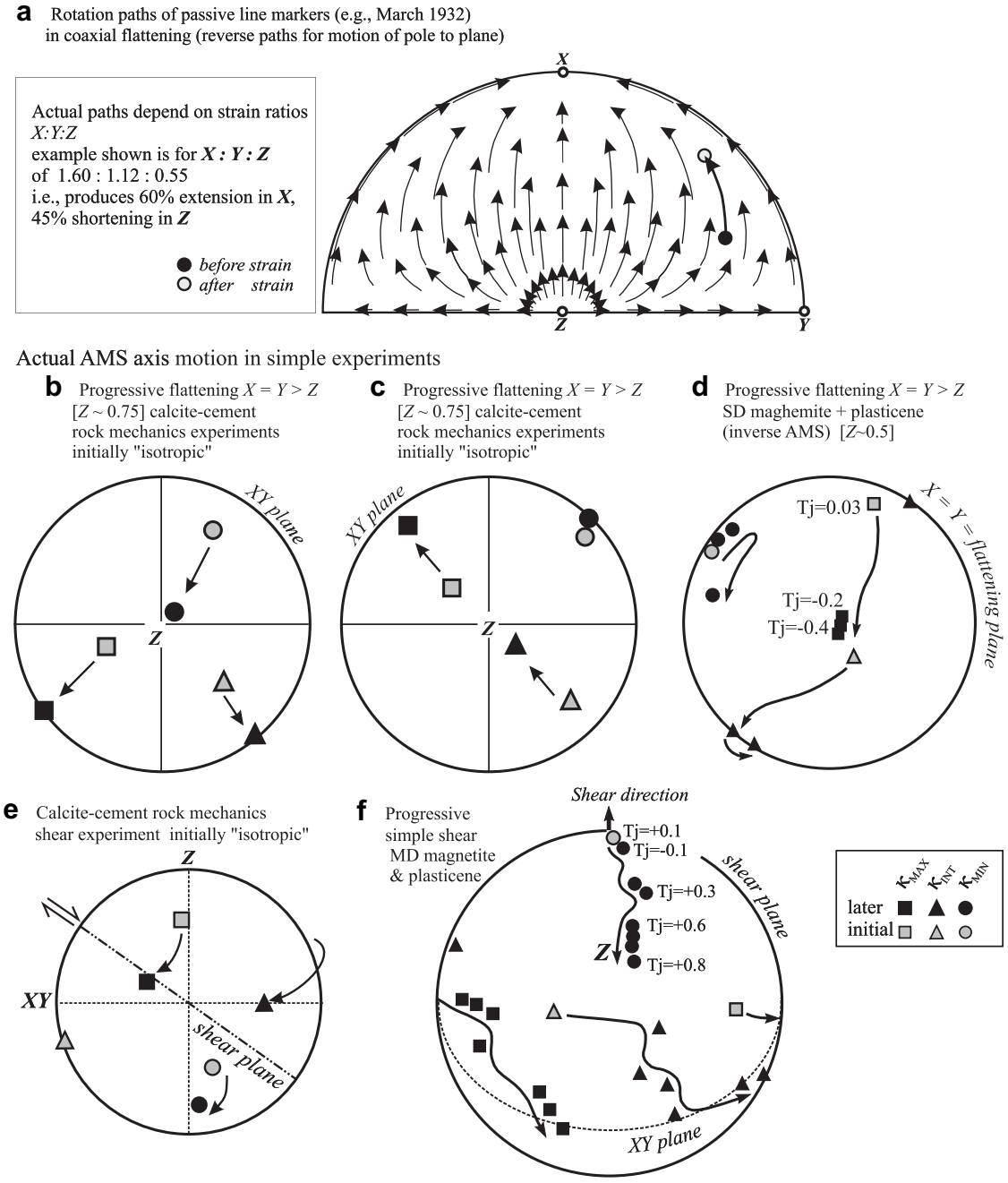

Fig. 17. (a) March (1932) predicted the spin-paths for passive line elements undergoing coaxial homogeneous strain. (These are very sensitive to the *X, Y* and *Z magnitudes*). (b–d) Rock mechanics experiments (100 or 150 MPa, $10^{-5}s^{-1}$) using calcite-analoguerocks show migration of AMS axes that only approximately follows the sense of Marchian rotation and does not agree quantitatively. (e–f) Shear experiments also show the rotation of AMS axes approximately in the sense expected by progressive finite strain, but with no quantitative corroboration.

cleavage and mineral lineation define *XY* and *X* respectively, which correspond to the AMS axes but AARM axes do not (Fig. 19a–d). It is remarkable that such well-defined slaty cleavage may bear quite discordant sub-fabrics of magnetite due to late non-coaxial increments of strain.

9. Summary

Reproducible AMS results are obtained for standard specimens (8 cm^3 or 10.5 cm^3 right-cylinder) if they are sufficiently homogeneous and if the grain size is not too large. Typically, measurement takes minutes; specimen preparation is minimal so that AMS provides considerable practical advantages over Universal-stage petrography, photometry, neutron and X-ray goniometry. The latter techniques are desirably mineral-specific but they are time-consuming to execute and learn, involve statistical uncertainties sophisticated instrumentation and are limited to few minerals of restricted grain-sizes.

Routine AMS measurements by structural geologists usually use low fields in an inexpensive A.C. induction coil instrument (e.g., AGICO, Brno, Czech Republic; Sapphire Instruments, Kingsville Ontario). The anisotropic response is a complex summation and averaging process of the different magnetic responses of the OD of hundreds of crystals in the specimen (Eqs. (8) and (9)). Each

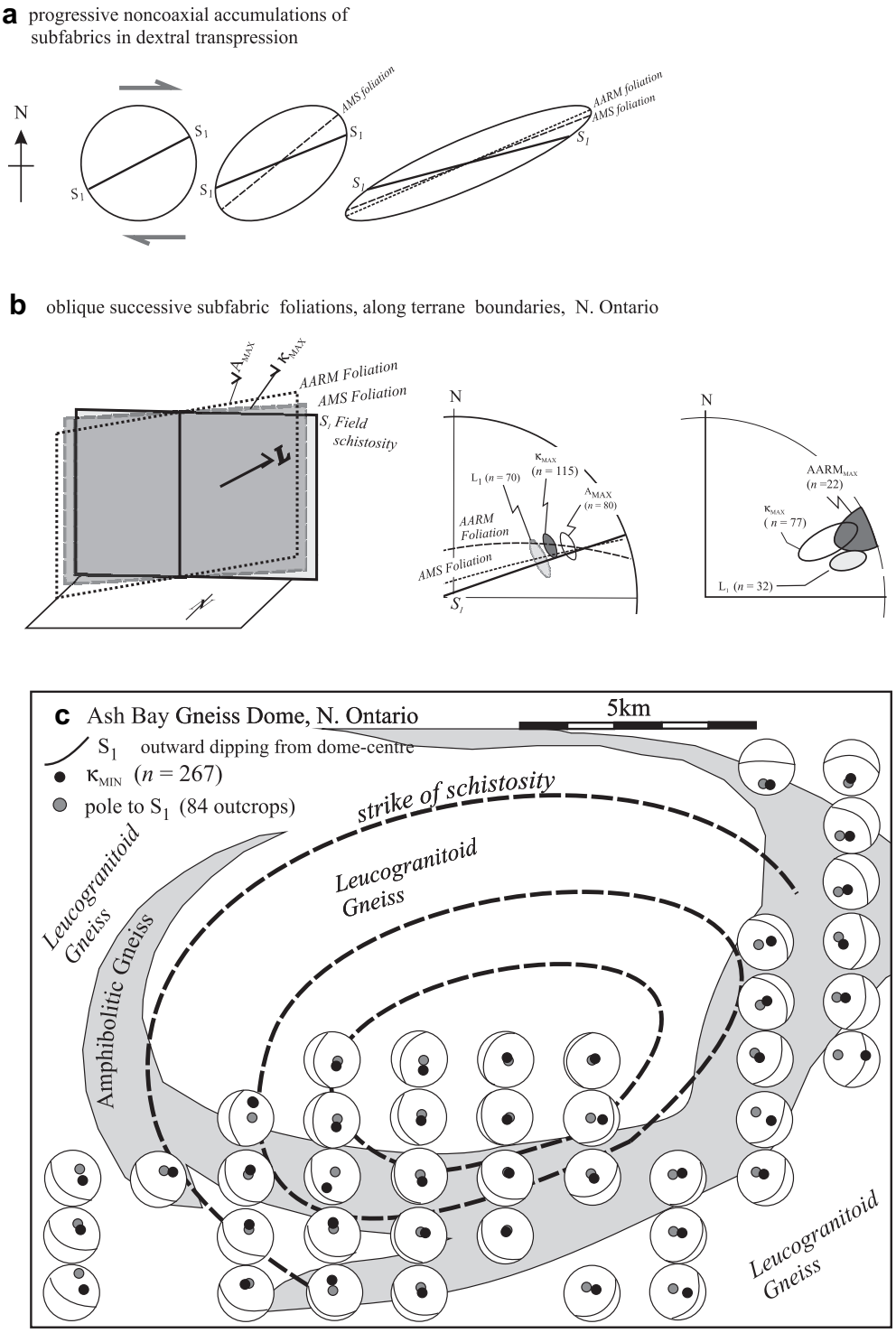

Fig. 18. (a) During progressive, non-coaxial strain earlier foliation planes may lag the spin of the finite strain ellipsoid. The result is that successive planes of flattening may superimpose on one another. Numerous studies by the authors in northern Ontario and northern Minnesota show that, the field schistosity (quartz-feldspar), AMS due to mafic silicate, and AARM fabrics due to magnetite all develop at slightly different angles at successive stages. (b) This is evident along the Archean terrane boundaries. (c) It is also evident in the inflation of the Ash Bay Gneiss dome, where the domal dips of quartz-feldspar schistosity are less than the dips of the AMS foliation (Borradaile and Dehls, 1993; Borradaile and Gauthier, 2003; Borradaile et al., 1989, 1993).

mineral has an intrinsic susceptibility response (diamagnetic, paramagnetic, "ferro"-magnetic) related directly to crystal structure. This is possibly complicated by inclusions and rather involved for specific minerals of very high susceptibility (Borradaile and Jackson, 2004; Owens, 1974; Hrouda, 1987, 1993). For a tectonite with a single-event homogeneous fabric the orientations and magnitudes of the principal axes κ_{MAX}, κ_{INT}, κ_{MIN} of the AMS ellipsoid are readily measured and associated with L-S fabrics. Alone, the principal axial magnitudes and κ suffice to interpret the AMS fabrics for a suite of similar tectonites in terms of strain or petrofabric processes. Sometimes, AMS orientations correspond to those of other physical crystalline anisotropies e.g.,

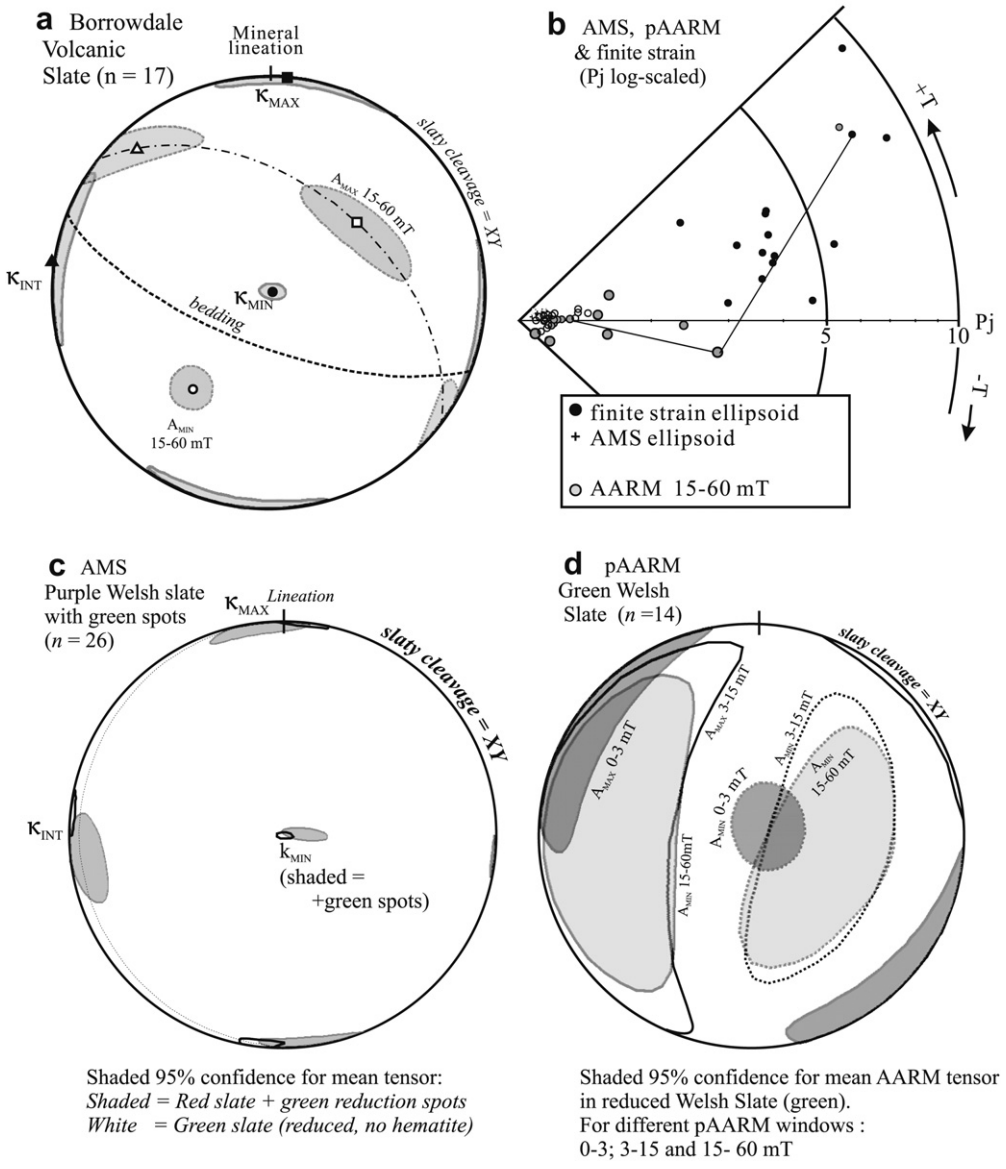

Fig. 19. Specific combined strain-AMS-AARM studies of two classic slates (Nakamura and Borradaile, 2001, 2003). (a) Borrowdale volcanic slate; AMS axes correspond to LS field fabric but AARM fabric does not. (b) AMS-AARM strain magnitudes are quite unrelated in the same specimen. (c) Welsh slate at Pennrhyn; AMS axes agree with slaty cleavage and lineation orientations. Reduced green beds and elliptical spots post-date cleavage formation and generate a later magnetite fabric, reducing the correspondence of AMS with cleavage. (d) AARM isolates the magnetite fabric in the green Welsh slates and corresponds to its L-S fabric for MD magnetite (0–3 mT). AARM cannot be determined for the red/purple Welsh Slate due to its high coercivity exceeding the maximum field of the AF demagnetizer (180 mT).

elastic wave velocity and permit further tectonic interpretation (Borradaile et al., 1999; Owens and Rutter, 1978).

Ideally, if all pure minerals possessed orthorhombic or tetragonal symmetry, principal susceptibilities would be parallel to crystal axes. In that case a well-aligned assemblage of crystals would yield a rock-AMS similar to the mineral AMS (Hrouda, 1987, 1993). However, even a homogeneous tectonite comprises many minerals and its bulk susceptibility (κ) and AMS tensor ($\boldsymbol{K}$) complexly merge the grains' physical responses (paramagnetic, etc.) (Eqs. (8) and (9)). To interpret AMS, we must consider all of the following: the grains' lattice orientations, their crystal-level AMS relation with the rock, their inclusions, and the grain-shape of high-κ minerals (Borradaile, 1987; Borradaile and Jackson, 2004; Borradaile and Werner, 1994; Richter et al., 1993a,b; Rochette, 1987a,b; Housen et al., 1993a,b; Martín-Hernández et al., 2001, 2003, 2004, 2005). Most rock-forming minerals have monoclinic or lower symmetry (and may include high-susceptibility impurities) so that their AMS does not directly correlate with crystal habit (Figs. 6 and 9) (Borradaile, 1994; Borradaile and Jackson, 2004; Borradaile and Werner, 1994; Lagroix and Borradaile, 2000a,b; Debacker et al, 2009; Renné et al., 2002). Therefore, most common crystal-symmetries reduce the correlation of AMS with petrofabric ODs.

Petrofabric comparisons with AMS require care since strain or OD-ellipsoids have unit-magnitude whereas the AMS ellipsoid for a specimen is weighted according to κ. K (and more complexly K) are complex summations of mineral abundances, susceptibilities, anisotropies and abundances (Eqs. (8) and (9)) . Thus, there are theoretical objections to the correlation of strain magnitudes or preferred-orientation (OD) strengths with finite strain (Fig. 15e–f). Tests of field examples verify this (Figs. 12, 15 and 16). (P_j, T_j) for the tectonite underestimate the values for the most anisotropic mineral

although the mean AMS axes for the tectonite and the petrofabric or strain ellipsoid may be nearly parallel.

AMS interpretation may be complicated where crystal or mineral-grain AMS is counter-intuitive to the petrofabric. For example, "inverse or "blended" fabrics result from the combination of incompatible AMS sub-fabrics. The first examples of inverse fabric were attributed to SD magnetite since the grain must have κ_{MIN} parallel to its long axis (Potter and Stephenson, 1988). A second class of counterintuitive associations of crystal and AMS axes occurs with diamagnetic minerals (since κ_{MAX} is the most negative value; Hamilton et al., 2004; Hrouda, 2004; Rochette, 1988), and with rare paramagnetic minerals that do not show a one-to-one correspondence of AMS axial magnitudes with crystal axes (Rochette et al., 1992; Chadima et al., 2009). A third use of "inverse fabric" is less fundamental and denotes only an unexpected association of AMS axes with some structural features such as cleavage, bedding, or mineral lineation.

In general, it is almost impossible to expect either perfectly "normal" or "inverse" alignments of AMS axes with PCO axes due to the mixing of different mineral sub-fabrics (Figs. 15 and 16). Moreover, most rock-forming minerals cannot perfectly align their AMS with and *L*–*S* fabric (Fig. 6). Blending of AMS sub-fabrics with different principal orientations may become quite complex, particularly if the two sub-fabrics are differently developed in successive outcrops (e.g., Housen et al., 1993a,b; Borradaile and Gauthier, 2003; Borradaile and Tarling, 1981, 1984; Evans et al., 2003; Trindade et al., 2001). However, a progression in net rock (*Tj, Pj*) in a sequence of outcrops may include changes in petrofabric, bulk susceptibility of the rock (κ), relative abundances of minerals or relative intensities of differently oriented sub-fabrics. The concept of a flexible strain ellipsoid reflects a progressive accumulation of events but the AMS ellipsoid sums contributions presented at discrete times and in discrete orientations from different mineral sub-fabrics (Figs. 15a and 16a). A fourth group of anomalous specimen-AMS orientations, including inverse fabric may rarely arise with distribution anisotropy in high-κ specimens. This is due to a *location-fabric* of abundant high- κ minerals, usually magnetite, so packed that their external fields interfere.

The interpretation of AMS in terms of petrofabric or strain axes requires knowledge of the mineral or sub-fabric sources of AMS in the specimens. Sophisticated laboratory procedures in rock magnetism may resolve many issues (e.g., Martín-Hernández and Hirt, 2004; Martín-Hernández and Ferré, 2007; Schmidt et al., 2007b; Hrouda et al., 1997; Hrouda, 2009) but the technology and expertise is usually unavailable and not strictly necessary for structural work. In section 6, we showed that processing the basic data (κ_{MAX}, κ_{INT}, κ_{MIN} and κ) for a suite of specimens will achieve nearly the same results, leading to the partial isolation of contributions from minerals or sub-fabrics of different κ, different AMS or different orientation. The simplest include plotting κ against the magnitudes of principal values (Henry, 1987; Henry and Daly, 1983; Borradaile and Henry, 1997), plotting κ against measures of anisotropy (*Pj, Tj*) (Rochette, 1987a,b; Borradaile and Sarvas, 1990; Nakamura and Borradaile, 2004) and performing such plots for sub-samples of different mean-κ (Borradaile and Gauthier, 2001). The mean-tensor, calculated using an algorithm supplied with common AMS instruments (Jelinek, 1978, AGICO, Sapphire Instruments) is a powerful directional statistic for a suite of specimens. Comparing the mean tensor for specimens normalized and not normalized by their mean susceptibility partially isolates sub-fabrics (Borradaile, 2001). Further commonly available laboratory facilities may identify minerals according to κ or AMS. These include mineral-separations, single-crystal measurements, reconstituting and aligning mineral separations and SEM microprobe analysis. The next level of sophistication, accessible in many palaeomagnetic laboratories, is the measurement of the anisotropy of remanence; this isolates the sub-fabric contribution of RBM of low-coercivity. However, this demands technical resources. For AIRM one needs a pulse magnetizer, simple AF demagnetizer and spinner magnetometer. The more desirable AARM technique requires a rather sophisticated AF demagnetizer and a spinner magnetometer.

Acknowledgments

We are sincerely grateful for the encouragement and succinct reviews by Dr. Joao Hibbert and two anonymous reviewers. This is contribution number 0903 of the Institute for Rock Magnetism, University of Minnesota, Minneapolis. Borradaile thanks NSERC (Ottawa) for continuous support for this project, 1979-present.

References

Almqvist, B.S.G., Hirt, A.M., Schmidt, V., Dietrich, D., 2009. Magnetic fabrics of the Morcles Nappe complex. Tectonophysics 466, 89–100.
Appel, E., 1987. Stress anisotropy in Ti-rich titanomagnetites. Physics of the Earth and Planetary Interiors 46, 233–240.
Aubourg, C., Robion, P., 2002. Composite ferromagnetic fabrics (magnetite, greigite) measured by AMS and partial AARM in weakly strained sandstones from western Makran. Geophysical Journal International 151, 729–737.
Aubourg, C., Rochette, P., Bergmüller, F., 1995. Composite magnetic fabric in weakly deformed black shales. Physics of the Earth and Planetary Interiors 87, 267–278.
Banerjee, S.K., Stacey, F.D., 1967. The high-field torque-meter method of measuring magnetic anisotropy in rocks. In: Collinson, D.W., Creer, K.M., Runcorn, S.K. (Eds.), Methods in Palaeomagnetism. Elsevier, Amsterdam, New York, pp. 470–476.
Bergmüller, F., Bärlocher, C., Geyer, B., Grieder, M., Heller, F., Zweifel, P., 1994. A torque magnetometer for measurements of the high-field anisotropy of rocks and crystals,. Measurements in Science and Technology 5, 1466–1470.
Blenkinsop, T., 2000. Deformation Microstructures and Mechanisms in Minerals and Rocks. Kluwer, Dordrecht. 150pp.
Boland, J.N., Fitzgerald, J.D., 1993. Defects and Processes in the Solid State, Geosciences Applications. Elsevier, Amsterdam, 470 pp.
Borradaile, G.J., 1981. Particulate flow of rock and the formation of cleavage. Tectonophysics 72, 305–321.
Borradaile, G.J., 1987. Anisotropy of magnetic susceptibility, rock composition versus strain. Tectonophysics 138, 327–329.
Borradaile, G.J., 1988. Magnetic susceptibility, petrofabrics, and strain, a review. Tectonophysics 156, 1–20.
Borradaile, G.J., 1991. Correlation of strain with anisotropy of magnetic susceptibility (AMS). Pure and Applied Geophysics 135, 15–29.
Borradaile, G.J., 1994. Paleomagnetism carried by crystal inclusions, the effect of preferred crystallographic orientation. Earth and Planetary Science Letters 126, 171–182.
Borradaile, G.J., 2001. Magnetic fabrics and petrofabrics; their orientation distributions and anisotropies. Journal of Structural Geology 23, 1581–1596.
Borradaile, G.J., 2003. Statistics of Earth Science Data. Springer-Verlag, 351 pp.
Borradaile, G.J., Alford, C., 1987. Relationship between magnetic susceptibility and strain in laboratory experiments. Tectonophysics 133, 121–135.
Borradaile, G.J., Alford, C., 1988. Experimental shear zones and magnetic fabrics. Journal of Structural Geology 10, 895–904.
Borradaile, G.J., Dehls, J.F., 1993. Regional kinematics inferred from magnetic subfabrics in Archaean rocks of northern Ontario, Canada. Journal of Structural Geology 15, 887–894.
Borradaile, G.J., Gauthier, D., 2001. AMS-detection of inverse fabrics without AARM, in ophiolite dikes. Geophysical Research Letters 28, 3517–3520.
Borradaile, G.J., Gauthier, D., 2003. Emplacement of an Archean gneiss dome, northern Ontario, Canada, inflation inferred from magnetic fabrics. Tectonics 22. doi:10.1029/2002TC001443.
Borradaile, G.J., Gauthier, D., 2006. Magnetic studies of magma-supply and sea-floor metamorphism, Troodos ophiolite dikes. Tectonophysics 418, 75–92.
Borradaile, G.J., Geneviciene, I., 2008. Late Proterozoic reconstructions of North-West Scotland and Central Canada: magnetic fabrics, paleomagnetism and tectonics. Journal of Structural Geology 30, 1466–1488. doi:10.1016/j.jsg.2008.07.009.
Borradaile, G.J., Henry, B., 1997. Tectonic applications of magnetic susceptibility and its anisotropy. Earth Science Reviews 42, 49–93.
Borradaile, G.J., Jackson, M., 2004. Anisotropy of magnetic susceptibility (AMS), magnetic petrofabrics of deformed rocks. In: Martín-Hernandez, F., Lünenburg, C.M., Aubourg, C., Jackson, M. (Eds.), Magnetic Fabrics. Geological Society of London Spec. Publ. No, 238, pp. 299–360.

Borradaile, G.J., Lagroix, F., 2001. Magnetic fabrics reveal upper mantle flow fabrics in the Troodos ophiolite complex, Cyprus. Journal of Structural Geology 23, 1299–1317.
Borradaile, G.J., McArthur, J., 1990. Experimental calcite fabrics in a synthetic weaker aggregate by coaxial and non-coaxial deformation. Journal of Structural Geology 12, 351–363.
Borradaile, G.J., Mothersill, J.S., 1984. Coaxial deformed and magnetic fabrics without simply correlated magnitudes of principal values. Physics of the Earth and Planetary Interiors 56, 254–265.
Borradaile, G.J., Puumala, M.A., 1989. Synthetic magnetic fabrics in plasticine. Tectonophysics 164, 73–78.
Borradaile, G.J., Sarvas, P., 1990. Magnetic susceptibility fabrics in slates, structural, mineralogical and lithological influences. Tectonophysics 172, 215–222.
Borradaile, G.J., Spark, R.N., 1991. Deformation of the Archean Quetico-Shebandowan subprovince boundary in the Canadian Shield near Kashabowie, northern Ontario. Canadian Journal of Earth Sciences 28, 116–125.
Borradaile, G.J., Stupavsky, M., 1995. Anisotropy of magnetic susceptibility, measurement schemes. Geophysical Research Letters 22, 1957–1960.
Borradaile, G.J., Tarling, D.H., 1981. The influence of deformation mechanisms on magnetic fabrics in weakly deformed rocks. Tectonophysics 77, 151–168.
Borradaile, G.J., Tarling, D.H., 1984. Strain partitioning and magnetic fabrics in particulate flow. Canadian Journal of Earth Sciences 21, 694–697.
Borradaile, G.J., Werner, T., 1994. Magnetic anisotropy of some phyllosilicates. Tectonophysics 235, 223–248.
Borradaile, G.J., Keeler, W., Alford, C., Sarvas, P., 1987. Anisotropy of magnetic susceptibility of some metamorphic minerals. Physics of the Earth and Planetary Interiors 48, 161–166.
Borradaile, G.J., MacKenzie, A., Jensen, E., 1990. Silicate versus trace mineral susceptibility in metamorphic rocks. Journal of Geophysical Research 95, 8447–8451.
Borradaile, G.J., Mothersill, J.S., Tarling, D.H., 1985. Sources of magnetic susceptibility in a slate. Earth and Planetary Science Letters 76, 336–340.
Borradaile, G.J., Stewart, R.A., Werner, T., 1993. Archean uplift of a subprovince boundary in the Canadian Shield, revealed by magnetic fabrics. Tectonophysics 227, 1–15.
Borradaile, G.J., Stupavsky, M., Trebilcock, D.-A., 2008. Induced magnetization of magnetite-titanomagnetite in alternating fields ranging from 400 A/m to 80,000 A/m; Low field susceptibility (100–400 A/m) and beyond). Pure and Applied Geophysics, 1–23. doi:10.1007/s00024-008-0361-5.
Borradaile, G.J., Tella, S., McArthur, J., 1989. Magnetic fabric as a kinematic indicator of faults, a test case. Annales de Tectonicae 3, 3–11.
Borradaile, G.J., Werner, T., Lagroix, F., 1999. Magnetic fabrics and anisotropy-controlled thrusting in the Kapuskasing structural zone, Canada. Tectonophysics 302, 241–256.
Borradaile, G.J., Puumala, M., Stupavsky, M., 1992. Anisotropy of complex magnetic susceptibility as an indicator of strain and petrofabric in rocks bearing sulphides. Tectonophysics 202, 309–318.
Borradaile, G.J., Sarvas, P., Dutka, R., Stewart, R., Stubley, M., 1988. Transpression in slates along the margin of an Archaean gneiss belt, northern Ontario-magnetic fabrics and petrofabrics. Canadian Journal of Earth Sciences 25, 1069–1077.
Brokmeier, H.G., 1994. Application of neutron diffraction to measure preferred orientations of geological materials. In: Bunge, H.J., Siegesmund, S., Skrotzki, W., Weber, K. (Eds.), Textures of Geological Materials. DGM Informationsgesellschaft, Oberursel, pp. 327–344.
Cañon-Tapia, E., 1996. Single-grain versus distribution anisotropy: a simple three-dimensional model. Physics of the Earth and Planetary Interiors 94, 149–158.
Chadima, M., Cajz, V., Týcová, P., 2009. On the interpretation of normal and inverse magnetic fabric in dikes, Examples from the Eger Graben, NW Bohemian Massif. Tectonophysics 466, 47–63.
Chadima, M., Hansen, A., Hirt, A., Hrouda, F., Siemes, H., 2004. Phyllosilicate preferred orientation as a control of magnetic fabric. In: Martín-Hernandez, F., Lünenburg, C.M., Aubourg, C., Jackson, M. (Eds.), Magnetic Fabrics. Geological Society of London, Special Publication, vol. 238, pp. 361–380.
Cifelli, F., Mattei, M., Chadima, M., Lenser, S., Hirt, A.M., 2009. The magnetic fabric in "undeformed clays", AMS and neutron texture analyses from the Rif Chain (Morocco). Tectonophysics 466, 79–88.
Constable, C., Tauxe, L., 1990. The Bootstrap method for magnetic susceptibility tensors. Journal of Geophysical Research 95, 8383–8395.
Daly, L., 1967. Possibilité d'existence dans les roches, de plusieurs anisotropies magnétiques superposées et leur séparation. Comptes Rendues d'Academie des Sciences, Paris, Série B 264, pp.1377–1380.
Daly, L., Zinsser, H., 1973. Étude comparative des anisotropies de susceptibilité et d'aimantation rémanente isotherme, conséquences pour l'analyse structurale et le paléomagnétisme. Annales de Géophysique 29, 189–200.
Debacker, T.N., Hirt, A.M., Sintubin, M., Robion, P., 2009. Differences between magnetic and mineral fabrics in low-grade, cleaved siliciclastic pelites, A case study from the Anglo-Brabant Deformation Belt (Belgium). Tectonophysics 466, 32–46.
de Wall, H., 2000. The field-dependence of AC susceptibility in titanomagnetites, implications for the anisotropy of magnetic susceptibility. Geophysical Research Letters 27, 2409–2411.
de Wall, H., Bestmann, M., Ullemeyer, K., 2000. Anisotropy of diamagnetic susceptibility in Thassos marble; a comparison between measured and modelled data. Journal of Structural Geology 22, 1761–1771.
Dunlop, D.J., Özdemir, Ö, 1997. Rock Magnetism, Fundamentals and Frontiers. Cambridge University Press, Cambridge, 573 pp.
Ellwood, B.B., Terrell, G.E., Cook, W.J., 1993. Frequency dependence and the electromagnetic susceptibility tensor in magnetic fabric studies. Physics of the Earth and Planetary Interiors 80, 65–74.
Evans, M.A., Lewchuk, M.T., Elmore, R.D., 2003. Strain partitioning of deformation mechanisms in limestones, examining the relationship of strain and anisotropy of magnetic susceptibility (AMS). Journal of Structural Geology 25, 1525–1549.
Ferré, E.C., 2002. Theoretical models of intermediate and inverse AMS fabrics. Geophysical Research Letters 29, 31–34.
Ferré, E.C., Martin-Hernandez, F., Teyssier, C., Jackson, M., 2004. Paramagnetic and ferromagnetic anisotropy of magnetic susceptibility in migmatites: measurements in high and low fields and kinematic implications. Geophysical Journal International 157, 1119–1129.
Flanders, P., 1974. Magnetostriction in some magnetic oxide compacted powders. IEEE Transactions on Magnetics MAG-10, 1050–1052.
Flinn, D., 1962. On folding during three-dimensional progressive deformation. Quarterly Journal of the Geological Society of London 118, 385–433.
Flinn, D., 1965. On the symmetry principle and the deformation ellipsoid. Geological Magazine 102, 36–45.
Friederich, D., 1995. Gefügeuntersuchungen an Amphiboliten der Bhömishen Masse unter besonderer Berücksichtigung der Anisotropie der magnetischen Suszetibiltät. Geotektonische Forschungen 82, 1–118.
Frizon De Lamotte, D., Souque, C., Grelaud, S., Robion, P., 2002. Early record of tectonic magnetic fabric during inversion of a sedimentary basin, examples from the Corbières transfer zone. Bulletin de la Societé de France 173, 461–469.
Frost, M.T., Siddans, A.W.B., 1979. A texture goniometer with variable radius and collimation for analysis of textures in rocks. Journal of Applied Crystallography 12, 564–569.
Fuller, M., 1963. Magnetic anisotropy and paleomagnetism. Journal of Geophysical Research 68, 293–309.
Gaillot, P., de Saint-Blanquat, M., Bouchez, J.-L., 2006. Effects of magnetic interactions in anisotropy of magnetic susceptibility: Models, experiments and implications for igneous rock fabrics quantification. Tectonophysics 418, 3–19.
Girdler, R.W., 1961. The measurement and computation of anisotropy of magnetic susceptibility in rocks. Geophysical Journal of the Royal Astronomical Society 5, 34–44.
Graham, J.W., 1954. Magnetic susceptibility anisotropy, an unexploited petrofabric element. Geological Society of America Bulletin 65, 1257–1258.
Graham, J.W., 1966. Significance of magnetic anisotropy in Appalachian sedimentary rocks. In: Steinhart, J.S., Smith, T.J. (Eds.), The Earth Beneath the Continents. Geophysical Monograph, 10. American Geophysical Union, Washington, pp. 627–648.
Granar, L., 1958. Magnetic measurements on Swedish varved sediments. Arkiv Fur Geofysik. 3, 1–40.
Grégoire, V., de Saint Blanquat, M., Nédelec, A., Bouchez, J.-L., 1995. Shape anisotropy versus magnetic interactions of magnetite grains, Experiments and application to AMS in granitic rocks. Geophysical Research Letters 22, 2765–2768.
Grégoire, V., Darrozes, J., Gaillot, P., Nédélec, A., 1998. Magnetite grain shape fabric and distribution anisotropy versus rock magnetic fabric: a three-dimensional case study. Journal of Structural Geology 20, 937–944.
Hamilton, T.D., Borradaile, G.J., Lagroix, F., 2004. Sub-fabric identification by standardization of AMS, an example of inferred neotectonic structures from Cyprus. In: Martín-Hernandez, F., Lünenburg, C.M., Aubourg, C., Jackson, M. (Eds.), Magnetic Fabrics. Geological Society of London Special Publication, vol. 238, pp. 527–540.
Hargraves, R.B., Johnson, D., Chan, C.Y., 1991. Distribution anisotropy: the cause of AMS in igneous rocks? Geophysical Research Letters 18, 2193–2196.
Henry, B., 1983. Interprétation quantitative de l'anisotropie de susceptibilité magnétique. Tectonophysics 91, 165–177.
Henry, B., 1989. Magnetic fabric and orientation tensor of minerals in rocks. Tectonophysics 165, 21–28.
Henry, B., 1990. Magnetic fabric implications for the relationships between deformation mode and grain-growth in slates from the Borrowdale Volcanic Group in the English Lake District. Tectonophysics 178, 225–230.
Henry, B., 1992. Modelling the relationship between magnetic fabric and strain in polymineralic rocks. Physics of the Earth and Planetary Interiors 70, 214–218.
Henry, B., Daly, L., 1983. From qualitative to quantitative magnetic anisotropy analysis, the prospect of finite strain calibration. Tectonophysics 98, 327–336.
Hext, G.R., 1963. The estimation of second-order tensors, with related tests and designs. Biometrika 50, 353–373.
Hirt, A.M., Lowrie, W., Clendenen, W.S., Kligfield, R., 1993. Correlation of strain and the anisotropy of magnetic susceptibility in the Onaping Formation; evidence for a near-circular origin of the Sudbury Basin. Tectonophysics 225, 231–254.
Hirt, A., Lowrie, W., Clendenen, W., Kligfield, R., 1988. The correlation of magnetic anisotropy with strain in the Chelmsford formation of the Sudbury Basin, Ontario. Tectonophysics 145, 177–189.
Hirt, A., Lowrie, W., Lunenburg, C., Lebit, H., Engelder, T., 2004. Magnetic fabric development in the Ordovician Martinsburg Formation, Pennsylvania. In: Martín-Hernandez, F., Lünenburg, C.M., Aubourg, C., Jackson, M. (Eds.), Magnetic Fabrics. Geological Society of London Special Publication, vol. 238, pp. 109–126.
Hobbs, B.E., Means, W.D., Williams, P.F., 1976. An Outline of Structural Geology. J. Wiley, Sons, New York, 571 pp.

Housen, B.A., van der Pluijm, B.A., 1990. Chlorite control of correlations between strain and anisotropy of magnetic susceptibility. Physics of the Earth and Planetary Interiors 61, 315–323.
Housen, B.A., van der Pluijm, B.A., 1991. Slaty cleavage development and magnetic anisotropy fabrics. Journal of Geophysical Research 96, 9937–9946.
Housen, B.A., Richter, C., van der Pluijm, B.A., 1993a. Composite magnetic anisotropy fabrics, experiments, numerical models, and implications for the quantification of rock fabrics. Tectonophysics 220, 1–12.
Housen, B.A., van der Pluijm, B.A., Van der Voo, R., 1993b. Magnetite dissolution and neocrystallization during cleavage formation, paleomagnetic study of the Martinsburg formation, Lehigh Gap, Pennsylvania. Journal of Geophysical Research 98, 13,799–13,813.
Hrouda, F., 1982. Magnetic anisotropy of rocks and its application in geology and geophysics. Geophysical Surveys 5, 37–82.
Hrouda, F., 1986. The effect of quartz on the magnetic anisotropy of quartzite. Studia Geophysica et Geodaetica 30, 39–45.
Hrouda, F., 1987. Mathematical model relationship between the paramagnetic anisotropy and strain in slates. Tectonophysics 142, 323–327.
Hrouda, F., 1992. Separation of a component of tectonic deformation from a complex magnetic fabric. Journal of Structural Geology 14, 65–71.
Hrouda, F., 1993. Theoretical models of magnetic anisotropy to strain relationship revisited. Physics of the Earth and Planetary Interiors 77, 237–249.
Hrouda, F., 2002a. Low-field variation of magnetic susceptibility and its effect on the anisotropy of magnetic susceptibility of rocks. Geophysical Journal International 150, 715–723.
Hrouda, F., 2002b. The use of the anisotropy of magnetic remanence in the resolution of the anisotropy of magnetic susceptibility into its ferromagnetic and paramagnetic components. Tectonophysics 347, 269–281.
Hrouda, F., 2004. Problems in interpreting AMS parameters in diamagnetic rocks. In: Martín-Hernández, F., Luneburg, C.M., Aubourg, C., Jackson, M. (Eds.), Magnetic Fabrics. Geological Society of London Special Publication, vol. 238, pp. 49–59.
Hrouda, F., 2007. Anisotropy of magnetic susceptibility of rocks in the Rayleigh Law region, Modeling errors arising from linear fit to non-linear data. Studia Geophysica et Geodaetica 51, 423–438.
Hrouda, F., 2009. Determination of field-independent and field-dependent components of anisotropy of susceptibility through standard AMS measurement in variable low fields I, Theory. Tectonophysics 466, 114–122.
Hrouda, F., Jelinek, V., 1990. Resolution of ferrimagnetic and paramagnetic anisotropies in rocks, using combined low-field and high-field measurements. Geophysical Journal International 103, 75–84.
Hrouda, F., Schulmann, K., 1990. Conversion of the magnetic susceptibility tensor into the orientation tensor in some rocks. Physics of the Earth and Planetary Interiors 63, 71–77.
Hrouda, F., Jelinek, V., Zapletal, K., 1997a. Refined technique for susceptibility resolution into ferromagnetic and paramagnetic components based on susceptibility temperature-variation measurement. Geophysical Joournal International 129, 715–719.
Hrouda, F., Jelinek, V., Zapletal, K., 1997b. Refined technique for susceptibility resolution into ferromagnetic and paramagnetic components based on susceptibility temperature-variation measurement. Geophysical Journal International 129, 715–719.
Hrouda, F., Henry, B., Borradaile, G., 2000. Limitations of tensor subtraction in isolating diamagnetic fabrics by magnetic anisotropy. Tectonophysics 322, 303–310.
Hrouda, F., Putis, M., Madaras, J., 2002. The Alpine overprints of the magnetic fabrics in the basement and cover rocks of the Veporic Unit (Western Carpathians, Slovakia). Tectonophysics 359, 271–288.
Hrouda, F., Faryad, S.W., Chlupácová, M., Jerábek, P., Kratinová, Z., 2009. Determination of field-independent and field-dependent components of anisotropy of susceptibility through standard AMS measurement in variable low fields II, An example from the ultramafic body and host granulitic rocks at Bory in the Moldanubian Zone of Western Moravia, Czech Republic. Tectonophysics 466, 123–134.
Hunt, C.P., Moskowitz, B.M., Banerjee, S.K., 1995. Magnetic properties of rocks and minerals. In: Ahrens, T.J. (Ed.), A Handbook of Physical Constants, vol. 3. Am. Geophys. Union, Washington, DC, pp. 189–204.
Ihmlé, P.F., Hirt, A.M., Lowrie, W., Dietrich, D., 1989. Inverse fabric in deformed limestones of the Morcles Nappe, Switzerland. Geophysical Research Letters 16, 1383–1386.
Ising, G., 1942. On the magnetic properties of varved clay. Arkiv för Matematik. Astronomi och Fysik 29A, 1–37.
Jackson, M.J., 1991. Anisotropy of magnetic remanence, a brief review of mineralogical sources, physical origins, and geological applications, and comparison with susceptibility anisotropy. Pure and Applied Geophysics 136, 1–28.
Jackson, M.J., Borradaile, G., 1991. On the origin of the magnetic fabric in purple Cambrian slates of north Wales. Tectonophysics 194, 49–58.
Jackson, M.J., Tauxe, L., 1991. Anisotropy of magnetic susceptibility and remanence, developments in the characterization of tectonic, sedimentary, and igneous fabric. Reviews of Geophysics 29, 371–376. suppl. (IUGG Report-Contributions in Geomagnetism, Paleomagnetism).
Jackson, M.J., Gruber, W., Marvin, J.A., Banerjee, S.K., 1988. Partial anhysteretic remanence and its anisotropy, applications and grain-size dependence. Geophysical Research Letters 15, 440–443.
Jackson, M., Borradaile, G.J., Hudleston, P., Banerjee, S., 1993. Experimental deformation of synthetic magnetite-bearing calcite sandstones; effects on remanence, bulk magnetic properties, and magnetic anisotropy. Journal of Geophysical Research 98, 383–401.
Jackson, M., Moskowitz, B., Rosenbaum, J., Kissel, C., 1998. Field-dependence of AC susceptibility in titanomagnetites. Earth and Planetary Science Letters 157, 129–139.
Jackson, M., Sprowl, D., Ellwood, B., 1989. Anisotropies of partial anhysteretic remanence and susceptibility in compacted black shales, grainsize- and composition-dependent magnetic fabric. Geophysical Research Letters 16, 1063–1066.
Jelínek, V., 1976. The Statistical Theory of Measuring Anisotropy of Magnetic Susceptibility of Rocks and its Application. Geophyzika, Brno.
Jelínek, V., 1978. Statistical processing of anisotropy of magnetic susceptibility measures on groups of specimens. Studia geophisica et geodetica 22, 50–62.
Jelínek, V., 1981. Characterization of the magnetic fabrics of rocks. Tectonophysics 79, T63–T67.
Jelínek, V., 1985. The physical principles of measuring magnetic anisotropy with the torque magnetometer. Travaux Géophysiques 33, 177–198.
Jelínek, V., 1993. Theory and measurement of the anisotropy of isothermal remanent magnetization of rocks. Travaux Géophysiques 37, 124–134.
Jelínek, V., Pokorný, J., 1997. Some new concepts in technology of transformer bridges for measuring susceptibility anisotropy of rocks. Physics and Chemistry of the Earth 22, 179–181.
Jezek, J., Hrouda, F., 2002. Software for modeling the magnetic anisotropy of strained rocks. Computers in Geosciences 28, 1061–1068.
Jezek, J., Hrouda, F., 2004. Determination of the orientation of magnetic minerals from the anisotropy of magnetic susceptibility. In: Martín-Hernandez, F., Lünenburg, C.M., Aubourg, C., Jackson, M. (Eds.), Magnetic Fabrics. Geological Society of London Special Publication, vol. 238, pp. 9–20.
Johns, M., Jackson, M., 1991. Compositional control of anisotropy of remanent and induced magnetization in synthetic samples. Geophysical Research Letters 18, 1293–1296.
Johns, M.K., Jackson, M.J., Hudleston, P.J., 1992. Compositional control of magnetic anisotropy in the Thomson formation, east-central Minnesota. Tectonophysics 210, 45–58.
Kelso, P.R., Tikoff, B., Jackson, M., Sun, W., 2002. A new method for the separation of paramagnetic and ferromagnetic susceptibility anisotropy using low field and high field methods. Geophysical Journal International 151, 345–359.
Kissel, C., Barrier, E., Laj, C., Lee, T.-Q., 1986. Magnetic fabric in "undeformed" marine clays from compressional zones. Tectonics 5, 769–781.
Klerk, J., Brabers, V.A.M., Kuipers, A.J.M., 1977. Magnetostriction of the mixed series Fe3−xTixO4. Journale de Physique 38, 87–189. Colloque C-1.
Knipe, R.J., Rutter, E.H., 1994. Deformation mechanisms, rheology and tectonics. Geological Society of London Special Publication 54 535pp.
Lagroix, F., Borradaile, G.J., 2000a. Magnetic fabric interpretation complicated by inclusions in mafic silicates. Tectonophysics 325, 207–225.
Lagroix, F., Borradaile, G.J., 2000b. Tectonics of the circum-Troodos sedimentary cover of Cyprus, from rock magnetic and structural observations. Journal of Structural Geology 22, 453–469.
March, A., 1932. Mathematische Theorie der Regelung nach der Korngestalt bei affiner Deformation. Zeitschrift für Kristallographie 81, 285–297.
Martin-Hernandez, F., Ferre, E.C., 2007. Separation of paramagnetic and ferrimagnetic anisotropies: a review. Journal of Geophysical Research 112. doi:10.1029/2006JB004340.
Martín-Hernández, F., Hirt, A.M., 2001. Separation of ferrimagnetic and paramagnetic anisotropies using a high-field torsion magnetometer. Tectonphysics 337, 209–221.
Martín-Hernández, F., Hirt, A.M., 2003. The anisotropy of magnetic susceptibility in biotite, muscovite and chlorite single crystals. Tectonophysics 367, 13–28.
Martín-Hernández, F., Hirt, A.M., 2004. A method for the separation of paramagnetic, ferrimagnetic and haematite magnetic subfabrics using high-field torque magnetometry. Geophysical Journal International 157, 117–127.
Martín-Hernández, F., Kunze, K., Julivert, M., Hirt, A.M., 2005. Mathematical simulations of anisotropy of magnetic susceptibility on composite fabrics. Journal of geophysical Research 110 (B06102). doi:10.1029/2004JB003505.
Martín-Hernández, F., Dekkers, M.J., Bominaar-Silkens, I.M.A., Maan, J.C., 2008. Magnetic anisotropy behaviour of pyrrhotite as determined by low- and high-field experiments. Geophysical Journal International 174, 42–54.
McCabe, C., Jackson, M.J., Ellwood, B.B., 1985. Magnetic anisotropy in the Trenton limestone, results of a new technique, anisotropy of anhysteretic susceptibility. Geophysical Research Letters 12, 333–336.
Moskowitz, B.M., 1993. High-temperature magnetostriction of magnetite and titanomagnetites. Journal of Geophysical Research 98, 359–371.
Muxworthy, A.R., Williams, W., 2004. Distribution anisotropy: the influence of magnetic interactions on the anisotropy of magnetic remanence. In: Martín-Hernández, F., Lüneburg, C.M., Aubourg, C., Jackson, M. (Eds.), Magnetic Fabrics. Geological Society of London Special Publication, vol. 238, pp. 37–48.
Nagata, T., 1961. Rock Magnetism. Maruzen, Tokyo, 350 pp.
Nagata, T., 1970. Basic magnetic properties of rocks under the effect of mechanical stresses. Tectonophysics 9, 167–195.
Nakamura, N., Borradaile, G., 2001a. Strain, anisotropy of anhysteretic remanence, and anisotropy of magnetic susceptibility in a slaty tuff. Physics of the Earth and Planetary Interiors 125, 85–93.
Nakamura, N., Borradaile, G., 2001b. Do reduction spots predate finite strain? A magnetic diagnosis of Cambrian slates in North Wales. Tectonophysics 340, 133–139.

Nakamura, N., Borradaile, G.J., 2004. Metamorphic control of magnetic susceptibility and magnetic fabrics, a 3-D projection. In: Martín-Hernandez, F., Lünenburg, C.M., Aubourg, C., Jackson, M. (Eds.), Magnetic Fabrics. Geological Society of London Special Publication, vol. 238, pp. 61–68.
Nicolas, A., 1987. Principles of Rock Deformation. Kluwer, Dordrecht. 208 pages.
Nicolas, A., Poirier, J.P., 1976. Crystalline Plasticity and Solid State Flow in Metamorphic Rocks. J. Wiley and Sons, New York, 444 pp.
Nye, J.F., 1957. Physical Properties of Crystals. Oxford University Press, London. 322 pp.
Oertel, G., 1983. The relationship of strain and preferred orientation of phyllosilicate grains in rocks, a review. Tectonophysics 100, 413–447.
Owens, W.H., 1974. Mathematical model studies on factors affecting the magnetic anisotropy of deformed rocks. Tectonophysics 24, 115–131.
Owens, W.H., 2000a. Error estimates in the measurement of anisotropic magnetic susceptibility. Geophysical Journal International 142, 516–526.
Owens, W.H., 2000b. Statistical applications to second-rank tensors in magnetic fabric analysis. Geophysical Journal International 142, 527–538.
Owens, W.H., Rutter, E.H., 1978. The development of magnetic susceptibility anisotropy through crystallographic preferred orientation in a calcite rock. Physics of the Earth and Planetary Interiors 16, 215–222.
Paaschier, C.W., Trouw, A.J., 2005. Microtectonics. Springer-Verlag, 366 pp.
Parés, J.M., 2004. How deformed are weakly deformed mudrocks? In: Martín-Hernández, F., Lüneburg, C.M., Aubourg, C., Jackson, M. (Eds.), Magnetic Fabrics Geological Society of London Special Publication, vol. 238, pp. 191–204.
Parés, J.M., van der Pluijm, B.A., 2002a. Phyllosilicate fabric characterization by Low-Temperature Anisotropy of Magnetic Susceptibility (LT-AMS). Geophysical Research Letters. doi:10.1029/2002GL015459.
Parés, J.M., van der Pluijm, B.A., 2002b. Phyllosilicate fabric characterization by Low-Temperature Anisotropy of Magnetic Susceptibility (LT-AMS). Geophysiocal Journal International 129, 715–719.
Parés, J.M., van der Pluijm, B., Dinarès-Turell, J., 1999. Evolution of magnetic fabrics during incipient deformation of mudrocks (Pyrenees, northern Spain). Tectonophysics 307, 1–14.
Poirier, J.-P., 1985. Creep of Crystals. Cambridge University Press, 260 pp.
Petrovsky, E., Kapicka, A., 2006. On determination of the Curie point from thermomagnetic curves. Journal of Geophysical Research 111. doi:10.1029/2006JB004507.
Pokorný, J., Suza, P., Hrouda, F., 2004. Anisotropy of magnetic susceptibility of rocks measured in variable weak magnetic fields using the KLY-4S Kappabridge. In: Martín-Hernandez, F., Lünenburg, C.M., Aubourg, C., Jackson, M. (Eds.), Magnetic Fabrics. Geological Society of London Special Publication, vol. 238, pp. 69–76.
Potter, D.K., 2004. A comparison of anisotropy of magnetic remanence methods – a user's guide for application to paleomagnetism and magnetic fabric studies. In: Martín-Hernández, F., Lünenburg, C.M., Aubourg, C., Jackson, M. (Eds.), Magnetic Fabrics. Geological Society of London Special Publication, vol. 238, pp. 21–35.
Potter, D.K., Stephenson, A., 1988. Single-domain particles in rocks and magnetic fabric analysis. Geophysical Research Letters 15, 1097–1100.
Ramsay, J.G., 1967. Folding and Fracturing of Rocks. McGraw-Hill, New York, 578 pp.
Ramsay, J.G., Huber, M.I., 1983. The Techniques of Modern Structural Geology. Volume I, Strain analysis. Academic Press, 307 pp.
Rathore, J.S., 1979. Magnetic susceptibility anisotropy in the Cambrian slate belt of north Wales and correlation with strain. Tectonophysics 53, 83–97.
Rathore, J.S., 1980. The magnetic fabrics of some slates from the Borrowdale Volcanic Group in the English Lake District and their correlations with strains. Tectonophysics 67, 207–220.
Renné, P.R., Scott, G.R., Glen, J.M.G., Feinberg, J.M., 2002. Oriented inclusions of magnetite in clinopyroxene; source of stable remanent magnetization in gabbros of the Messum Complex, Namibia. Geochemistry, Geophysics, Geosystems - G^3 3, 11.
Revol, J., Day, R., Fuller, M., 1977. Effect of uniaxial compressive stress upon remanent magnetization, stress cycling and domain state dependence. Journal of Geomagnetism and Geoelectricity 30, 593–605.
Richter, C., van der Pluijm, B.A., 1994. Separation of paramagnetic and ferrimagnetic susceptibilities using low temperature magnetic susceptibilities and comparison with high field methods. Physics of the Earth and Planetary Interiors 82, 111–121.
Richter, C., van der Pluijm, B.A., Housen, B.A., 1993a. The quantification of crystallographic preferred orientation using magnetic anisotropy. Journal of Structural Geology 15, 113–116.
Richter, C., Ratschbacher, L., Frisch, W., 1993b. Magnetic fabrics, crystallographic preferred orientation, and strain of progressively metamorphosed pelites in the Helvetic zone of the central Alps (Quartenschiefer formation). Journal of Geophysical Research 98, 9557–9570.
Robion, P., Frizon de Lamotte, D., Kissel, C., Aubourg, C., 1995. Tectonic versus mineralogical contribution to the magnetic fabrics of epimetamorphic slaty rocks, an example from the Ardennes massif (France-Belgium). Journal of Structural Geology 17, 1111–1124.
Robion, P., Kissel, C., Frizon de Lamotte, D., Lorand, J.P., Guezou, J.C., 1997. Magnetic mineralogy and metamorphic zonation in the Ardenne massif (France-Belgium). Tectonophysics 271, 231–248.
Rochette, P., 1987a. Magnetic susceptibility of the rock matrix related to magnetic fabric studies. Journal of Structural Geology 9, 1015–1020.
Rochette, P., 1987b. Metamorphic control of the mineralogy of black shales in the Swiss Alps, toward the use of "magnetic isograds". Earth and Planetary Science Letters 84, 446–456.
Rochette, P., 1988. Inverse magnetic fabric in carbonate-bearing rocks. Earth, Planetary Science Letters 90, 229–237.
Rochette, P., Fillion, G., 1988. Identification of multi-component anisotropies in rocks using various field and temperature values in a cryogenic magnetometer. Physics of the Earth and Planetary Interiors 51, 379–386.
Rochette, P., Vialon, P., 1984. Development of planar and linear fabrics in Dauphinois shales and slates (French Alps) studied by magnetic anisotropy and its mineralogical control. Journal of Structural Geology 6, 33–38.
Rochette, P., Aubourg, C., Perrin, M., 1999. Is this magnetic fabric normal? A review and case study in volcanic formations. Tectonophysics 307, 219–234.
Rochette, P., Jackson, M.J., Aubourg, C., 1992. Rock magnetism and the interpretation of anisotropy of magnetic susceptibility. Reviews of Geophysics 30, 209–226.
Sander, B., 1970. An Introduction to the Study of Fabrics of Geological Bodies (English translation and reprint of 1930 German edition). Pergamon Press, Oxford, 641 pp.
Scheidegger, A.E., 1965. On the statistics of the orientation of bedding planes, grain axes, and similar sedimentological data. U.S. Geol. Survey, Prof. Paper 525-C, 164–167.
Schmidt, V.A., Ellwood, B.B., Nagata, T., Noltimier, H.C., Hrouda, F., Wagner, J.-J., 1988. The measurement of anisotropy of magnetic susceptibility using a cryogenic (SQUID) magnetometer and a comparison with results obtained from a torsion-fibre magnetometer. Physics of the Earth and Planetary Interiors 51, 365–378.
Schmidt, V., Gunther, D., Hirt, A.M., 2006. Magnetic anisotropy of calcite at room-temperature. Tectonophysics 418, 63–73.
Schmidt, V., Hirt, A.M., Hametner, K., Gunther, D., 2007a. Magnetic anisotropy of carbonate minerals at room temperature and 77 K. 92, 1673–1684.
Schmidt, V., Hirt, A.M., Rosselli, P., Martín-Hernández, F., 2007b. Separation of diamagnetic and paramagnetic anisotropy by high-field, low-temperature torque measurements. Geophysical Journal International 168, 40–47.
Siddans, A.W.B., Henry, B., Kligfield, R., Lowrie, W., Hirt, A., Percevault, M.N., 1984. Finite strain patterns and their significance in Permian rocks of the Alpes Maritmes (France). Journal of Structural Geology 6, 339–368.
Stacey, F.D., Banerjee, S.K., 1974. The Physical Principles of Rock Magnetism. Elsevier, Amsterdam, 195 pp.
Stephenson, A., 1993. Three-axis static alternating-field demagnetization of rocks and the identification of NRM, GRM, and anisotropy. Journal of Geophysical Research 98, 373–381.
Stephenson, A., 1994. Distribution anisotropy, two simple models for magnetic lineation and foliation. Physics of the Earth and Planetary Interiors 82, 49–53.
Stephenson, A., Potter, D.K., 1987. Gyroremanent magnetizations in dilute anisotropic dispersions of gamma ferric oxide particles from magnetic recording tape. IEEE Transactions on Magnetics 23, 3820–3830.
Stephenson, A., Sadikun, S., Potter, D.K., 1986. A theoretical and experimental comparison of the anisotropies of magnetic susceptibility and remanence in rocks and minerals. Geophysiccal Journal of the Royal Astronomical Society 84, 185–200.
Stoner, E.C., 1945. The demagnetizing factors for ellipsoids. Philosophical Magazine 36, 803–821.
Sun, W.-W., Hudleston, P.J., Jackson, M., 1995. Magnetic and petrofabric studies in the multiply deformed Thompson Formtion, east-central Minnesota. Tectonophysics 249, 109–124.
Syono, Y., 1960. Magnetic susceptibility of some rock forming silicate minerals such as amphiboles, biotites, cordierites and garnets. Journal of Geomagnetism and Geoelectricity 11, 85–93.
Tarling, D.H., Hrouda, F., 1993. The Magnetic Anisotropy of Rocks. Chapman, Hall, London, 217 pp.
Taylor, S.R., McLelland, S.M., 1985. The Continental Crust, its Compositions and Evolution. Blackwell, Oxford. 312pp.
Tauxe, L., 1998. Paleomagnetic Principles and Practice. Kluwer, Dordecht, 299 pp.
Trindade, R.I.F., Bouchez, J.L., Bolle, O., Nedelec, A., Peschler, A., Poitrasson, F., 2001. Secondary fabrics revealed by remanence anisotropy: methodological study and examples from plutonic rocks. Geophysical Journal International 147, 310–318.
Tullis, T.E., 1976. Experiments on the origin of slaty cleavage and schistosity. Geological Society of America Bulletin 87, 745–753.
Ullemeyer, K., Braun, G., Dahms, M., Kruhl, J.H., OlesenØ, N., Siegesmund, S., 2000. Texture analysis of a muscovite-bearing quartzite: a comparison of some currently used techniques. Journal of Structural Geology 22, 1541–1557.
Uyeda, S., Fuller, M.D., Belshé, J.C., Girdler, R.W., 1963. Anisotropy of magnetic susceptibility of rocks and minerals. Journal of Geophysical Research 68, 279–291.
Vincenz, S.A., 1965. Frequency dependence of magnetic susceptibility of rocks in weak alternating fields. Journal of Geophysical Research 70, 1371–1377.
Voight, W., Kinoshita, S., 1907. Bestimmung absoluter Werte von Magnetiserungszahlen, inbesondere für Kristalle. Annale der Physik 24, 492–514.
Werner, T., Borradaile, G.J., 1996. Paleoremanence dispersal across a transpressed Archean terrain; deflection of anisotropy or by late compression? Journal of Geophysical research 101, 5531–5545.
Werner, T., 1997. Experimental designs for determination of the anisotropy of remanence-test of the efficiency of least-squares and bootstrap methods applied to metamorphic rocks from southern Poland. Physics and Chemistry of the Earth 22, 131–136.

Woodcock, N.H., 1977. Specification of fabric shapes using an Eigenvalue method. Geological Society of America Bulletin 88, 1231–1236.
Wörm, H.-U., 1998. On the superparamagnetic-stable single domain transition for magnetite, and frequency dependence of susceptibility. Geophysical Journal International 133, 201–206.
Wörm, H.-U., Clark, D., Dekkers, M.J., 1993. Magnetic susceptibility of pyrrhotite: grain size, field and frequency dependence. Geophysical Journal International 114, 127–137.
Zapletal, K., 1990. Low-field susceptibility anisotropy of some biotite crystals. Physics of the Earth and Planetary Interiors 63, 85–97.